UNIVERSITY OF CALIFORNIA SAN DIEGO

Spatiotemporal Variability of Seawater Carbonate Chemistry in Diverse Coral Reef Environments in South East Asia and Australia

A dissertation submitted in partial satisfaction of the
requirements for the degree Doctor of Philosophy

in

Oceanography

by

Samuel Andrew Ho'onewanewaonalani Kekuewa

Committee in charge:

Professor Andreas J. Andersson, Chair
Professor James Leichter
Professor Todd Martz
Professor Jonathan Shurin
Professor Linda Wegley-Kelly

2024

The Dissertation of Samuel Andrew Ho'onewanewaonalani Kekuewa is approved, and it is acceptable in quality and form for publication on microfilm and electronically.

University of California San Diego

2024

TABLE OF CONTENTS

Signature Page iii

Table of Contents iv

List of Tables v

List of Figures vii

Acknowledgments viii

Vita xi

Abstract of the Dissertation xii

Chapter 1: Introduction 1

Chapter 2: Temporal and Spatial Variabilities of Chemical and Physical Parameters on the Heron Island Coral Reef Platform 12

Chapter 3: Multi-scale coral reef seawater carbonate chemistry variability at Dongsha and Taiping Islands in the South China Sea 42

Chapter 4: Effect of seaweed cultivation on spatial seawater carbonate chemistry across Onna-son Reef 95

Chapter 5: Conclusion 134

LIST OF TABLES

Chapter 2

Table 2.1: Instrument deployment information for each site.....18

Table 2.2: Seawater temperature, salinity, DO, and pH variability from autonomous sensors.....24

Table 2.3: Seawater temperature, salinity, DO, DIC, TA, pH, Ω_{Ar}, and pCO_2 variability from spatial surveys.....27

Table 2.4: One-way anova statistics between means of seawater temperature, salinity, DO, DIC, TA, pH, Ω_{Ar}, and pCO_2 between each survey.....28

Chapter 3

Table 3.1: Description of habitats and sampling scheme for each spatial survey 70

Table 3.2: Instrument deployment information for each site.....71

Table 3.3: Seawater temperature, DO, and pH variability from autonomous sensors.....72

Table 3.4: Observed time of day of minimum and maximum seawater temperature, salinity, DO, and pH values from autonomous sensors.....73

Table 3.5: Slope, R^2, and associated *p*-value of dTA-dDIC and dDO-$dDIC_{NCP}$ as well as mean dDIC, dTA, and dDO for all individual spatial surveys 74

Table S3.1: Seawater temperature, DO, DIC, TA, pH, Ω_{Ar}, and pCO_2 variability from spatial surveys 75

Table S3.1: Extended seawater temperature, DO, DIC, TA, pH, Ω_{Ar}, and pCO_2 variability from spatial surveys.....76

Chapter 4

Table 4.1: Mean environmental conditions and measured carbonate chemistry parameters 113

Table S4.1: Mean environmental conditions and calculated carbonate chemistry parameters ...114

Table S4.2: Mean dTA, dDIC, dDO, dDICNCP, and corresponding slopes and R2 for each individual survey.....115

LIST OF FIGURES

Chapter 1

Figure 1.1: Map of study sites....7

Chapter 2

Figure 2.1: Details of study site....17

Figure 2.2: Temporal variability of environmental conditions and seawater biogeochemistry on Heron Reef Platform....22

Figure 2.3: Depth averaged water column velocity and direction....23

Figure 2.4: Lateral spatiotemporal variability of measured seawater salinity and temperature across Heron Reef Platform....25

Figure 2.5: Lateral spatiotemporal variability of measured seawater DO, DIC, and TA across Heron Reef Platform....25

Figure 2.6: Lateral spatiotemporal variability of calculated seawater Ω_{Ar}, pH_T, and pCO_2 across Heron Reef Platform....26

Figure 2.7: Property-property plots of seawater DIC and TA and seawater DIC_{NCP} and DO relative to offshore from spatial surveys....29

Figure 2.8: Lateral spatiotemporal variability of seawater DIC and TA and seawater DIC_{NCP} and DO relative to offshore across Heron Reef Platform....30

Chapter 3

Figure 3.1: Details of study sites....77

Figure 3.2: Hourly climatology and means of seawater temperature, pH, and DO from autonomous sensors from each study site....78

Figure 3.3: Lateral spatiotemporal variability of measured seawater DIC, and TA across each spatial habitat....79

Figure 3.4: Seawater temperature, pH, DO, and Ω_{Ar} as a function of habitat/spatial scale and time of day....80

Figure 3.5: Property-property plots of seawater DIC and TA and seawater DIC_{NCP} and DO relative to offshore from spatial surveys....81

Figure 3.6: Ridge plot and projections of seawater temperature, pH, DO, and Ω_{Ar} from the current day, 2050, and 2100 as a function of habitat/spatial survey following CMIP6 RCP 8.5 temperature increases and an annual 1.15 umol kg^{-1} increase in nDIC 82

Figure 3.7: Global coral reef TA anomalies relative to the open-ocean in comparison to observations from this study 83

Figure S3.1: Scatter plot of DO-pH from autonomous sensors 84

Chapter 4

Figure 4.1: Current velocity, current trajectory, significant wave heights, and mean sea level for each survey.....116

Figure 4.2: Lateral spatiotemporal variability of seawater DIC, TA, and pH across Onna-son Reef in the Fall.....117

Figure 4.3: Lateral spatiotemporal variability of seawater DIC, TA, and pH across Onna-son Reef in the Winter 118

Figure 4.4: Lateral spatiotemporal variability of seawater DIC, TA, and pH across Onna-son Reef in the Spring 119

Figure 4.5: Property-property plots of seawater DIC and TA and seawater DIC_{NCP} and DO relative to offshore from spatial surveys.....120

Figure S4.1: Spatial variability of calculated carbon chemistry parameters from Fall surveys ..121

Figure S4.2: Spatial variability of calculated carbon chemistry parameters from Spring surveys 122

Figure S4.3: Spatial variability of calculated carbon chemistry parameters from Winter surveys 123

Figure S4.4: Property-property plots of seawater DIC and TA and seawater DIC_{NCP} and DO relative to offshore from spatial surveys separated by time of day 124

ACKNOWLEDGMENTS

There are many people who have supported me, trained me, and mentored me throughout my dissertation who I would like to acknowledge.

First, I would like to acknowledge my thesis advisor, Andreas Andersson for training me as a scientist and providing me with the opportunities to be successful. I have grown much throughout my time working with alongside you and am a better person and scientist because of your mentorship. I would also like to thank my committee members James Leichter, Todd Martz, Jonathan Shurin, and Linda Wegley-Kelly for expanding my research interests and helping me disseminate my scientific research to a broader community.

Further, I would like to extend my gratitude to the Scripps Institution of Oceanography, National Sun Yat-sen University, and Okinawa Institute of Science and Technology communities in general. Particularly, I'd first like to acknowledge the support of past and present lab members of the Scripps Coastal and Open Ocean Biogeochemistry Lab in particular Alyssa Griffin, Travis Courtney, Tyler Cyronak, Ariel Pezner, Max Rintoul, Cheyenne Bridges, and Steven Flemig for countless shared experiences in both the lab and the field. I am also grateful to Captain Hayashi, Satoshi Mitarai, and the Mitarai lab in Okinawa and Yi Wei, Yi-Bei Liang, and Keryea Soong in Taiwan for your hospitality and facilitating field research.

I'd like to further acknowledge that my friends, family, and teachers that have assisted me along the way. I will forever be grateful to Jane Teranes who provided me the opportunity to pursue my graduate studies in the first place. You are missed but will never be forgotten. Thank you also to Jennifer Haase for introducing me to Earth Science research during the 2016 Scripps Undergraduate Research Fellowship. Outside of research, thank you to my mother, Kimberly

Leikam, father, David Kekuewa, and siblings, Daria and David Kekuewa, for the endless support and providing me a constant reminder to value the smaller things in life.

I would like to further acknowledge the overwhelming support that Allison Ho has provided throughout my dissertation. Alli has always been my biggest advocate and constantly motivated me to continue onward during rough times and to pursue research interests that aligned with me. Thank you for the endless adventures and providing me a home to come back to, this dissertation may not have been possible without you. Lastly, thank you to Wiley Wolfe, Zach Skelton, Momme Hell, Zach Quinlan, Alaina Smith, Kelli Mullane, and Stephanie Matthews for hanging out with me and for their constant friendship and support throughout the years.

I would like to further thank Scripps Institution of Oceanography, NTU and Okinawa Institute of Science and Technology for institutional support and to the volunteers and staff at those institutions who facilitated this research. I would like to also thank Sharyn Kilpatrick for processing countless travel and research reimbursements, the graduate office: Gilbert Bertado, Denise Darling, Maureen McGreevy, Maureen McCormick, Josh Reeves, Shelley Weisel, and Olivia Padilla for your support throughout my time at Scripps, and to the dive locker: Christian McDonald, Richard Walsh, Ashleigh Palinkas., and Brett Pickering for facilitating SCUBA diving. Lastly, a huge acknowledgement and thank you to Keiara Auzenne and the EDI fellows who supported me through some of my toughest times of my dissertation.

This research would not have been possible without financial support from the Tribal Membership Initiative Fellowship, National Science Foundation, Australian Research Council, NOAA Office of Oceanic and Atmospheric Research, Shepard Foundation, and Robert Buzzelli Endowed Fellowship.

It is with the utmost gratitude that I acknowledge and thank all the co-authors of my dissertation: Andreas Andersson, Travis Courtney, Tyler Cyronak, Bradley Eyre, Theo Kindeberg, Laura Stoltenberg, Ariel Pezner, Max Rintoul, Keryea Soong, Yi Wei, and Satoshi Mitarai. Thank you all so much for your time spent in the field, lab, meetings, emails, and edits to support these research projects. I have learned so much from you all and would not have been able to complete this dissertation without your support.

Chapter 2, in full, is a reprint of the material as it appears in Kekuewa SAH, Courtney TA, Cyronak T, Kindeberg T, Eyre BD,' Stoltenberg L, Andersson AJ. Temporal and Spatial Variabilities of Chemical and Physical Parameters on the Heron Island Coral Reef Platform. *Aquatic Geochemistry* 2021. The dissertation author was the primary investigator and author of this paper.

Chapter 3, in full, is currently being prepared for submission for publication of the material. Kekuewa SAH, Pezner AK, Courtney TA, Wei Y, Soong K, Rintoul MS, Andersson AJ. The dissertation author was the primary researcher and author of this material.

Chapter 4, in full, is currently being prepared for submission for publication of the material. Kekuewa SAH, Rintoul MS, Courtney TA, Pezner AK, Mitarai S, Andersson AJ. The dissertation author was the primary investigator and author of this material.

VITA

2017 Bachelor of Science in Earth Sciences (Minor in Marine Sciences), University of California San Diego

2020 Master of Science in Oceanography, University of California San Diego

2024 Doctor of Philosophy in Oceanography, University of California San Diego

PUBLICATIONS

Lampe RH, Coale TH, Forsch KO, Jabre LJ, **Kekuewa S**, Bertrand EM, Horák A, Oborník M, Rabines AJ, Rowland E, Zheng H, Barbeau KA, Andersson AJ, Allen AE. 2023. Short-term acidification promotes diverse iron acquisition and conservation mechanisms in upwelling-associated phytoplankton. *Nature Communications*. https://doi.org/10.1038/s41467-023-42949-1

Pezner AK, Courtney TA, Barkley HC, Chou WC, Chu HC, Clements SM, Cyronak T, DeGrandpre MD, **Kekuewa SAH**, Kline DI, Liang Y-B, Martz TB, Mitarai S, Page HN, Rintoul MS, Smith JE, Soong K, Takeshita Y, Tresguerres M, Wei Y, Yates KK, Andersson AJ. 2023. Increasing hypoxia on global coral reefs under ocean warming. *Nature Climate Change*. https://doi.org/10.1038/s41558-023-01619-2

Rintoul M, Courtney T, Dohner J, Giddings S, Inoha K, **Kekuewa S**, Mitarai S, Monismith S, Pezner A, Andersson A. 2022. The Effects of Light Intensity and Flow Speed on Biogeochemical Variability within a Fringing Coral Reef in Onna-son, Okinawa, Japan. *Journal of Geophysical Research – Oceans*. https://doi.org/10.1029/2021JC018369

Kekuewa SAH, Courtney TA, Cyronak T, Andersson AJ. 2022. Seasonal nearshore ocean acidification and deoxygenation in the Southern California Bight. *Scientific Reports*. https://doi.org/10.1038/s41598-022- 21831-y

Kekuewa SAH, Courtney TA, Cyronak T, Kindeberg T, Eyre BD, Stoltenberg L, Andersson AJ. 2021. Temporal and Spatial Variabilities of Chemical and Physical Parameters on the Heron Island Coral Reef Platform. *Aquatic Geochemistry*. https://doi.org/10.1007/s10498-021-09400-7

ABSTRACT OF THE DISSERTATION

Spatiotemporal Variability of Seawater Carbonate Chemistry in Diverse Coral Reef Environments in South East Asia and Australia

by

Samuel Andrew Ho'onewanewaonalani Kekuewa

Doctor of Philosophy in Oceanography

University of California San Diego, 2024

Professor Andreas J. Andersson, Chair

Coral reefs are under threat from global environmental perturbations including ocean warming, acidification, and deoxygenation. The degree to which these perturbations will affect coral reefs is dependent on a range of factors including the local hydrodynamics and biogeochemical processes, both which vary widely across space and time. Consequently, not all coral reefs will be affected equally due to differences in local properties and processes. To develop predictive capacity for how coral reefs will be affected by ocean acidification (OA) it is necessary to first understand the current seawater CO_2 chemistry variability and drivers. In this dissertation, autonomous sensors and discrete seawater samples were used to characterize the natural spatial

and temporal variability of seawater CO_2 chemistry across different reef scales and habitats in Australia and South East Asia (i.e., Heron Island, Great Barrier Reef; Dongsha Atoll and Taiping Island, South China Sea; and Onna-son Reef, Okinawa). In Heron Island, the largest spatial and temporal variability in seawater chemistry was associated with the most shallow, western region of the platform that also had the longest residence time. Interactions between reef geomorphology and timing of the tidal cycle greatly influenced chemical gradients and variability leading to some unexpected trends and patterns. On Dongsha, elevated pH and aragonite saturation state (Ω_{Ar}) were observed inside a semi-enclosed lagoon during both day and night. Future projections showed that this environment will not cross, detrimental aragonite thresholds (e.g., $\Omega_{Ar} < 2.92$) as frequently as patch reefs and the large-scale lagoon of Dongsha. However, concurrent high water temperature and hypoxia indicated that this environment will not offer respite to taxa sensitive to OA. In Onna-son, the influence of seaweed cultivation on seawater chemistry during spring was compared to times of no cultivation during fall and winter. pH elevation was observed during both spring (+0.13 units) and fall (+0.10 units), but it was not possible to separate the role of cultivated seaweed from natural taxa. This dissertation demonstrates current coral reef seawater CO_2 chemistry conditions and biochemical function, information that will be critical for making rigorous projections for the future.

CHAPTER 1: Introduction

Despite covering less than 1% of the ocean floor (Smith, 1978), coral reefs provide ecologically, and economically important ecosystem services valued at trillions of dollars (Costanza et al., 2014). For example, coral reefs are home to more than 25% of global marine species, supporting important fisheries that feed more than 500 million people and creating economically important revenue to local communities through tourism and fisheries (Costanza et al., 1997). Furthermore, the complex, rigid habitats that coral reefs create provide coastline protection from storms and erosion by dissipating an average of 97% of wave energy from reaching the shoreline (Ferrario et al., 2014). Currently, coral reefs are under threat from multiple global stressors such as warming, ocean acidification (OA), deoxygenation, and sea level rise, as well as local stressors such as disease, eutrophication, overfishing, and other disturbances that synergistically may increase the mortality of coral reefs (Hoegh-Guldberg et al., 2007; Hughes et al., 2017). By the year 2100, seawater temperature is projected to increase by 3.5°C coincident with a decrease of seawater pH and dissolved oxygen by 0.40 and 13 μmol kg^{-1}, respectively, following the highest gas emission scenario (Kwiatkowski et al., 2020). Due to these phenomena, global coral cover has declined by more than 50% between 1957 to 2007 (Bruno et al., 2007, Wilkinson et al., 2008; De'ath et al., 2009; Eddy et al., 2018). These declines are predicted to continue in the future (Hoegh-Guldberg et al., 2007).

Coral reefs may be particularly vulnerable to OA as their skeletal structures are created out of calcium carbonate ($CaCO_3$). OA is a direct result of anthropogenic CO_2 emissions and land-use changes that result in increased oceanic uptake of CO_2, a shift in seawater carbonate chemistry equilibrium, and a decrease in seawater pH (e.g., Raven et al., 2005; Doney et al., 2009). OA has been shown to increase $CaCO_3$ dissolution and bioerosion on coral reefs (Andersson et al., 2009;

Wisshak et al., 2012; Eyre et al., 2014) and decrease coral calcification rates (Kleypas et al., 1999; Gattuso et al., 1999; Langdon and Atkinson, 2005; Albright et al., 2013), potentially resulting in a state of net coral reef erosion (Andersson and Gledhill, 2013; Eyre et al., 2014). However, not all coral reefs will be affected by OA and other global stressors the same way due to different benthic compositions (e.g., sand flats, seagrass, algal mats, coral and algal composition), reef type (e.g., atoll, barrier, fringing, platform), and local environmental drivers. To gain a predictive capacity for how coral reefs may be affected in the future we need to first understand the current physicochemical variability and drivers across multiple temporal (hourly, daily, seasonally) and spatial scales (100's m^2 100's km^2) in different reef environments and habitats (Andersson and Mackenzie, 2012; Andersson et al., 2015; Edmunds et al., 2016).

In most coral reef habitats, daily seawater carbonate chemistry variability is mainly controlled by net reef metabolism, which includes the influence of net community production (NCP) and net community calcification (NCC). NCP refers to the net sum of primary production and total respiration while NCC refers to the net sum of gross calcification and gross $CaCO_3$ dissolution (Smith and Key, 1975). Positive NCP refers to net organic carbon production, which increases dissolved inorganic carbon ($DIC = [CO_2] + [HCO_3^-] + [CO_3^{2-}]$) with minor changes in total alkalinity ($TA = [HCO_3^-] + 2[CO_3^{2-}] + [B(OH)_4^-] + [OH^-] – [H^+] \pm$ other minor constituents) from nutrient uptake and release (Zeebe and Wolf-Gladrow, 2001). Positive NCC refers to net $CaCO_3$ production, which decreases TA and DIC in a 2:1 ratio, and vice versa for negative NCP and NCC. However, complexity is added as both processes vary over temporal and spatial scales and are controlled by light and nutrient availability, temperature, seawater flow rates, benthic community composition, carbonate chemistry, and other local factors (e.g., terrestrial runoff and oceanic organic matter inputs) (Watanabe et al., 2006; Kleypas et al., 2011; Falter et al., 2013;

Page et al., 2016; Courtney et al., 2018; Page et al., 2019). In addition, the chemical variability in any given coral reef habitat is influenced by the seawater depth, flow trajectory, chemical memory, and residence time (Falter et al., 2013; Page et al., 2018; Cyronak et al., 2020), wherein a shallower depth results in a greater biomass to seawater volume ratio, which may allow enhanced biogeochemical modification of the overlying seawater in comparison to a deeper depth with lower biomass to seawater volume ratio (Koweek et al., 2015; Cyronak et al., 2020). Similarly, a longer residence time allows for longer duration of interaction between the benthos and overlying seawater, which results in enhanced biogeochemical modification of the overlying seawater (Falter et al., 2013). However, depending on the benthic habitats, flow trajectory, and rates of NCP and NCC, the net effect on the overlying seawater carbonate chemistry may balance out (Andersson et al., 2014). That is to say that the net effect of NCP and NCC could be balanced out if the seawater trajectory flows through various benthic habitats with opposite influences on the seawater chemistry or if the relative rates of NCP and NCC are of similar magnitude. Understanding how the cumulative effect of these various drivers and controls modulate seawater carbon chemistry variability in different coral reef environments and habitats is imperative for ascertaining how coral reefs will be impacted in the future.

We currently lack a comprehensive understanding for how coral reefs are responding to the individual and synergistic effects of both global and local stressors (Rogers, 1990; Anthony et al., 2008; Chan and Connolly, 2013; Eyre et al., 2014; Camp et al., 2017; Bell et al., 2022). A number of studies have reported the impact of OA and various stressors on coral reefs and their subsequent natural physicochemical variability across smaller sized spatial scales (i.e., population to community) (Santos et al., 2011; Koweek et al., 2015; Albright et al., 2015) with fewer studies that illustrate ecosystem to platform wide spatial scales (Andersson et al., 2014; Yeakel et al.,

2015; Takeshita et al., 2018; Courtney et al., 2018; Page et al., 2019; Kekuewa et al., 2021). This results in a distorted perspective of coral reef biogeochemical variability wherein small scale variability and its drivers are extrapolated to large scale, ecosystem and reef scales, without properly accounting for the full range and relative importance of different benthic habitats (e.g., seagrass beds, patch reefs, fore reef, sand flats, algal mats) and physical features. To fully understand how anthropogenic change is going to affect coral reef ecosystems and their various habitats, it is critical to capture the physiochemical variability between and across multiple spatial and temporal scales to assess habitat specific biogeochemical footprints and to extrapolate to make informed predictions at the ecosystem level (Andersson et al., 2015; Edmunds et al., 2016).

The theme of this dissertation aims to address three overarching research questions in contrasting reef environments:

1.) What is the natural spatial and temporal variability of seawater physicochemical parameters across different coral reef systems and habitats?

2.) How do coral reef chemical conditions deviate from the open ocean and what is the relative influence of organic and inorganic carbon cycling in modifying coral reef seawater carbonate chemistry?

3.) How do local properties and drivers influence local extremes that may exacerbate or alleviate ocean acidification on different temporal and spatial scales, i.e., what is the potential for a reef and/or habitat to serve as refugia from ocean acidification?

To address these overarching questions, I propose to leverage discrete seawater samples collected at various spatial scales paired alongside autonomous physical-biogeochemical sensors deployed

at various habitats across distinct coral reefs to capture both the spatial and temporal variability of seawater CO_2 chemistry parameters. These data will provide current-day baseline conditions and variability of seawater CO_2 chemistry parameters, but also show the relative importance of the inorganic and organic carbon cycle in driving these conditions. The broader goal of this dissertation intends to leverage observations in a range of geographically distinct coral reef environments and in unique habitats within these environments to gain a broad understanding of how local properties (e.g., geomorphology, depth and size of the reef, community composition, etc.) may influence the mean and variability of CO_2 chemistry parameters. Since local processes have a significantly greater influence on the local variability than the long-term secular increase in atmospheric CO_2, the information from this dissertation will contribute to enhancing our predictive capacity of how coral reef seawater chemistry may be affected in the near future owing to climate change and OA. Specifically, this dissertation focuses on four distinct reef sites - Heron Island Reef, Great Barrier Reef, Australia; Dongsha Atoll and Taiping Island, South China Sea, Taiwan; and Onna-son Reef, Okinawa, Japan (Figure 1).

In **Chapter 2**, I characterize the spatiotemporal variability of seawater carbonate chemistry parameters across the Heron Island coral reef platform, Great Barrier Reef, Australia. Utilizing both discrete seawater samples and autonomous sensors I assess the impact of local geomorphology and tidal isolation on the Heron Island coral reef platform. Using these observations, I highlight differences with previously modeled biogeochemical variability across the reef and demonstrate the need for increase spatial monitoring during different tidal regimes and times of day.

In **Chapter 3**, I focus on two coral reefs in the South China Sea – Dongsha Atoll and Taiping Island. Dongsha Atoll has an area of ~600 km^2 with a lagoon as wide as 28 km and an

average depth of 10 m. Dongsha Atoll is a unique study site due to its diversity in benthic habitats (e.g., fore reef, reef flats, patch reefs, sand flats, seagrass beds), size of patch reefs, percent coral cover, extent of forereef, and the presence of large internal waves on the forereef. In comparison, Taiping Island is an oceanic reef that consists of similar coral reef habitats (seagrass beds, sand flats, and corals), but has less opportunity to modify seawater CO_2 chemistry due to short residence times compared to Dongsha. By comparing observations across both systems, I assess how individual reef habitats and reef geomorphology contribute to the platform scale variability and account for differences in observed biogeochemical variability. Lastly, using these observations I calculate the projected effect of ongoing climate change conditions for each benthic habitat and assess the capacity for each habitat to act as a refugia to global warming, OA, and deoxygenation.

In **Chapter 4**, I focus on a fringing reef located in Onna-son, Okinawa, Japan. The Onna-son reef consists of a ~3 km long and 150 m wide reef flat consisting of sand, rubble, and algae. The lagoon behind the reef flat that ranges from 2-4 m deep and consists of sand, rubble, patch reefs, and both coral and seaweed farms with outlets to the ocean located at the northern, central, and southern regions of the reef. Uniquely, fishermen in Okinawa have employed parallel seaweed and coral aquaculture in this region for decades with an empirical understanding that this practice is beneficial to both the success of the seaweeds and the corals. Recently, seaweed aquaculture has also been proposed as an ocean-based CO_2 removal approach and a method to buffer coral reefs from OA (Duarte et al., 2017). However, little quantitative data exist to verify this hypothesis. Thus, this chapter assesses the biogeochemical footprint of the Onna-son seaweed aquaculture through Fall, 2019 and Winter, 2024 when seaweed is not growing and Spring, 2023 when seaweed is growing and harvesting. Further, these observations provide insight to the potential benefits of seaweed aquaculture such as increased calcification and pH amelioration.

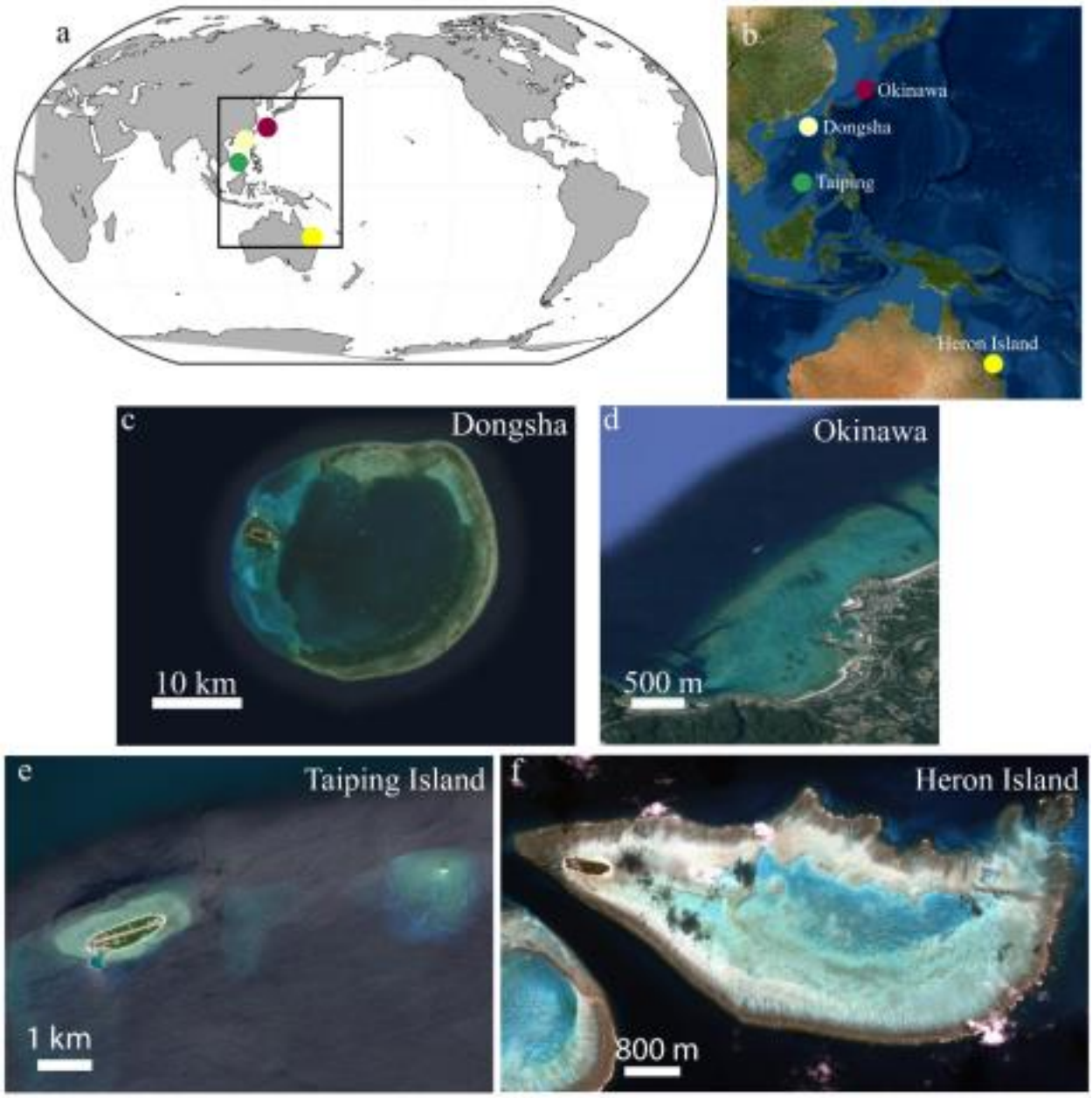

Figure 1.1. a) and b): World map and location of study sites in the Western Pacific. c) to f): larger scale maps of the study sites: c) Dongsha Atoll, d) Onna-son, Okinawa, e) Taiping Island, and f) Heron Island. All maps besides the world map and Heron Island map were generated via plot_google_map in MATLAB. The world map was generated in MATLAB via worldmap while the Heron Island image was provided by the Digital Globe Foundation.

References

Albright, R., Langdon, C., & Anthony, K. R. N. (2013). Dynamics of seawater carbonate chemistry, production, and calcification of a coral reef flat, central Great Barrier Reef. *Biogeosciences*, *10*(10), 6747-6758.

Albright, R., Benthuysen, J., Cantin, N., Caldeira, K., & Anthony, K. (2015). Coral reef metabolism and carbon chemistry dynamics of a coral reef flat. *Geophysical Research Letters*, *42*(10), 3980-3988.

Andersson, A. J., Kuffner, I. B., Mackenzie, F. T., Jokiel, P. L., Rodgers, K. S., & Tan, A. (2009). Net loss of $CaCO_3$ from coral reef communities due to human induced seawater acidification. *Biogeosciences Discussions*, *6*(1).

Andersson, A. J., & Mackenzie, F. T. (2012). Revisiting four scientific debates in ocean acidification research. *Biogeosciences*, *9*(3), 893-905.

Andersson, A. J., & Gledhill, D. (2013). Ocean acidification and coral reefs: effects on breakdown, dissolution, and net ecosystem calcification. *Annual review of marine science*, *5*, 321-348.

Andersson, A. J., Yeakel, K. L., Bates, N. R., & De Putron, S. J. (2014). Partial offsets in ocean acidification from changing coral reef biogeochemistry. *Nature Climate Change*, *4*(1), 56-61.

Andersson, A. J. (2015). A fundamental paradigm for coral reef carbonate sediment dissolution. *Frontiers in Marine Science*, *2*, 52.

Anthony, K. R., Kline, D. I., Diaz-Pulido, G., Dove, S. and Hoegh-Guldberg, O. (2008) Ocean acidification causes bleaching and productivity loss in coral reef builders, *Proceedings of the National Academy of Sciences*, 105(45), 17442-17446.

Bell, T., Manullang, C., Kumagai, N. H., Sakai, K., Suzuki, A., & Iguchi, A. (2022). Calcification responses of subtropical corals to ocean acidification: A case study from Sesoko Island, Okinawa, Japan. *Galaxea, Journal of Coral Reef Studies*, *24*(1), 51-61.

Bruno, J. F., & Selig, E. R. (2007). Regional decline of coral cover in the Indo-Pacific: timing, extent, and subregional comparisons. *PLoS one*, *2*(8), e711.

Camp, E.F., Nitschke, M.R., Rodolfo-Metalpa, R., Houlbreque, F., Gardner, S.G., Smith, D.J., Zampighi, M. and Suggett, D.J., (2017). Reef-building corals thrive within hot-acidified and deoxygenated waters. *Scientific reports*, *7*(1), p.2434.

Chan, N. C., & Connolly, S. R. (2013). Sensitivity of coral calcification to ocean acidification: A meta-analysis. *Global change biology*, *19*(1), 282-290.

Costanza, R., De Groot, R., Sutton, P., Van der Ploeg, S., Anderson, S. J., Kubiszewski, I., Farber, S., & Turner, R. K. (2014). Changes in the global value of ecosystem services. *Global environmental change*, *26*, 152-158.

Costanza, R., d'Arge, R., De Groot, R., Farber, S., Grasso, M., Hannon, B., Limburg, K., Naeem, S., O'neill, R. V., Paruelo, J., Raskin, R. G., & Van Den Belt, M. (1997). The value of the world's ecosystem services and natural capital. *nature*, *387*(6630), 253-260.

Courtney, T. A., De Carlo, E. H., Page, H. N., Bahr, K. D., Barro, A., Howins, N., Tabata, R., Terlouw, G., Rodgers, K. S., & Andersson, A. J. (2018). Recovery of reef-scale calcification following a bleaching event in Kāne'ohe Bay, Hawai'i. *Limnology and Oceanography Letters*, *3*(1), 1-9.

Cyronak, T., Takeshita, Y., Courtney, T. A., DeCarlo, E. H., Eyre, B. D., Kline, D. I., Martz, T., Page, H., Price, N. N., Smith, J., Stoltenberg, L., & Andersson, A. J. (2020). Diel temperature and pH variability scale with depth across diverse coral reef habitats. *Limnology and Oceanography Letters*, *5*(2), 193-203.

De'ath, G., Lough, J. M., & Fabricius, K. E. (2009). Declining coral calcification on the Great Barrier Reef. *Science*, *323*(5910), 116-119.

Doney, S. C., Fabry, V. J., Feely, R. A., & Kleypas, J. A. (2009). Ocean acidification: the other CO_2 problem. *Annual review of marine science*, *1*, 169-192.

Duarte, C. M., Wu, J., Xiao, X., Bruhn, A., & Krause-Jensen, D. (2017). Can seaweed farming play a role in climate change mitigation and adaptation?. *Frontiers in Marine Science*, *4*, 100.

Eddy, T. D., Cheung, W. W., & Bruno, J. F. (2018). Historical baselines of coral cover on tropical reefs as estimated by expert opinion. *PeerJ*, *6*, e4308.

Edmunds, P. J., Comeau, S., Lantz, C., Andersson, A., Briggs, C., Cohen, A., Gattuso, J. P., Grady, J. M., Gross, K., Johnson, M., Muller, E. B., & Carpenter, R. C. (2016). Integrating the effects of ocean acidification across functional scales on tropical coral reefs. *Bioscience*, *66*(5), 350-362.

Eyre, B. D., Andersson, A. J., & Cyronak, T. (2014). Benthic coral reef calcium carbonate dissolution in an acidifying ocean. *Nature Climate Change*, *4*(11), 969-976.

Falter, J. L., Lowe, R. J., Zhang, Z., & McCulloch, M. (2013). Physical and biological controls on the carbonate chemistry of coral reef waters: effects of metabolism, wave forcing, sea level, and geomorphology. *PloS one*, *8*(1), e53303.

Ferrario, F., Beck, M. W., Storlazzi, C. D., Micheli, F., Shepard, C. C., & Airoldi, L. (2014). The effectiveness of coral reefs for coastal hazard risk reduction and adaptation. *Nature communications*, *5*(1), 1-9.

Gattuso, J. P., Allemand, D., & Frankignoulle, M. (1999). Photosynthesis and calcification at cellular, organismal and community levels in coral reefs: a review on interactions and control by carbonate chemistry. *American zoologist*, *39*(1), 160-183.

Hoegh-Guldberg, O., Mumby, P. J., Hooten, A. J., Steneck, R. S., Greenfield, P., Gomez, E., Harvell, C. D., Sale, P. F., Edwards, A. J., Caldeira, K., Knowlton, N., & Hatziolos, M. (2007) Coral reefs under rapid climate change and ocean acidification S*cience*, *318*(5857), 1737-1742.

Hughes, T. P., Barnes, M. L., Bellwood, D. R., Cinner, J. E., Cumming, G. S., Jackson, J. B., Kleypas, J., van De Leemput, I. A., Lough, J. M., Morrison, T. H., Palumbi, S. R., & Scheffer, M. (2017). Coral reefs in the Anthropocene. *Nature*, *546*(7656), 82-90.

Kekuewa, S. A., Courtney, T. A., Cyronak, T., Kindeberg, T., Eyre, B. D., Stoltenberg, L., & Andersson, A. J. (2021). Temporal and Spatial Variabilities of Chemical and Physical Parameters on the Heron Island Coral Reef Platform. *Aquatic Geochemistry*, *27*(4), 241-268.

Kleypas, J. A., Buddemeier, R. W., Archer, D., Gattuso, J. P., Langdon, C., & Opdyke, B. N. (1999). Geochemical consequences of increased atmospheric carbon dioxide on coral reefs. *science*, *284*(5411), 118-120.

Kleypas, J. A., Anthony, K. R., & Gattuso, J. P. (2011). Coral reefs modify their seawater carbon chemistry–case study from a barrier reef (Moorea, French Polynesia). *Global change biology*, *17*(12), 3667-3678.

Koweek, D., Dunbar, R. B., Rogers, J. S., Williams, G. J., Price, N., Mucciarone, D., & Teneva, L. (2015). Environmental and ecological controls of coral community metabolism on Palmyra Atoll. *Coral Reefs*, *34*(1), 339-351.

Koweek, D. A., Dunbar, R. B., Monismith, S. G., Mucciarone, D. A., Woodson, C. B., & Samuel, L. (2015). High-resolution physical and biogeochemical variability from a shallow back reef on Ofu, American Samoa: An end-member perspective. *Coral Reefs*, *34*(3), 979-991.

Kwiatkowski, L., Torres, O., Bopp, L., Aumont, O., Chamberlain, M., Christian, J. R., Dunne, J. P., Gehlen, M., Ilyina, T. and John, J. G. (2020) Twenty-first century ocean warming, acidification, deoxygenation, and upper-ocean nutrient and primary production decline from CMIP6 model projections, *Biogeosciences*, 17(13), 3439-3470.

Langdon, C., & Atkinson, M. J. (2005). Effect of elevated pCO_2 on photosynthesis and calcification of corals and interactions with seasonal change in temperature/irradiance and nutrient enrichment. *Journal of Geophysical Research: Oceans*, *110*(C9).

Page, H. N., Andersson, A. J., Jokiel, P. L., Rodgers, K. U. S., Lebrato, M., Yeakel, K.Davidson, C., D'Angelo, S., & Bahr, K. D. (2016). Differential modification of seawater carbonate chemistry by major coral reef benthic communities. *Coral Reefs*, *35*(4), 1311-1325.

Page, H. N., Courtney, T. A., De Carlo, E. H., Howins, N. M., Koester, I., & Andersson, A. J. (2019). Spatiotemporal variability in seawater carbon chemistry for a coral reef flat in Kāne ʻohe Bay, Hawai ʻi. *Limnology and Oceanography*, *64*(3), 913-934.

Raven, J., Caldeira, K., Elderfield, H., Hoegh-Guldberg, O., Liss, P., Riebesell, U., Sheperd, J., Turley, C., & Watson, A. (2005). *Ocean acidification due to increasing atmospheric carbon dioxide*. The Royal Society.

Rogers, C. S. (1990). Responses of coral reefs and reef organisms to sedimentation. *Marine ecology progress series. Oldendorf*, *62*(1), 185-202.

Santos, I. R., Glud, R. N., Maher, D., Erler, D., & Eyre, B. D. (2011). Diel coral reef acidification driven by porewater advection in permeable carbonate sands, Heron Island, Great Barrier Reef. *Geophysical Research Letters*, *38*(3).

Smith, S. V., & Key, G. S. (1975). Carbon dioxide and metabolism in marine environments 1. *Limnology and Oceanography*, *20*(3), 493-495.

Smith, C. L. (1978). Coral reef fish communities: a compromise view. *Environmental Biology of Fishes*, *3*(1), 109-128.

Takeshita, Y., Cyronak, T., Martz, T. R., Kindeberg, T., & Andersson, A. J. (2018). Coral reef carbonate chemistry variability at different functional scales. *Frontiers in Marine Science*, *5*, 175.

Watanabe, A., Kayanne, H., Hata, H., Kudo, S., Nozaki, K., Kato, K., Negishi, A., Ikeda, Y., & Yamano, H. (2006). Analysis of the seawater CO_2 system in the barrier reef-lagoon system of Palau using total alkalinity-dissolved inorganic carbon diagrams. *Limnology and Oceanography*, *51*(4), 1614-1628.

Wilkinson, C. R., & Souter, D. (2008). Status of Caribbean coral reefs after bleaching and hurricanes in 2005.

Wisshak, M., Schönberg, C. H., Form, A., & Freiwald, A. (2012). Ocean acidification accelerates reef bioerosion. *PloS one*, 7, e45124.

Zeebe, R. E., & Wolf-Gladrow, D. (2001). CO_2 in seawater: equilibrium, kinetics, isotopes (Vol. 65). *Gulf Professional Publishing.*

CHAPTER 2

Temporal and Spatial Variabilities of Chemical and Physical Parameters on the Heron Island Coral Reef Platform

Kekuewa SAH, Courtney TA, Cyronak T, Kindeberg T, Eyre BD, Stoltenberg L, Andersson AJ

Aquatic Geochemistry
https://doi.org/10.1007/s10498-021-09400-7

ORIGINAL ARTICLE

Temporal and Spatial Variabilities of Chemical and Physical Parameters on the Heron Island Coral Reef Platform

Samuel A. H. Kekuewa[1] · Travis A. Courtney[1,2] · Tyler Cyronak[3] · Theodor Kindeberg[4] · Bradley D. Eyre[5] · Laura Stoltenberg[5] · Andreas J. Andersson[1]

Received: 3 March 2021 / Accepted: 13 September 2021

Abstract

Globally, coral reefs are threatened by ocean warming and acidification. The degree to which acidification will impact reefs is dependent on the local hydrodynamics, benthic community composition, and biogeochemical processes, all of which vary on different temporal and spatial scales. Characterizing the natural spatiotemporal variability of seawater carbonate chemistry across different reefs is critical for elucidating future impacts on coral reefs. To date, most studies have focused on select habitats, whereas fewer studies have focused on reef scale variability. Here, we investigate the temporal and spatial seawater physicochemical variability across the entire Heron Island coral reef platform, Great Barrier Reef, Australia, for a limited duration of six days. Autonomous sensor measurements at three sites across the platform were complemented by reef-wide boat surveys and discrete sampling of seawater carbonate chemistry during the morning and evening. Variability in both temporal and spatial physicochemical properties were predominantly driven by solar irradiance (and its effect on biological activity) and the semidiurnal tidal cycles but were influenced by the local geomorphology resulting in isolation of the platform during low tide and rapid flooding during rising tides. As a result, seawater from previous tidal cycles was sometimes trapped in different parts of the reef leading to unexpected biogeochemical trends in space and time. This study illustrates the differences and limitations of data obtained from high-frequency measurements in a few locations compared to low-frequency measurements at high spatial resolution and coverage, showing the need for a combined approach to develop predictive capability of seawater physicochemical properties on coral reefs.

Keywords Coral reef · Ocean acidification · Carbonate chemistry · Heron Island · Great Barrier Reef · Metabolism

✉ Samuel A. H. Kekuewa
kekuewa.sam@gmail.com

✉ Andreas J. Andersson
aandersson@ucsd.edu

Extended author information available on the last page of the article

Published online: 04 October 2021

1 Introduction

Despite covering less than one percent of the ocean surface, coral reefs are one of the most biologically diverse and economically important marine ecosystems (Crossland et al. 1991; Costanza et al. 1997, 2014). Some of the ecosystem services that coral reefs provide include protection for coastlines, fisheries, and tourism (Moberg and Folke 1999; Pandolfi et al. 2005; Brander et al. 2007). Coral reefs are currently under threat due to global environmental change associated with ocean warming (Hughes et al. 2003; Carpenter et al. 2008; Hoegh-Guldberg et al. 2010; Hughes et al. 2018a) and acidification (Hoegh-Guldberg et al. 2007) in addition to local disturbances such as overfishing (Jackson et al. 2001), eutrophication (Bell 1992; Bruno et al. 2003), and sedimentation (Rogers 1990). For the past several decades, increased research attention has been focused on the effects of ocean acidification (OA) on marine calcifiers due to the demonstrated effects on the formation and destruction of calcium carbonate ($CaCO_3$) shells and structures (Orr et al. 2005; Jokiel et al. 2008; Kleypas et al. 2009; Hofmann et al. 2010; Hendriks et al. 2010; McCulloch et al. 2012). It has been proposed that OA will have deleterious effects on coral reefs through the combination of decreasing calcification (Kleypas et al. 1999; Gattuso et al. 1999; Langdon and Atkinson 2005; De'ath et al. 2009; Albright et al. 2013; Chan and Connolly 2013; Comeau et al. 2013; Johnson et al. 2014; Albright et al. 2018) and increasing $CaCO_3$ dissolution and bioerosion (Andersson et al. 2009; Wisshak et al. 2012; Eyre et al. 2014, 2018), potentially leading to a state of net reef erosion (Andersson and Gledhill 2013; Eyre et al. 2018). However, the effects of OA may not be equal across coral reef ecosystems and habitats due to local factors influencing seawater carbonate chemistry, such as reef metabolism, community composition, residence time, flow rates, and water depth (Marshall et al. 2000; Manzello et al. 2010, 2012; Kapsenberg and Cyronak 2019; Cyronak et al. 2020).

On most coral reefs, daily variability in seawater carbonate chemistry is most strongly influenced by net metabolism, or the balance between net community calcification (NCC) and net community production (NCP). On a coral reef, NCC represents the net sum of calcification and $CaCO_3$ dissolution, while NCP is the net sum of photosynthesis and total respiration. Positive NCC decreases total alkalinity (TA) and dissolved inorganic carbon (DIC) in a ratio of 2:1 leading to a decrease in pH, whereas positive NCP primarily reduces DIC with only minor influence on TA leading to an increase in pH (Smith and Key 1975; Smith and Kinsey 1978; Atkinson and Smith 1983; Chisholm and Gattuso 1991). In contrast, negative NCC (i.e., net dissolution) increases pH and negative NCP (i.e., net respiration) decreases pH. The rates of NCC and NCP carry over multiple spatiotemporal scales and are controlled by many factors including community composition, light intensity, temperature, nutrition and nutrient concentrations, carbonate chemistry, flow rates, and external inputs of organic material from terrestrial and marine environments (Langdon and Atkinson 2005; Watanabe et al. 2006; Carilli et al. 2009; Kleypas et al. 2011; Falter et al. 2013; Venti et al. 2014; Cyronak et al. 2014a; Page et al. 2016, 2019; Courtney et al. 2018; Hughes et al. 2018b; Stoltenberg et al. 2021). The net effect of these processes on seawater carbonate chemistry is modified by physical factors such as the local bathymetry, geomorphology, and hydrodynamics. In particular, seawater depth, flow trajectory, and residence time are strongly linked to the magnitude of change in seawater carbonate chemistry parameters on coral reefs (Page et al. 2019; Cyronak et al. 2020). With shallower depth, the biomass to seawater volume ratio often increases, which allows for a

greater change in the overlying seawater carbon chemistry (Falter et al. 2013; Koweek et al. 2015a, b; Page et al. 2019; Cyronak et al. 2018, 2020). Similarly, a longer residence time allows for extended contact time between the benthos and seawater, and thus, greater modification in the mean seawater TA and DIC. Depending on the balance of NCC and NCP, flow trajectories, and the influence of different habitats, the net effect on seawater carbonate chemistry parameters (e.g., pH, aragonite saturation state, pCO_2) may balance out (Andersson et al. 2014; Page et al. 2019). That is, if NCC and NCP are of similar magnitude, there is little to no change in seawater pH, and similarly, if a water parcel's flow trajectory crosses habitats with opposite influence on pH, the net effect on pH is zero. Consequently, to understand future effects of OA on coral reefs, it is imperative to first understand the current natural spatial and temporal ranges, variability, and drivers of seawater carbonate chemistry in different reef environments (Andersson and Mackenzie 2012; Falter et al. 2013; Page et al. 2016, 2017; Takeshita et al. 2018).

To date, numerous biogeochemical studies have focused on individual coral reef habitats (e.g., Santos et al. 2011; Shaw et al. 2012; Koweek et al. 2015a, b; Albright et al. 2015; DeCarlo et al. 2017), whereas fewer studies have targeted entire reef ecosystems that encompass multiple habitats and benthic communities (e.g., fore reef, back reef, lagoon, sea grass, sand flats) (Suzuki and Kawahata 2003; Watanabe et al. 2006; Andersson et al. 2014; Shamberger et al. 2018; Courtney et al. 2018; Page et al. 2019). In the context of anthropogenically driven global environmental change, it is important to understand the ecosystem-level effects of OA and warming, which require the ability to integrate effects across different spatiotemporal scales and scale up to the ecosystem level (Edmunds et al. 2016). To do this successfully, studies targeting the biogeochemical function of entire reef systems are required.

One reef that has been studied extensively in the context of OA through the use of both experimental and field-based studies is Heron Reef, which is located on the southern Great Barrier Reef (GBR) of Australia (e.g., Anthony et al. 2008; Cyronak et al. 2013a, b; Dove et al. 2013; Kline et al. 2015; Brown et al. 2018, 2020). Several field studies have measured seawater carbonate chemistry in specific habitats or portions of the reef (e.g., Anthony et al. 2011; Santos et al. 2011; Kline et al. 2012, 2015; Georgiou et al. 2015; Cyronak et al. 2014b; Albright et al. 2015; Stoltenberg et al. 2020), but with no observational study characterizing the variability across the entire reef platform. Mongin and Baird (2014) attempted to characterize the reef scale seawater carbonate chemistry of the Heron Reef platform using a coupled hydrodynamic and biogeochemical model. They concluded that the major driver of carbonate chemistry variability at a given location was controlled by the benthic community composition and the flow trajectory but had limited biogeochemical data to validate their model output (Mongin and Baird 2014). Consequently, platform-wide spatial and temporal surveys of seawater carbon chemistry are needed to better understand how local physical and biological drivers affect physicochemical variability across Heron Reef.

In this study, we used a combination of autonomous sensors and reef-wide boat surveys to characterize the natural spatiotemporal variability of seawater carbonate chemistry parameters across the entire Heron Reef platform during October 2015. Here, we primarily focus on two questions: (1) What is the natural spatiotemporal variability of seawater carbonate chemistry parameters across the Heron Reef platform? (2) What is the relative importance of NCC and NCP in modifying seawater carbonate chemistry across the reef platform? We also assess and discuss how our observations align with the general model results by Mongin and Baird (2014).

2 Methods

2.1 Site Description

Heron Island is located at 23.45° S, 151.92° E, in the Capricorn Bunker Group along the southern portion of the Great Barrier Reef, Australia, ~ 70 km from the coast. Heron Island is a small coral cay (0.16 km^2) surrounded by a reef platform (27 km^2) that is dominated by lagoon and reef flat environments. The lagoon is encircled by a fore reef and reef crest. Depths within the lagoon and reef flat range from less than 1 m to 4 m, with a maximum depth near the center of the lagoon. Outside of the lagoon the reef slope community composition is predominantly hard coral cover (~ 60–80%) with low amounts of fleshy macroalgae (~ 2%) (Brown et al. 2018). In comparison, the inner lagoon is predominantly comprised of permeable carbonate sand flats (Glud et al. 2008) with lower amounts of hard coral cover (~ 20%) and higher amounts of fleshy macroalgae (25%) (Fig. 1; Brown et al. 2018; Allen Coral Atlas 2020). Water circulation across Heron Reef is tide and wind driven, primarily moving from east to west (Mongin and Baird 2014) at rates ranging from 1 to 30 cm s^{-1} (Gourlay and Hacker 1999; Anthony et al. 2013). Heron Reef experiences a semidiurnal tidal regime with tidal fluctuations up to 3 m during spring tides (Phinn et al. 2012). During low tide, the Heron Reef lagoon is isolated from the adjacent ocean, with seawater spilling over the reef crest during incoming tides (Gourlay and Hacker 2008; Mongin and Baird 2014).

2.2 Environmental and Chemical Measurements

Autonomous instruments were deployed at three stations covering the extent of the Heron Reef platform from October 9, 2015, to October 15, 2015, to capture high-resolution temporal variability (Fig. 1; Table 1). Station 1 (depth = 0.63 ± 0.28 m; mean ± SD) was located in the western part of the lagoon and according to the Allen Coral Atlas (2020) was composed of coral rubble (24%) and carbonate sand flats (76%), Station 2 (depth = 2.22 ± 0.60 m) was located in the center of the lagoon and was in close proximity to large coral colonies (18%) and permeable carbonate sand flats (82%), and Station 3 (depth = 1.55 ± 0.72 m) was located in the eastern part, close to the reef crest and composed of coral rubble (16%), coral (3%), macroalgae (3%), and permeable carbonate sand flats (78%) (Fig. 1; Allen Coral Atlas 2020). In addition to autonomous measurements, spatial surveys were conducted by boat to collect discrete seawater samples across the lagoon at 07:35 and 19:21 on October 13, 2015, as well as 08:34 on October 14, 2015. Due to the shallow depths of the lagoon, these surveys were restricted to tidal conditions sufficiently high to allow for safe navigation (i.e., + 1.2 m relative to mean lower low water). All data are available at BCO-DMO (https://www.bco-dmo.org/dataset/839261).

2.2.1 Autonomous Sensors

All three stations were equipped with SeapHOx sensors that measured temperature (°C), salinity (g kg^{-1}), pressure (PSIG), pH, and dissolved oxygen (DO; mL L^{-1}) every 30 min (Martz et al. 2010). Each SeapHOx consisted of a Honeywell Durafet III pH sensor (Martz et al. 2010), an Aanderaa 3835 oxygen optode, and a SBE-37 MicroCAT conductivity–temperature–depth (CTD) profiler. The SeapHOx oxygen optode and CTD were factory calibrated for temperature (± 0.002 °C), DO (± 5%), salinity (± 0.0002), and pressure

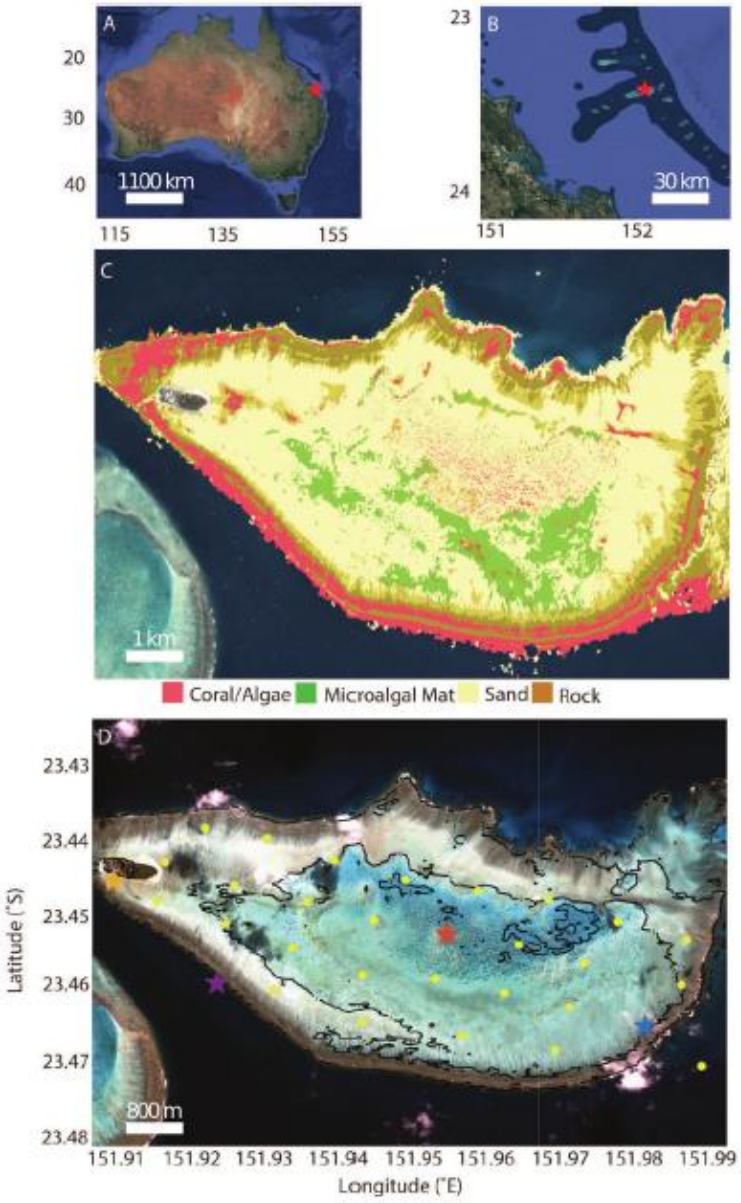

Fig. 1 **a** and **b** Location of Heron Reef (red star) on the Great Barrier Reef, Australia. **c** Benthic community map and **d** sampling locations of the present study. Yellow symbols in **d** indicate discrete sampling stations for spatial surveys, while stars indicate autonomous sensor locations (Station 1: orange, Station 2: red, Station 3: blue, and the Heron MAPCO2 mooring: purple). Black lines indicate the 1-, 3-, and 4-m depth contours. Credit: **a** Google Earth, **b** Google Earth, **c** Allen Coral Atlas (2020), **d** Digital Globe Foundation

Table 1 Autonomous sensor deployment locations, depths, instruments, parameters, and benthic habitats and zonations

Station	Longitude	Latitude	Average depth (m)	Instruments	Parameters measured	Benthic habitat and zonation
1	23.444° S	151.913° E	0.63 ± 0.28	SeapHOx	T, S, P, DO, pH	Coral rubble near to Heron Island
2	23.451° S	151.958° E	2.22 ± 0.60	SeapHOx	T, S, P, DO, pH	Coral colonies surrounded by sand flats in center of lagoon
				ADCP	Current velocity	
				ECO-*PAR*	PAR	
				ECO-*FLNTU*	Chl *a*	
3	23.464° S	151.985° E	1.55 ± 0.72	SeapHOx	T, S, P, DO, pH	Coral rubble near eastern reef crest

(±0.1%). The pH Durafet sensor was cross-calibrated with discrete seawater samples collected in a water tank prior to deployment following standard procedure (Bresnahan et al. 2014) and compared to additional validation samples collected in situ. The accuracy of the Durafet pH sensors throughout the deployment was calculated to be ±0.01 from the validation samples. Additional sensors were deployed at Station 2, including a Nortek acoustic Doppler current profiler (ADCP; Aquadopp 1 MHz,), a Wetlabs photosynthetically active radiation (PAR; µE m^{-2} s^{-1}) sensor (ECO-PARSB), and a Wetlabs Ecosensor (ECO-FLNTUSB) to measure Chlorophyll *a* (Chl *a*; µg L^{-1}). The ADCP collected current data every 10 min in 0.5-m depth bins. Starting from 0.4 m above the sensor, the ADCP sampled to a max height of 3.4 m above the bottom. PAR and Chl *a* sensors collected data every 10 min, with each data point representing an average of 10 points measured every 6 s. The instruments were secured to either proximal substrate or cinder blocks at each station.

Outside the southwestern portion of the Heron Reef platform was a surface MAPCO2 mooring managed by B. Tilbrook at the Commonwealth Scientific and Industrial Research Organization (CSIRO; Tilbrook et al. 2012). The mooring was equipped with a Battelle Memorial Institute CO_2 system and a Seabird SBE 16plusV2, recording seawater temperature, salinity, xCO_{2sw}, and xCO_{2air} every 2-h (Sutton et al. 2014). The system calculates xCO_2 in air that has been equilibrated with seawater. For each measurement, the system is calibrated with a zero and a nonzero CO_2 reference gas provided by NOAA Earth System Research Laboratory (ESRL) and traceable to World Meteorological Organization (WMO) standards. The accuracy and precision of both air and seawater xCO_2 measurements are typically better than 2 µmol mol^{-1}. The mooring was re-deployed after servicing on September 23, 2015. Quality controlled data were provided by the joint efforts of the CSIRO Marine and Atmospheric Research and NOAA Pacific Marine Environmental Laboratory (PMEL) through support by Australia's Integrated Marine Observing System (Tilbrook et al. 2012).

2.2.2 Spatial Sampling Procedure

Three lagoon-wide sampling surveys were conducted across the Heron Reef lagoon during the morning ($n=2$) in full daylight and during the evening ($n=1$) between October 13 and 14, 2015, in full darkness. Due to boating hazards associated with low tide, all surveys were conducted at tides exceeding MLLW by 1.2 m. Seawater samples were collected from the surface using a bucket and line at 28 stations inside the lagoon and 1 station outside of the reef (Fig. 1). The duration of each survey was on average 2 h. Samples for seawater carbonate chemistry were carefully collected from the bucket into 250-mL Corning Pyrex glass bottles avoiding entrainment of bubbles. Bottles were rinsed three times before samples were collected, which were immediately poisoned with 100 µL saturated solution of mercuric chloride ($HgCl_2$) to prevent biological activity (Dickson et al. 2007). Measurements of sea surface temperature (±0.3 °C), DO (±0.2 mg L^{-1}), and salinity (±0.1) were made using a YSI Professional Plus handheld multi-parameter instrument (YSI 6600 V2). Salinity was calibrated to seawater certified reference materials (CRM) provided by the Dickson Lab at Scripps Institution of Oceanography, and DO was calibrated to 100% water-saturated air prior to each survey.

2.3 Sample Analyses

All seawater samples were transported to and analyzed at the Scripps Coastal and Open Ocean Biogeochemistry lab in La Jolla, CA, USA, in April of 2016, 6 months after collection. Seawater samples were analyzed for dissolved inorganic carbon (DIC) via an automated infrared inorganic carbon analyzer (AIRICA, *Marianda*) with a LI-COR 7000. Total alkalinity (TA) was measured via potentiometric, open-cell acid titrations (0.1 N HCl) with a system developed by the Dickson Lab at Scripps Institution of Oceanography (SIO) (Dickson et al. 2007). Accuracy and precision of the instruments were validated against CRMs provided by the Dickson Lab (mean offset ± 1SD of TA = 2.22 ± 0.36 µmol kg^{-1}, $n = 20$; DIC = − 0.86 ± 1.78 µmol kg^{-1}, $n = 18$). For all samples, CRMs were analyzed at the beginning and the end of the day, and also every fifth sample for DIC and every tenth sample for TA in order to ensure that there was no instrumental drift.

2.4 Data Analyses and Calculations

ADCP directional data were corrected for the local magnetic declination at the time of the study (9.44 ± 0.24 °E). Speed and direction were converted into U and V components, depth integrated throughout the water column, and recalculated as vectors. DO measurements from the SeapHOx were corrected for salinity according to the manufacturer (*Aanderaa*). Additionally, pressure measurements by the SeapHOx sensors were cross-calibrated in a shallow holding tank and converted into depth units (m). Due to high reflection of irradiance from the light-colored, sandy benthos during daytime and generally low Chl *a* concentrations, daytime Chl *a* measurement was considered spurious (personal communication with the manufacturer Seabird, Inc). Consequently, only nighttime Chl *a* data were used to assess the Chl *a* content.

Carbonate chemistry variables were calculated using CO2SYS for MATLAB (version 2.1; van Heuven et al. 2011) and inputs of DIC and TA at in situ temperature and salinity. The dissociation constants, K_1^* and K_2^* were based on Mehrbach et al. (1973) refit by Dickson and Millero (1987), $KHSO_4$ from Dickson (1990), and $[B]_T$ from Uppstrom (1974) were used. Air and seawater pCO_2 for the Heron Island MAPCO2 data were calculated using measured xCO_{2Air}, xCO_{2SW}, sea surface temperature, salinity, and air pressure following the procedure of Takahashi et al. (2009).

Lomb–Scargle periodograms were calculated for water column depth, seawater temperature, salinity, pH_T, DO, and pCO_2 using *plomb* in MATLAB. In order to ascertain any significant differences of physicochemical parameters between each individual spatial survey, multiple one-way analysis of variance (ANOVA) tests were conducted ($\alpha = 0.05$) in MATLAB. The seawater chemistry parameters obtained from discrete seawater samples were spatially interpolated for each survey using a cubic interpolation in MATLAB and superimposed on a georeferenced map of Heron Reef (Digital Globe Foundation).

In order to assess the influence of reef metabolism on biogeochemical parameters (i.e., TA, DIC, and DO), the difference between reef and offshore values were calculated and denoted dTA, dDIC, and dDO. The relative contribution from reef NCC and NCP was estimated using graphical vector analysis (Deffeyes 1965; Cyronak et al. 2018) and type II linear regressions in MATLAB (lsqfitma.m, http://www.mbari.org/staff/etp3/regress.htm) based on the assumption that NCC alters TA and DIC in a ratio of 2:1, while NCP has negligible influence on TA in coral reef environments (Smith and Key 1975; Smith and Kinsey

1978; Atkinson and Smith 1983; Chisholm and Gattuso 1991). Furthermore, changes in DIC owing to NCP only ($dDIC_{NCP}$) were compared to dDO for a rough approximation of the quotient of carbon to oxygen uptake and release during photosynthesis and respiration (Q) (Bolden et al. 2019). $dDIC_{NCP}$ was calculated according to the following expression, correcting for the contribution of NCC to changes in DIC:

$$dDIC_{NCP} = \left(dDIC - \frac{1}{2}(dTA)\right). \quad (1)$$

3 Results

3.1 Environmental Conditions

The tidal range at Heron Reef during our study was 1.61 ± 0.09 m (mean ± SD) (Fig. 2). At Station 2, there was a mean westward current of 0.11 ± 0.05 m s^{-1} with the strongest current speeds (0.22 m s^{-1}) observed during ebb close to low tide (Figs. 2 and 3). At high tide when the lagoonal seawater mixed with the adjacent ocean, average current speed was slower (~ 0.04 m s^{-1}) and lacked a dominant direction (Fig. 2). Station 1 was the shallowest site with an average depth of 0.63 ± 0.28 m, Station 2 was the deepest site with an average depth of 2.22 ± 0.60 m, and Station 3 had an average depth of 1.55 ± 0.72 m.

Sea surface temperature (SST) and salinity for all three stations had an average value of 23.1 ± 1.2 °C and 35.8 ± 0.1, respectively, throughout the deployment. SST varied primarily on a diurnal timescale, with the daily maximum temperature lagging midday maximum PAR by 3 h (Fig. 2). Daily minimum temperatures were observed just prior to sunrise and coincided with low tide. In addition to the diurnal trend, small variations in SST were also observed in association with the semidiurnal tidal cycle. There was no obvious daily trend observed for salinity, but salinity did gradually increase throughout the study from 35.7 to 35.9 (Fig. 2). The average DO and pH for the three stations were 195 ± 29 µmol kg^{-1} and 8.09 ± 0.04, respectively (Fig. 2). Similar to SST, DO and pH were dominated by diurnal variations at all three stations. Daily maximum DO and pH values were also observed lagging midday maximum PAR by 3 h with the highest maximum DO and pH values recorded on days with higher PAR (Fig. 2). The daily minimum DO and pH values were observed in the early morning right before sunrise (Fig. 2).

Although the general temporal trends in temperature, pH, and DO were similar at the three stations, the maximum, minimum, and the diel mean and range were often different between stations (Fig. 2, Table 2). Station 1, the shallowest station, experienced the greatest diel range in all parameters and typically experienced the highest and lowest temperature on a given day (Table 2). Station 1 also experienced the lowest pH and DO at night but had similar maximum values as Station 3 during the day. Station 2, the deepest station in the middle of the lagoon, experienced the smallest diel range in all parameters, while Station 3 experienced a diel range somewhere between Stations 1 and 2 (Fig. 2; Table 2). On several days, a distinct secondary maxima and minima were observed at Station 3 during flood tide. Chl *a* concentration was slightly elevated following sunset with an overall averaged value of 0.22 ± 0.05 µg L^{-1}.

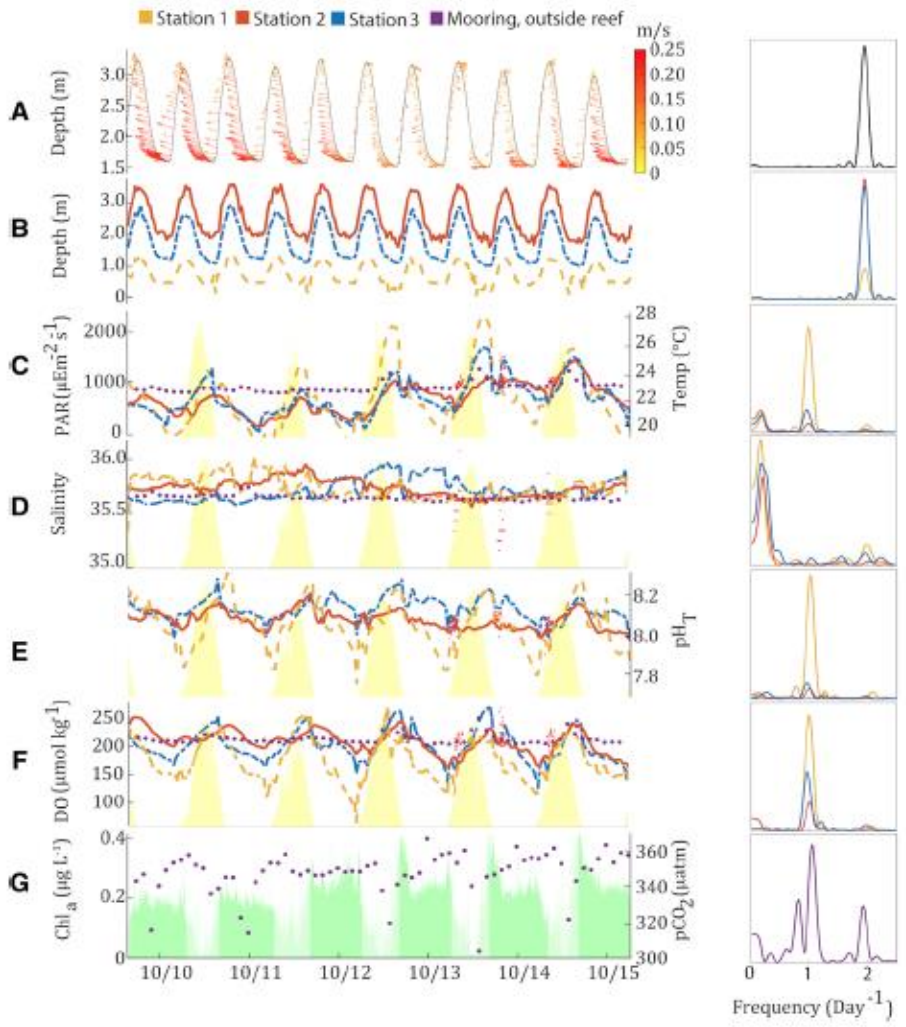

Fig. 2 **a** Depth integrated current velocity and direction (vectors) in relationship to sea surface height at Station 2. SeapHOx measurements every 30 min at Stations 1, 2, and 3 showing **b** depth, **c** sea surface temperature, **d** salinity, **e** pH_T, and **f** DO. Yellow shading shows PAR (**b**–**f**), and green shading shows Chl *a* (**g**) measured every 10 min at Station 2. Dark green shows nighttime values, while light green shows spurious daytime values (see main text). Red symbols in **b**–**f** indicate data from discrete samples. Purple symbols indicate measurements from the MAPCO2 mooring every 2 h outside the reef in the Wistari Channel. The right panels show a periodogram of the associated parameter and station from left panels of **a** depth from the ADCP, **b** depth from SeapHOx, **c** sea surface temperature, **d** salinity, **e** pH_T, **f** DO, and **g** pCO_2

From the MAPCO2 buoy outside of the reef, average diel temperature and salinity were 22.9 ± 0.3 °C and 35.7 ± 0.02, respectively. Diel signals in temperature were similar to inside the lagoon but with much lower variability (Fig. 2). The average pCO_2 outside the reef was 342 ± 11 µatm throughout the study and had a mean diel range of 42 ± 13 µatm with lower values during the day and higher values during the night (Fig. 2).

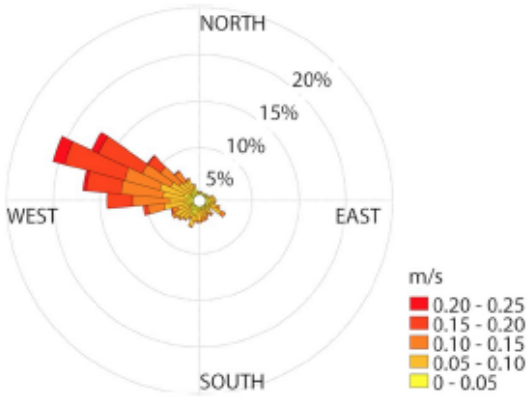

Fig. 3 Rose plot illustrating integrated water column velocity and flow direction at Station 2

3.2 Spatial Carbonate Chemistry Variability

Spatial gradients in physical (SST and S) and chemical (DO, DIC, TA, pH, Ω_a, and pCO_2) parameters were observed across the Heron Reef platform during both the morning and evening surveys (Figs. 4, 5, and 6) but were spotty and lacked uniform directional trends. In general, the spatial range of values for all parameters except for salinity was greater during the evening survey compared to the morning surveys (Table 3). Similarly, all parameters with the exception of salinity showed distinct covariance across the reef, although this was most prominent during the evening survey. Mean SST, DO, pH, and Ω_{ar} during the morning surveys were lower compared to the evening surveys, while DIC, TA, and pCO_2 were higher, with all parameters showing detectable differences between morning and evening (1-way ANOVA, $p<0.05$) except for TA (Tables 3, 4). There were no detectable differences between the two morning surveys for any of the parameters (1-way ANOVA, $p>0.05$).

During morning surveys, patches of colder seawater were observed near the center of the reef (Fig. 4). DO, DIC, and TA demonstrated similar patchiness as SST, with patches of lower DO corresponding to higher DIC and TA (Fig. 5). Calculated carbonate parameters (pH, Ω_{ar}, pCO_2) followed similar trends. Salinity showed a gradient across the reef with higher values on the eastern side compared to the western side with the strongest gradient observed on October 13 (Fig. 4).

During the evening survey, the spatial gradients were dominated by a water mass in the western part of the lagoon that had warmer SST, higher DO, pH, and Ω_{ar}, and lower DIC, TA, and pCO_2 compared to other parts of the lagoon (Fig. 6). A smaller south to north gradient in these parameters was also discernible, while variations in salinity across the reef were within the precision of the instrument.

Comparison of discrete measurements of pH and DO in the surface seawater during spatial surveys with the coincident means of autonomous measurements at the benthos (0.5–3.3 m depth) revealed a mean offset in pH of 0.00 ± 0.04 and DO of $+30 \pm 17$ µmol kg^{-1} for all survey data (Fig. 2). In addition to potential differences between the surface and the benthos, it should be reminded that the spatial surveys included multiple locations over a wider area than the autonomous sensors located at Stations 1, 2, and 3.

Table 2 Average diel mean (± SD) and diel range (± SD) of seawater temperature, salinity, DO, and pH from SeapHOx data across all three stations from October 9 to October 15, 2015

	Station 1				Station 2				Station 3			
	Diel mean	Range	Min	Max	Diel mean	Range	Min	Max	Diel mean	Range	Min	Max
Temp (°C)	23.1 ± 0.6	5.3 ± 1.4	20.0	27.9	23.1 ± 0.8	1.9 ± 0.4	21.5	25.2	23.1 ± 0.6	3.1 ± 0.5	21.1	26.0
Salinity	35.8 ± 0.1	0.3 ± 0.1	35.0	36.2	35.8 ± 0.1	0.2 ± 0.1	35.6	36.0	35.8 ± 0.1	0.2 ± 0.1	35.6	36.0
DO (μmol kg^{-1})	181 ± 6	137 ± 45	66	276	215 ± 10	59 ± 17	169	261	209 ± 8	111 ± 21	129	278
pH_T	8.05 ± 0.01	0.46 ± 0.03	7.79	8.31	8.08 ± 0.02	0.13 ± 0.08	7.98	8.20	8.14 ± 0.03	0.24 ± 0.04	8.00	8.30

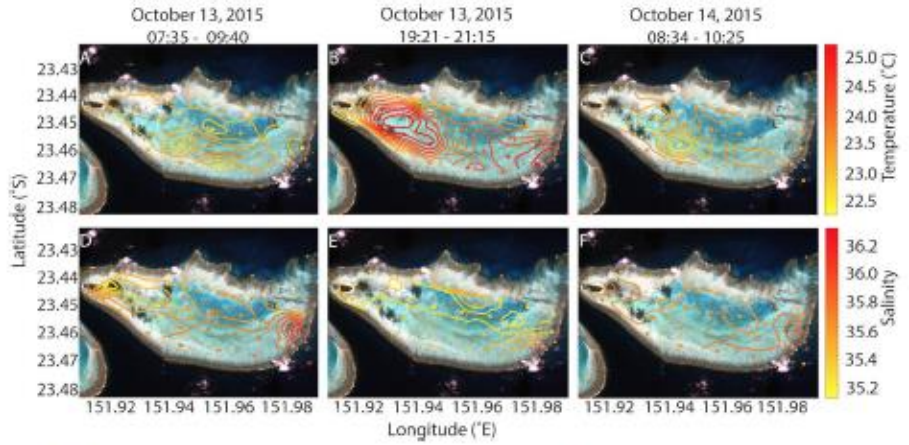

Fig. 4 Spatial distribution of sea surface temperature (**a**–**c**) and salinity (**d**–**f**) on Heron Reef in the morning (**a**, **d**) and evening (**b**, **e**) of October 13, 2015, and the morning (**c**, **f**) of October 14, 2015. Contour line intervals represent 0.3 °C and 0.1, respectively

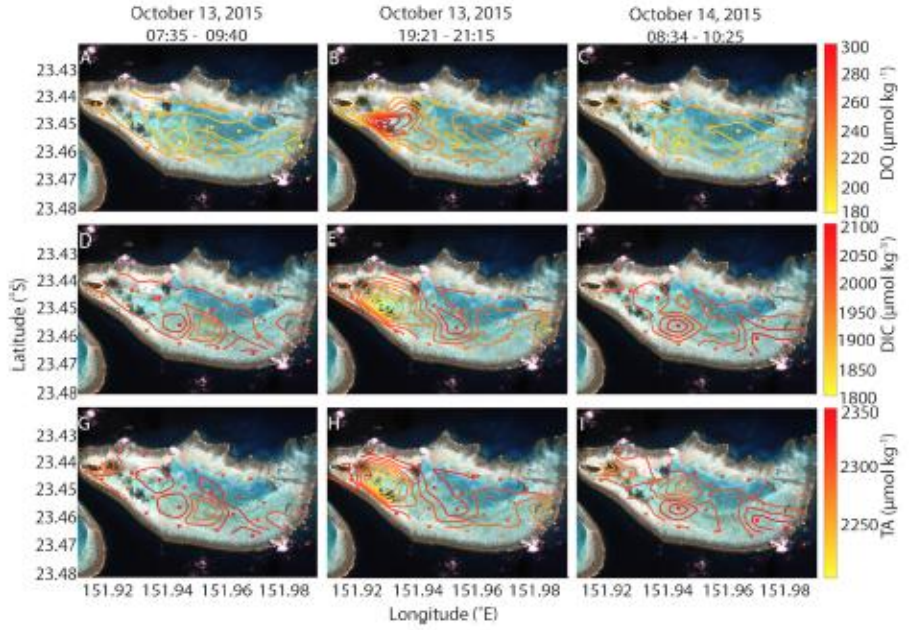

Fig. 5 Spatial distribution of DO (**a**–**c**), DIC (**d**–**f**) and TA (**g**–**i**) on Heron Reef in the morning (**a**, **d**, **g**) and evening (**b**, **e**, **h**) of October 13, 2015, and the morning (**c**, **f**, **i**) of October 14, 2015. Contour line intervals represent 12 μmol kg^{-1}, 30 μmol kg^{-1}, and 15 μmol kg^{-1}, respectively

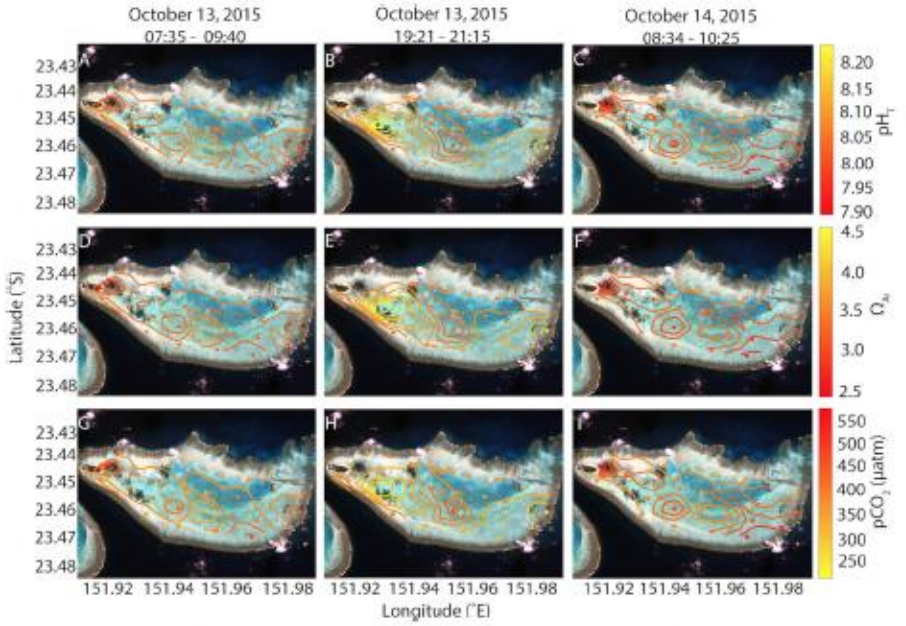

Fig. 6 Spatial distribution of pH_T (**a**–**c**), Ω_{ar} (**d**–**f**), and pCO_2 (**g**–**i**) on Heron Reef in the morning (**a**, **d**, **g**) and evening (**b**, **e**, **h**) of October 13, 2015, and the morning (**c**, **f**, **i**) of October 14, 2015. Contour line intervals represent 0.03 units, 0.2 units, and 40 µatm, respectively

3.3 Biogeochemical Modification of Seawater Chemistry on Heron Reef

TA, DIC, and DO measurements across the Heron Reef showed both depletion and repletion (i.e., both positive and negative dTA, dDIC, and dDO) compared to the seawater conditions outside of the lagoon for all surveys (Figs. 7 and 8). The observed anomalies were different between each survey with the evening survey having both the largest observations of TA depletion (net calcification) and repletion (net dissolution), but in different parts of the reef (Fig. 7a, b). Observations from the morning surveys predominantly showed depletion of DO and repletion of DIC_{NCP} (i.e., net respiration and heterotrophy) whereas the evening survey mostly revealed the opposite (i.e., net production and autotrophy), albeit with some exceptions (Fig. 7c, d). Instances of TA repletion were almost exclusively associated with net respiration while TA depletion was observed along conditions of either net respiration or net production. Despite measurable changes in dTA, dDIC, and dDO across Heron Reef, it was difficult to discern clear spatial patterns of depletion and repletion of these parameters. In general, during morning surveys, dDO and dDIC appeared to be negative and positive, respectively, in the interior of the lagoon while close to neutral or positive at the edges of the reef except for in the eastern part (Fig. 8). To some extent, the opposite was observed for the evening survey, but with greater patchiness. dTA was also very patchy and the clearest trend was observed during the evening survey with mostly positive values in the north transitioning to negative values in the southeastern part of the reef (Fig. 8).

Table 3 Mean (± SD), range, minimum (Min), and maximum (Max) values of physical and biogeochemical seawater properties for three spatial surveys conducted between October 13 and 14, 2015

	Oct 13, 15 07:35–09:40				Oct 13, 15 19:21–21:15				Oct 14, 15 08:34–10:25			
	Mean	Range	Min	Max	Mean	Range	Min	Max	Mean	Range	Min	Max
Temp (°C)	23.1 ± 0.3	1.3	22.4	23.7	23.9 ± 0.8	2.4	22.8	25.2	23.3 ± 0.3	1.4	22.2	23.6
Salinity	35.6 ± 0.2	1.1	35.2	36.3	35.3 ± 0.1	0.6	35.2	35.8	35.6 ± 0.1	0.4	35.5	35.9
DO (μmol kg^{-1})	214 ± 13	48	185	233	233 ± 23	92	206	298	219 ± 14	48	191	239
DIC (μmol kg^{-1})	2013 ± 27	151	1930	2081	1970 ± 57	201	1801	2062	2017 ± 31	114	1975	2089
TA (μmol kg^{-1})	2313 ± 13	69	2277	2346	2299 ± 29	111	2219	2330	2306 ± 20	102	2241	2343
pH_T	8.06 ± 0.03	0.15	7.98	8.13	8.09 ± 0.04	0.24	7.99	8.23	8.03 ± 0.05	0.19	7.90	8.09
Ω_{ar}	3.34 ± 0.19	0.96	2.84	3.80	3.63 ± 0.30	1.47	3.03	4.50	3.23 ± 0.28	1.14	2.44	3.58
pCO_2 (μatm)	377 ± 35	162	300	462	340 ± 46	242	217	459	404 ± 56	219	344	563

Table 4 One-way analysis of variance (ANOVA) showing difference between means (Δ mean) of Surveys 1, 2, and 3 and associated lower and upper 95% confidence interval alongside *p*-values for each parameter

	Survey 1–Survey 2				Survey 1–Survey 3				Survey 2–Survey 3			
	Δ mean	Lower 95%	Upper 95%	*p*	Δ mean	Lower 95%	Upper 95%	*p*	Δ mean	Lower 95%	Upper 95%	*p*
Temp (°C)	− 0.8	− 1.1	− 0.5	< 0.001	− 0.2	− 0.5	0.1	0.27	0.6	0.3	0.9	< 0.001
Salinity	0.3	0.2	0.42	< 0.001	0.0	− 0.1	0.1	0.96	− 0.3	− 0.4	− 0.2	< 0.001
DO (µmol kg^{-1})	− 19	− 29	− 8	< 0.001	− 4	− 15	6	0.58	14	4	25	0.005
DIC (µmol kg^{-1})	43	18	68	< 0.001	− 4	− 29	21	0.94	− 47	− 72	− 21	< 0.001
TA (µmol kg^{-1})	14	1	28	0.003	7	− 6	20	0.44	− 7	− 21	6	0.39
pH_T	− 0.03	− 0.06	− 0.01	< 0.001	0.02	0.00	0.05	0.06	0.06	0.03	0.08	< 0.001
Ω_{ar}	− 0.29	− 0.45	− 0.12	< 0.001	0.12	− 0.05	0.28	0.21	0.40	0.24	0.57	< 0.001
pCO_2 (µatm)	36	8	65	0.002	− 26	− 55	2	0.08	− 63	− 91	− 34	< 0.001

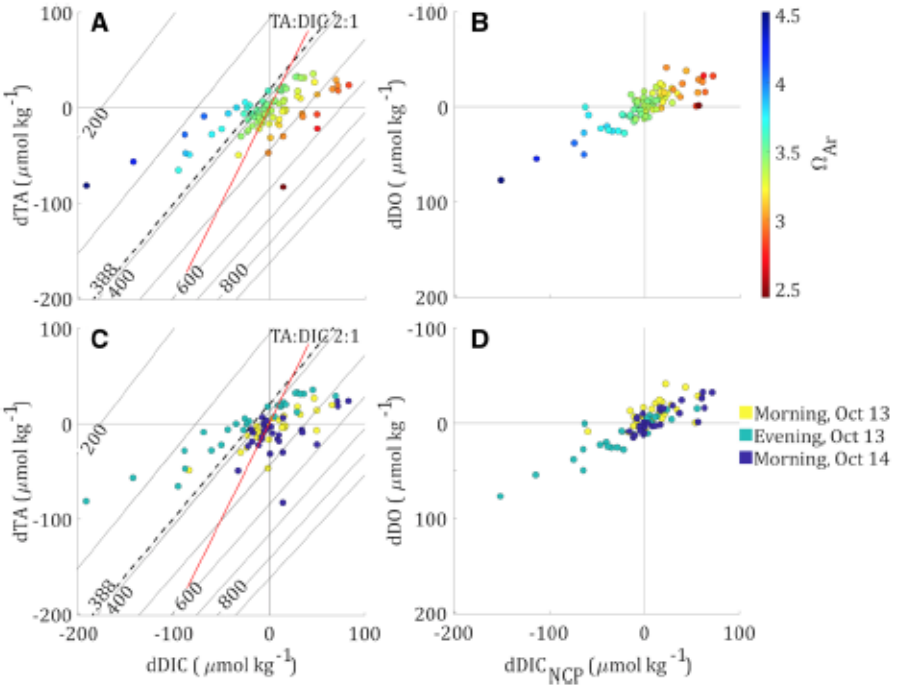

Fig. 7 Property-property plots of the difference between reef and offshore salinity normalized properties; (**a**, **c**) dTA vs. dDIC and (**b**, **d**) dDO vs. $dDIC_{NCP}$ with colors in (**a**, **b**) indicating aragonite saturation state and in (**c**, **d**) showing each spatial survey. Black contour lines show pCO_2 with a contour interval of 100 uatm. The dashed line shows the average pCO_2 of the air from the MAPCO2 buoy. Type II linear regressions of dTA vs. dDIC and for dDO vs. $dDIC_{NCP}$ were: $dTA = 0.45dDIC - 4.65$ ($R^2 = 0.50$) and $dDO = 0.49dDIC_{NCP} - 0.31$ ($R^2 = 0.75$), respectively. Red line demonstrates the TA/DIC 2:1 stoichiometric ratio

Changes in seawater Ω_{ar} and pCO_2 appeared to mostly track changes resulting from photosynthesis or respiration as inferred from dDO and $dDIC_{NCP}$ trends (Fig. 7b). The highest Ω_{ar} and lowest pCO_2 were associated with the most positive values of dDO and most negative values of $dDIC_{NCP}$, while the lowest Ω_{ar} and highest pCO_2 were largely associated with more negative values of dDO and more positive values of $dDIC_{NCP}$ (Fig. 7c). However, the minimum and maximum of Ω_{ar} and pCO_2, respectively, coincided with a combination of repletion in DIC_{NCP} (net respiration) and depletion in TA (net calcification) (Fig. 7a, b). Linear regression (type II) of all the dTA-dDIC data revealed a slope of 0.45 ($R^2 = 0.50$), further confirming that organic carbon cycling (NCP) had a greater influence on the variability of Ω_{ar}, pH, and pCO_2 than inorganic carbon cycling (NCC). The slope of individual surveys ranged from 0.41 to 0.52. The ratio of DO to DIC_{NCP} changes revealed an overall slope of − 0.49 ($R^2 = 0.75$) with individual surveys ranging from − 0.45 to − 0.51.

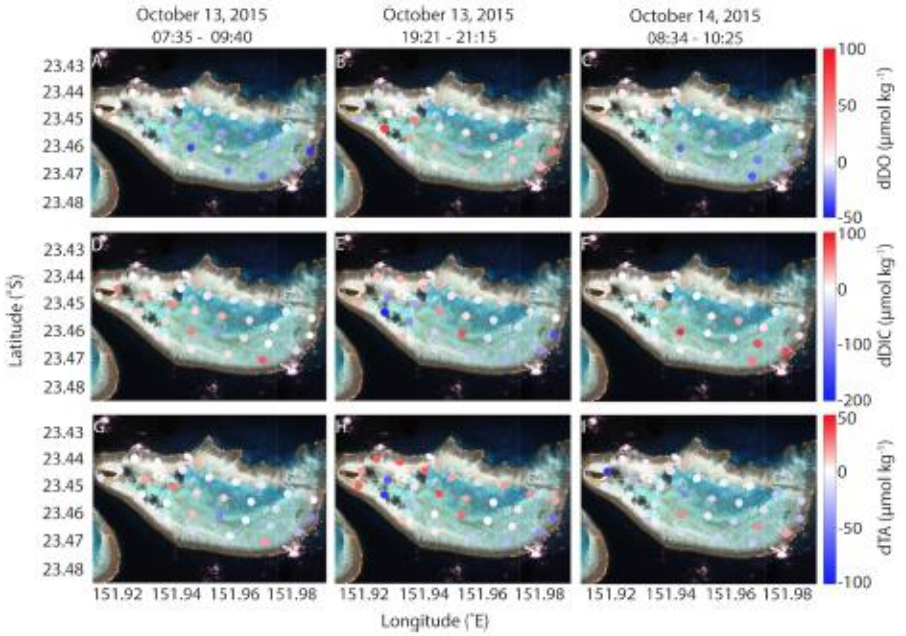

Fig. 8 Colored scatter dots of dDO (**a**–**c**), dDIC (**d**–**f**), and dTA (**g**–**i**) on Heron Reef in the morning (**a**, **d**, **g**) and evening (**b**, **e**, **h**) of October 13, 2015, and the morning (**c**, **f**, **i**) of October 14, 2015. Note that the scale of the colorbar differs between parameters

4 Discussion

4.1 Natural Variability of Seawater Carbonate Chemistry Across Heron Reef

This study showed that the temporal and spatial variabilities of seawater physical and chemical parameters at Heron Reef were a result of a combination of the diel light cycle, net community metabolism, and the local hydrodynamics. The hydrodynamics were strongly influenced by the local reef geomorphology and tidal cycle, which resulted in temporal isolation of the reef platform from the surrounding ocean during low tide. As a result, ocean water spilled over the reef crest during flood tide and drained in the western end during ebb tide. These features were reflected in the higher flow speeds and consistent flow direction observed during tidal isolation and the slower flow speeds and variable directions observed during flood tides (Fig. 2a) but led to some unexpected temporal and spatial variability in biogeochemical parameters. The magnitude of variability was also strongly influenced by depth, which has been highlighted in several other studies (Falter et al. 2013; Page et al. 2019; Cyronak et al. 2020).

The primary frequency of variability in temperature, DO, and pH was clearly linked to the diel light cycle. The observed lag (~ 3 h) between extremes in these parameters and peak insolation was possibly also extended by the afternoon low tide amplifying the effects of solar heating and reef metabolism on the associated shallower and smaller seawater volume. The secondary, smaller variations in these parameters coincided with the semi-diurnal tidal frequencies at all stations and was particularly prominent

at Station 3 (Fig. 2). This was likely due to its close proximity to the reef crest, which amplified the contrast between seawater conditions developed during isolation at low tide and the properties of the ocean water flowing onto the reef during rising tides. An interesting diel signal was evident in the Chl *a* data, but it was in all likelihood spurious during daytime as discussed in the Methods section (Fig. 2). Nonetheless, the nighttime mean Chl *a* content was similar to previously observed values on Heron Reef (Steven et al. 1998).

Observed differences in the mean values and daily ranges of seawater temperature, DO, and pH between the autonomous sensor stations were attributed to water depth, their location in relation to the prevalent flow trajectories, and possibly the benthic community composition in the case of pH and DO variability. Most notably, the mean daily range in seawater temperature, pH, and DO for each sensor station was negatively correlated with the mean depth of the overlying water column, with the largest daily range observed alongside the shallowest depth and vice versa (Table 2, Figs. 2, 4, 5, 6). This follows the established effects of increased biomass to seawater volume ratio (Falter et al. 2013; Koweek et al. 2015a, b; Takeshita et al. 2018; Page et al. 2019; Cyronak et al. 2020) and the increased contact time between seawater and the benthos due to increased bottom friction in shallower waters (Gourlay and Hacker 2008; Falter et al. 2013; Mongin and Baird 2014). However, in the present case, the flow trajectory likely also played an important role on the observed daily range and would be most prominent at Station 1 due to the location in the western part of the reef (i.e., downstream during ebb tide), which likely tracked the cumulative biogeochemical modifications occurring on the reef to a larger extent than the other stations (cf. Mongin and Baird 2014). Nonetheless, because this was also the shallowest station, it is difficult to discern the local metabolic influence from the chemical memory originating upstream.

The diel signal and the underlying drivers of variability in the sensor data at Stations 1–3 were less apparent in the spatial boat surveys. This was partly due to the fact that spatial surveys were restricted to a minimum tidal depth of + 1.2 m relative to the mean lower low water (MLLW) due to navigational safety, and thus, only took place during high tides in the morning (~ 07:30) and in the evening (~ 19:20). This prevented us from characterizing the spatial variability during the local extrema anticipated during low tide in the mid-afternoon and at night before sunrise (e.g., Shamberger et al. 2011; Albright et al. 2015; Page et al. 2017; Takeshita et al. 2018). Furthermore, as a result of the tidal restriction on the spatial surveys, these results reflected gradients resulting from the metabolic imprint of the previous low tide, and potentially even older seawater (Mongin and Baird 2014), combined with ocean water flowing over the reef with the rising tide. Consequently, during morning spatial surveys, parts of the platform revealed the remnant metabolic signal from the previous low tide at night (i.e., low SST, DO, pH) while parts of the lagoon in the evening revealed the remnants of the daytime signal (i.e., high SST, DO, pH). As a result, the evening spatial survey had higher mean SST, pH, DO, and Ω_{ar} and lower DIC, TA, and pCO_2 compared to morning surveys despite the evening surveys being conducted in full darkness ~ 1.5 h after sunset (Table 3). A larger range of values were also observed for all parameters during the evening spatial survey, which was attributed to a greater influence of daytime production on seawater chemistry compared to the influence of nighttime respiration (Table 3; Page et al. 2016, 2019).

Compared to spatial surveys in other reef environments showing distinct spatial distribution of gradients in carbonate chemistry (e.g., offshore to inshore; Andersson et al. 2014; Courtney et al. 2018; Page et al. 2019), the patchy spatial distribution of carbonate chemistry at Heron Reef showed little directional uniformity at the scale of the whole reef. This

was most likely an effect of the reef morphology, wherein the temporal isolation of the lagoon during low tide and subsequent flooding of the lagoon during rising tides coincided with the timing of the spatial surveys. The incoming tide pushed the oceanic water across the shallow reef crest and into the deeper lagoon, entraining portions of the lagoon water (Gourlay and Hacker 2008; Mongin and Baird 2014). As a result, patches of older seawater were encountered in different parts of the reef during the spatial surveys. This was most prominent during the evening survey and reflected by the elevated SST, DO, pH, and Ω_{ar} and reduced DIC and TA in the lagoon near the western end of the reef (Figs. 4, 5, 6).

Because of the complex flow dynamics coincident with the spatial surveys, it is challenging to assess the relative influence of different benthic communities on the overlying seawater biogeochemistry from these data. Daytime enhanced biological uptake of DIC and TA would be expected for the coral-algal dominated reef flat communities relative to the microalgal mat and sand dominated lagoon areas (Fig. 1 c) (e.g., Kline et al. 2012; Mongin and Baird 2014; Albright et al. 2015; Kline et al. 2015; Page et al. 2019; Cyronak et al. 2020; Brown et al. 2020; but see also discussion in Page et al. 2017) whereas the opposite would be expected at night owing to predominantly metabolic $CaCO_3$ dissolution within the sand areas (Santos et al. 2011; Cyronak et al. 2013a, b; McMahon et al. 2013; Stoltenberg et al. 2021). Despite distinct observations of both TA and DIC depletion and repletion in different parts of the reef (Fig. 8), the absence of specific flow trajectories and water residence time associated with these changes prohibit our ability to relate these changes to specific habitats on the reef. Instead, the most prominent biogeochemical feature (i.e., the low DIC and TA, high DO, pH, and Ω_{ar}) characterized in the western part of the reef during the evening survey coincided with shallow depths and long residence times as modeled by Mongin and Baird (2014) during conditions of rising tide and low wind conditions (the spatial surveys occurred in no wind (Oct. 13) to very light wind (Oct. 14) conditions). The longer residence time would allow for greater biological modification of the seawater although the net change in pH and Ω_{ar} would be dependent on the balance of photosynthesis/respiration and calcification/dissolution (Mongin and Baird 2014). However, opposed to the results of Mongin and Baird (2014) who projected declines in seawater Ω_{ar} and pH as a function of age in the western part of the reef (cf. Figure 7c, d in Mongin and Baird 2014), we observed the opposite with an increase in Ω_{ar} and pH (Fig. 6). Instead, our evening survey more closely matched the Mongin and Baird (2014) base model results observed during the day (cf. Figure 9a in Mongin and Baird 2014), but there could be many factors contributing to this divergence including a simple mismatch between the timing of the two studies (and the timing and amplitude of low and high tide) or the parameterization of calcification to organic carbon production in the model. Importantly, the two studies were conducted at different times of the year (January vs. October) with potential implications for seasonally varying relative importance of biogeochemical processes (see Stoltenberg et al. 2020, 2021). Further modeling efforts similar to Mongin and Baird (2014) utilizing the spatial surveys from this study as validation may therefore be necessary to improve our understanding of the patterns and processes associated with Heron Reef platform biogeochemical processes. Such efforts should be accompanied by additional spatial biogeochemical observations at different tidal configurations, seasons, and during low-tide conditions.

4.2 Importance of Biogeochemical Processes on Heron Reef Carbonate Chemistry

The imprint of biogeochemical processes on seawater chemistry on Heron Reef was evident from both the autonomous sensor measurements and the discrete samples from spatial surveys. Compared to the diel ranges of DO (30 ± 13 µmol kg^{-1}) and pCO_2 (42 ± 13 µatm) measured at the MAPCO2 mooring outside the reef, the diel and spatial ranges of DO (diel range = 137 ± 45 µmol kg^{-1} and spatial range = 92 µmol kg^{-1}) and pCO_2 (spatial range = 242 µatm) were much greater inside the reef. Similarly, the depletion and repletion of reef TA, DIC, and DO relative to off-reef conditions explicitly showed the influence of NCC and NCP. The coincident observations of conditions indicating net calcification (− dTA) and net $CaCO_3$ dissolution (+ dTA), as well as net organic carbon production (− $dDIC_{NCP}$; + dDO) and net respiration (+ $dDIC_{NCP}$; − dDO) in different parts of the reef during all surveys were probably partly due to differential habitat characteristics (Figs. 7 and 8), but were also a result of the entrainment of older seawater as previously discussed and potentially mixing of pore water (high DIC and low DO) into the water column. The fact that net $CaCO_3$ dissolution was almost exclusively associated with net respiration and heterotrophy support the notion that dissolution on coral reefs is mainly driven by decomposition of organic matter (Morse and Mackenzie 1990; Andersson 2015). In contrast, net calcification signals were observed in the seawater with either positive or negative NCP signatures, although the former combination was more common than the latter. Temporal co-occurrences of net calcification and net respiration in reef environments are not unusual and have been reported widely (e.g., Watanabe et al. 2006; Bates et al. 2010; Yeakel et al. 2015). Typically, it arises from a separation in time (e.g., night vs. day) and/or space (e.g., fore reef vs. back reef) between net respiration and net production, while net calcification proceeds due to high abundance of calcifiers, low dissolution rates and/or dissolution thresholds that have not been exceeded (McMahon et al. 2018; Takeshita et al. 2018; Kessler et al. 2020). It may also occur in response to external input of organic matter from either terrestrial or oceanic sources that may drive coral heterotrophy and increased calcification (Suzuki and Kawahata 2003; Yeakel et al. 2015; DeCarlo et al. 2015, 2017). In regard to Heron Reef, McMahon et al. (2013) and Stoltenberg et al. (2021) reported occurrences of net dissolution at slack tide in the western part at $\Omega_{ar} > 3$, which agrees with the present observations (Fig. 7). However, this dissolution signal likely originated from within the pore water–sediment system where Ω_{ar} is substantially lower than in the water column (Walter and Morse 1985; Kessler et al. 2020). Stoltenberg et al. (2021) suggested that up to 78% of the NCC signal at night on Heron Reef comes from within the pore water–sediment system. In the present study, morning surveys conducted in full daylight predominantly revealed seawater carbonate chemistry reflecting net heterotrophic conditions, while the evening survey conducted in full darkness predominantly revealed net autotrophic conditions. We suggest that these counterintuitive results were due to the entrainment of older seawater from the previous low tides at night and afternoon, respectively, which also explain the lack of uniform spatial patterns across the reef. It should also be noted that the observed biogeochemical signals are relative to the adjacent source water and reflect the net of all physical and biogeochemical modifications that occur on the reef platform including influences from the sediment pore water system.

The overall slope of dTA-dDIC (0.45; $R^2 = 0.50$) showed that the variability in seawater Ω_{ar}, pH, and pCO_2 on Heron Reef was primarily driven by net organic carbon production (i.e., NCP) relative to net inorganic carbon production (i.e., NCC), which agrees with previous studies (Kline et al. 2012; McMahon et al. 2013; Albright et al. 2015; Kline et al. 2015). This was also evident from assessment of net production/respiration alone, which showed strong

covariance with seawater Ω_{ar} as a function of the extent of dDO and $dDIC_{NCP}$ anomalies. Notably the slope of dDO and $dDIC_{NCP}$ equaled − 0.49 (R^2=0.75), which was substantially different from the idealized oxygen/carbon quotient in reefs close to − 1 (Kinsey 1985; Falter et al. 2012). Although recent research has suggested that the quotient may be more variable than previously assumed (Bolden et al. 2019), not accounting for gas exchange of oxygen (loss during autotrophy; uptake during heterotrophy) would underestimate the slope of dDO and $dDIC_{NCP}$. However, given the calm wind-conditions during the sampling surveys this effect would be rather small. Other additional mechanisms responsible for the observed $dDO/dDIC_{NCP}$ ratio may in part be due to mixing with pore water high in DIC and low oxygen content or the capture of oxygen bubbles on different substrates as hypothesized by Bolden et al. (2019).

5 Concluding Remarks

It is evident from this study that whole reef spatial surveys of carbonate chemistry add additional perspectives to the drivers of spatiotemporal variability on coral reefs than those revealed by autonomous sensors and modeling output alone. Ideally, these different research approaches should be conducted in parallel with the goal of refining model parameterization to the extent numerical simulations can reproduce physical and chemical parameters in both space and time with a high degree of confidence. Spatial surveys and/or high-resolution arrays of autonomous sensors may be particularly valuable in this context but are limited by factors such as navigational restrictions and cost. The current spatial data were clearly limited by the restriction to high tide conditions, which consequently omitted the most extreme environmental conditions anticipated during low tide. These extreme conditions may be particularly relevant in evaluating physiological stress and/or tolerance of reef organisms, while spatial heterogeneity characterized during such extremes may be important for identifying potential areas of refuge in the context of heat stress events and future acidification (van Hooidonk et al. 2013; Palumbi et al. 2014; Kapsenberg and Cyronak 2019). Several studies have suggested that corals exposed to large fluctuations in seawater temperature and pH experience enhanced resilience and tolerance to ocean warming and acidification compared to corals exposed to more stable conditions (e.g., Camp et al. 2017; Enochs et al. 2018; Safaie et al. 2018). However, areas of large fluctuations are more likely to experience unusual extremes that could exceed physiological thresholds, so it is important to consider organisms' resilience and tolerance in the context of both chronic and acute perturbations.

Similar to other coral reef studies (e.g., Shamberger et al. 2011; Lowe and Falter 2015; Eyre et al. 2018; Page et al. 2019; Cyronak et al. 2020), the present study showed that different portions of Heron Reef experienced varied levels of spatial and temporal means and ranges of physiochemical properties, which were controlled by depth, geomorphology, benthic community composition, seawater flow trajectory, and residence times. In a future high-CO_2 world some of these controls may change due to sea level rise (Lowe et al. 2016), changes in community composition (Andersson et al. 2014), species-specific interactions (Brown et al. 2018), and potentially intensified atmospheric currents (Zhang et al. 2013; England et al. 2014) that could modify the spatiotemporal patterns and variability of seawater physiochemical properties.

In the context of targeting observations during extreme environmental conditions, it is important to recognize that most spatial investigations are restricted to daytime conditions due to navigational constraints in the dark, which has biased conclusions toward

daytime metabolic performance of coral reefs (Suzuki and Kawahata 2003; Watanabe et al. 2006; Andersson et al. 2014; Courtney et al. 2018; Shamberger et al. 2018; Page et al. 2019). This study was the first time we were able to complete a reef scale survey in full darkness, but ironically this survey mostly revealed the remnant daytime metabolic signal due to the specific properties of Heron Reef. However, the physical and chemical properties of Heron Reef are not unique and there are probably many reefs with comparable properties that may undergo similar controls of the spatiotemporal variability in physical and chemical parameters (Rees et al. 2003; McKinney 2009). At the same time, it is important to recognize that the spatiotemporal variability and gradients observed at Heron Reef are different from what has been reported in previous spatial surveys (Andersson et al. 2014; Courtney et al. 2018; Page et al. 2019), highlighting the importance of assessing each reef independently. Future studies at Heron Reef should ideally target reef scale sampling during extreme conditions associated with the daily light and tidal cycles to ascertain the full natural spatial and temporal variability of seawater carbonate chemistry and ecosystem functioning of coral reef ecosystems.

Acknowledgements We would like to thank the Heron Island Research Station staff for their help with facilitating this project. We are also grateful for the constructive feedback by two anonymous reviewers and the associate editor that significantly improved this manuscript. The research was supported by funding from NSF OCE 12-55042 (AJA) and Australian Council Discovery Grant 150102092 (BDE and AJA).

References

Albright R, Langdon C, Anthony K (2013) Dynamics of seawater carbonate chemistry, production, and calcification of a coral reef flat, central Great Barrier Reef. Biogeosci Discuss 10(5):7641–7676

Albright R, Benthuysen J, Cantin N, Caldeira K, Anthony K (2015) Coral reef metabolism and carbon chemistry dynamics of a coral reef flat. Geophys Res Lett 42(10):3980–3988

Albright R, Takeshita Y, Koweek DA, Ninokawa A, Wolfe K, Rivlin T, Nebuchina Y, Young J, Caldeira K (2018) Carbon dioxide addition to coral reef waters suppresses net community calcification. Nature 555(7697):516–519

Allen Coral Atlas (2020) Imagery, maps and monitoring of the world's tropical coral reefs. https://doi.org/10.5281/zenodo.3833242

Andersson A, Kuffner I, Mackenzie F, Jokiel P, Rodgers K, Tan A (2009) Net loss of $CaCO_3$ from coral reef communities due to human induced seawater acidification. Biogeosci Discuss 6(1)

Andersson A, Mackenzie F (2012) Revisiting four scientific debates in ocean acidification research. Biogeosciences 9(3):893–905

Andersson AJ, Gledhill D (2013) Ocean acidification and coral reefs: effects on breakdown, dissolution, and net ecosystem calcification. Ann Rev Mar Sci 5:321–348

Andersson AJ, Yeakel KL, Bates NR, De Putron SJ (2014) Partial offsets in ocean acidification from changing coral reef biogeochemistry. Nat Clim Chang 4(1):56–61

Andersson AJ (2015) A fundamental paradigm for coral reef carbonate sediment dissolution. Front Mar Sci 2:52

Anthony KR, Kline DI, Diaz-Pulido G, Dove S, Hoegh-Guldberg O (2008) Ocean acidification causes bleaching and productivity loss in coral reef builders. Proc Natl Acad Sci 105(45):17442–17446

Anthony KR, Kleypas JA, Gattuso JP (2011) Coral reefs modify their seawater carbon chemistry–implications for impacts of ocean acidification. Glob Change Biol 17(12):3655–3666

Anthony KR, Diaz-Pulido G, Verlinden N, Tilbrook B, Andersson A (2013) Benthic buffers and boosters of ocean acidification on coral reefs. Biogeosci Discuss 10(2):4897–4909

Atkinson MJ, Smith SV (1983) C: N: P ratios of benthic marine plants 1. Limnol Oceanogr 28(3):568–574

Bates N, Amat A, Andersson A (2010) Feedbacks and responses of coral calcification on the Bermuda reef system to seasonal changes in biological processes and ocean acidification. Biogeosciences 7(8):2509–2530

Bell P (1992) Eutrophication and coral reefs—some examples in the Great Barrier Reef lagoon. Water Res 26(5):553–568

Bolden IW, Sachs JP, Gagnon AC (2019) Temporally-variable productivity quotients on a coral atoll: implications for estimates of reef metabolism. Mar Chem 217:103707
Brander KM (2007) Global fish production and climate change. Proc Natl Acad Sci 104(50):19709–19714
Bresnahan PJ Jr, Martz TR, Takeshita Y, Johnson KS, LaShomb M (2014) Best practices for autonomous measurement of seawater pH with the Honeywell Durafet. Methods Oceanogr 9:44–60
Brown KT, Bender-Champ D, Kubicek A, van der Zande R, Achlatis M, Hoegh-Guldberg O, Dove SG (2018) The dynamics of coral-algal interactions in space and time on the southern Great Barrier Reef. Front Mar Sci 5:181
Brown KT, Bender-Champ D, Achlatis M, van Der Zande RM, Kubicek A, Martin SB, Castro-Sanguino C, Dove SG, Hoegh-Guldberg O (2020) Habitat-specific biogenic production and erosion influences net framework and sediment coral reef carbonate budgets. Limnol Oceanogr 66:349–365
Bruno JF, Stachowicz JJ, Bertness MD (2003) Inclusion of facilitation into ecological theory. Trends Ecol Evol 18(3):119–125
Camp EF, Nitschke MR, Rodolfo-Metalpa R, Houlbreque F, Gardner SG, Smith DJ, Zampighi M, Suggett DJ (2017) Reef-building corals thrive within hot-acidified and deoxygenated waters. Sci Rep 7(1):1–9
Carilli JE, Norris RD, Black BA, Walsh SM, McField M (2009) Local stressors reduce coral resilience to bleaching. PLoS ONE 4(7):e6324
Carpenter KE, Abrar M, Aeby G, Aronson RB, Banks S, Bruckner A, Chiriboga A, Cortés J, Delbeek JC, DeVantier L (2008) One-third of reef-building corals face elevated extinction risk from climate change and local impacts. Science 321(5888):560–563
Chan NC, Connolly SR (2013) Sensitivity of coral calcification to ocean acidification: a meta-analysis. Glob Change Biol 19(1):282–290
Chisholm JR, Gattuso JP (1991) Validation of the alkalinity anomaly technique for investigating calcification of photosynthesis in coral reef communities. Limnol Oceanogr 36(6):1232–1239
Comeau S, Carpenter R, Edmunds P (2013) Coral reef calcifiers buffer their response to ocean acidification using both bicarbonate and carbonate. Proc R Soc B Biol Sci 280(1753):20122374
Costanza R, d'Arge R, De Groot R, Farber S, Grasso M, Hannon B, Limburg K, Naeem S, O'neill RV, Paruelo J (1997) The value of the world's ecosystem services and natural capital. Nature 387(6630):253–260
Costanza R, De Groot R, Sutton P, Van der Ploeg S, Anderson SJ, Kubiszewski I, Farber S, Turner RK (2014) Changes in the global value of ecosystem services. Glob Environ Chang 26:152–158
Courtney T, De Carlo E, Page H, Bahr K, Barro A, Howins N, Tabata R, Terlouw G, Rodgers K, Andersson A (2018) Recovery of reef-scale calcification following a bleaching event in Kāne'ohe Bay, Hawai'i. Limnol Oceanogr Lett 3(1):1–9
Crossland C, Hatcher B, Smith S (1991) Role of coral reefs in global ocean production. Coral reefs 10(2):55–64
Cyronak T, Santos IR, Eyre BD (2013a) Permeable coral reef sediment dissolution driven by elevated pCO_2 and pore water advection. Geophysical Research Letters 40(18):4876–4881
Cyronak T, Santos IR, McMahon A, Eyre BD (2013b) Carbon cycling hysteresis in permeable carbonate sands over a diel cycle: implications for ocean acidification. Limnology and Oceanography 58(1):131–143
Cyronak T, Schulz KG, Santos IR, Eyre BD (2014a) Enhanced acidification of global coral reefs driven by regional biogeochemical feedbacks. Geophys Res Lett 41(15):5538–5546
Cyronak T, Santos IR, Erler DV, Maher DT, Eyre BD (2014b) Drivers of pCO_2 variability in two contrasting coral reef lagoons: The influence of submarine groundwater discharge. Global Biogeochem Cycles 28(4):398–414
Cyronak T, Andersson AJ, Langdon C, Albright R, Bates NR, Caldeira K, Carlton R, Corredor JE, Dunbar RB, Enochs I (2018) Taking the metabolic pulse of the world's coral reefs. PLoS ONE 13(1):e0190872
Cyronak T, Takeshita Y, Courtney TA, DeCarlo EH, Eyre BD, Kline DI, Martz T, Page H, Price NN, Smith J (2020) Diel temperature and pH variability scale with depth across diverse coral reef habitats. Limnol Oceanogr Lett 5(2):193–203
De'ath G, Lough JM, Fabricius KE (2009) Declining coral calcification on the Great Barrier Reef. Science 323(5910):116–119
DeCarlo TM, Karnauskas KB, Davis KA, Wong GT (2015) Climate modulates internal wave activity in the Northern South China Sea. Geophys Res Lett 42(3):831–838
DeCarlo TM, Cohen AL, Wong GT, Shiah FK, Lentz SJ, Davis KA, Shamberger KE, Lohmann P (2017) Community production modulates coral reef pH and the sensitivity of ecosystem calcification to ocean acidification. J Geophys Res Oceans 122(1):745–761

Deffeyes KS (1965) Carbonate equilibria: a graphic and algebraic approach 1. Limnol Oceanogr 10(3):412–426
Dickson A, Millero FJ (1987) A comparison of the equilibrium constants for the dissociation of carbonic acid in seawater media. Deep Sea Res Part A Oceanogr Res Pap 34(10):1733–1743
Dickson AG (1990) Thermodynamics of the dissociation of boric acid in synthetic seawater from 273.15 to 318.15 K. Deep Sea Res Part A Oceanogr Res Pap 37(5):755–766
Dickson AG, Sabine CL, Christian JR (2007) Guide to best practices for ocean CO_2 measurements. North Pacific Marine Science Organization
Dove SG, Kline DI, Pantos O, Angly FE, Tyson GW, Hoegh-Guldberg O (2013) Future reef decalcification under a business-as-usual CO_2 emission scenario. Proc Natl Acad Sci 110(38):15342–15347
Edmunds PJ, Comeau S, Lantz C, Andersson A, Briggs C, Cohen A, Gattuso J-P, Grady JM, Gross K, Johnson M (2016) Integrating the effects of ocean acidification across functional scales on tropical coral reefs. Bioscience 66(5):350–362
England MH, McGregor S, Spence P, Meehl GA, Timmermann A, Cai W, Gupta AS, McPhaden MJ, Purich A, Santoso A (2014) Recent intensification of wind-driven circulation in the Pacific and the ongoing warming hiatus. Nat Clim Chang 3:222–227
Enochs IC, Manzello DP, Jones PJ, Aguilar C, Cohen K, Valentino L, Schopmeyer S, Kolodziej G, Jankulak M, Lirman D (2018) The influence of diel carbonate chemistry fluctuations on the calcification rate of Acropora cervicornis under present day and future acidification conditions. J Exp Mar Biol Ecol 506:135–143
Eyre BD, Andersson AJ, Cyronak T (2014) Benthic coral reef calcium carbonate dissolution in an acidifying ocean. Nat Clim Chang 4(11):969–976
Eyre BD, Cyronak T, Drupp P, De Carlo EH, Sachs JP, Andersson AJ (2018) Coral reefs will transition to net dissolving before end of century. Science 359(6378):908–911
Falter JL, Lowe RJ, Atkinson MJ, Cuet P (2012) Seasonal coupling and de-coupling of net calcification rates from coral reef metabolism and carbonate chemistry at Ningaloo Reef, Western Australia. J Geophys Res Oceans 117(C5)
Falter JL, Lowe RJ, Zhang Z, McCulloch M (2013) Physical and biological controls on the carbonate chemistry of coral reef waters: effects of metabolism, wave forcing, sea level, and geomorphology. PLoS ONE 8(1):e53303
Gattuso J-P, Allemand D, Frankignoulle M (1999) Photosynthesis and calcification at cellular, organismal and community levels in coral reefs: a review on interactions and control by carbonate chemistry. Am Zool 39(1):160–183
Georgiou L, Falter J, Trotter J, Kline DI, Holcomb M, Dove SG, Hoegh-Guldberg O, McCulloch M (2015) pH homeostasis during coral calcification in a free ocean CO_2 enrichment (FOCE) experiment, Heron Island reef flat, Great Barrier Reef. Proc Natl Acad Sci 112(43):13219–13224
Glud RN, Eyre BD, Patten N (2008) Biogeochemical responses to mass coral spawning at the Great Barrier Reef: effects on respiration and primary production. Limnol Oceanogr 53(3):1014–1024
Gourlay M, Hacker JL (1999) Influence of waves and winds on reef-top currents at Heron Island, Southern Great Barrier Reef. In: Coasts and Ports (1999) Challenges and directions for the new century; Proceedings of the 14th Australasian coastal and ocean engineering conference and the 7th Australasian port and harbour conference. National Committee on Coastal and Ocean Engineering, Institution of…, p 209
Gourlay MR, Hacker JL (2008) Reef-top currents in vicinity of Heron Island boat harbour, Great Barrier Reef, Australia: 2. Specific influences of tides meteorological events and waves.
Hendriks IE, Duarte CM, Álvarez M (2010) Vulnerability of marine biodiversity to ocean acidification: a meta-analysis. Estuar Coast Shelf Sci 86(2):157–164
Hoegh-Guldberg O, Mumby PJ, Hooten AJ, Steneck RS, Greenfield P, Gomez E, Harvell CD, Sale PF, Edwards AJ, Caldeira K (2007) Coral reefs under rapid climate change and ocean acidification. Science 318(5857):1737–1742
Hoegh-Guldberg O, Bruno JF (2010) The impact of climate change on the world's marine ecosystems. Science 328(5985):1523–1528
Hofmann GE, Barry JP, Edmunds PJ, Gates RD, Hutchins DA, Klinger T, Sewell MA (2010) The effect of ocean acidification on calcifying organisms in marine ecosystems: an organism-to-ecosystem perspective. Annu Rev Ecol Evol Syst 41:127–147
Hughes TP, Baird AH, Bellwood DR, Card M, Connolly SR, Folke C, Grosberg R, Hoegh-Guldberg O, Jackson JB, Kleypas J (2003) Climate change, human impacts, and the resilience of coral reefs. Science 301(5635):929–933
Hughes TP, Kerry JT, Baird AH, Connolly SR, Dietzel A, Eakin CM, Heron SF, Hoey AS, Hoogenboom MO, Liu G (2018a) Global warming transforms coral reef assemblages. Nature 556(7702):492–496

Hughes TP, Anderson KD, Connolly SR, Heron SF, Kerry JT, Lough JM, Baird AH, Baum JK, Berumen ML, Bridge TC (2018b) Spatial and temporal patterns of mass bleaching of corals in the Anthropocene. Science 359(6371):80–83

Jackson JB, Kirby MX, Berger WH, Bjorndal KA, Botsford LW, Bourque BJ, Bradbury RH, Cooke R, Erlandson J, Estes JA (2001) Historical overfishing and the recent collapse of coastal ecosystems. Science 293(5530):629–637

Johnson MD, Price NN, Smith JE (2014) Contrasting effects of ocean acidification on tropical fleshy and calcareous algae. PeerJ 2:e411

Jokiel P, Rodgers K, Kuffner I, Andersson A, Cox E, Mackenzie F (2008) Ocean acidification and calcifying reef organisms: a mesocosm investigation. Coral Reefs 27(3):473–483

Kapsenberg L, Cyronak T (2019) Ocean acidification refugia in variable environments. Glob Change Biol 25(10):3201–3214

Kessler AJ, Rogers A, Cyronak T, Bourke MF, Hasler-Sheetal H, Glud RN, Greening C, Meysman FJ, Eyre BD, Cook PL (2020) Pore water conditions driving calcium carbonate dissolution in reef sands. Geochimica et Cosmochimica Acta 279:16–28

Kinsey D (1985) Metabolism, calcification and production: I systems level studies. Proc Fifth Inter Coral Reef Congr 4:503–542

Kleypas JA, Buddemeier RW, Archer D, Gattuso J-P, Langdon C, Opdyke BN (1999) Geochemical consequences of increased atmospheric carbon dioxide on coral reefs. Science 284(5411):118–120

Kleypas JA, Yates KK (2009) Coral reefs and ocean acidification. Oceanography 22(4):108–117

Kleypas JA, Anthony KR, Gattuso JP (2011) Coral reefs modify their seawater carbon chemistry–case study from a barrier reef (Moorea, French Polynesia). Glob Change Biol 17(12):3667–3678

Kline DI, Teneva L, Schneider K, Miard T, Chai A, Marker M, Headley K, Opdyke B, Nash M, Valetich M (2012) A short-term in situ CO_2 enrichment experiment on Heron Island (GBR). Sci Rep 2(1):1–9

Kline DI, Teneva L, Hauri C, Schneider K, Miard T, Chai A, Marker M, Dunbar R, Caldeira K, Lazar B (2015) Six month in situ high-resolution carbonate chemistry and temperature study on a coral reef flat reveals asynchronous pH and temperature anomalies. PLoS ONE 10(6):e0127648

Koweek D, Dunbar RB, Rogers JS, Williams GJ, Price N, Mucciarone D, Teneva L (2015a) Environmental and ecological controls of coral community metabolism on Palmyra Atoll. Coral Reefs 34(1):339–351

Koweek DA, Dunbar RB, Monismith SG, Mucciarone DA, Woodson CB, Samuel L (2015b) High-resolution physical and biogeochemical variability from a shallow back reef on Ofu, American Samoa: an end-member perspective. Coral Reefs 34(3):979–991

Langdon C, Atkinson M (2005) Effect of elevated pCO_2 on photosynthesis and calcification of corals and interactions with seasonal change in temperature/irradiance and nutrient enrichment. J Geophys Res Oceans 110(C9)

Lowe RJ, Falter JL (2015) Oceanic forcing of coral reefs. Ann Rev Mar Sci 7:43–66

Lowe RJ, Pivan X, Falter J, Symonds G, Gruber R (2016) Rising sea levels will reduce extreme temperature variations in tide-dominated reef habitats. Sci Adv 2(8):e1600825

Manzello DP (2010) Ocean acidification hotspots: spatiotemporal dynamics of the seawater CO_2 system of eastern Pacific coral reefs. Limnol Oceanogr 55(1):239–248

Manzello DP, Enochs IC, Melo N, Gledhill DK, Johns EM (2012) Ocean acidification refugia of the Florida Reef Tract. PLoS ONE 7(7):e41715

Marshall P, Baird A (2000) Bleaching of corals on the Great Barrier Reef: differential susceptibilities among taxa. Coral Reefs 19(2):155–163

Martz TR, Connery JG, Johnson KS (2010) Testing the Honeywell Durafet® for seawater pH applications. Limnol Oceanogr Methods 8(5):172–184

McCulloch M, Falter J, Trotter J, Montagna P (2012) Coral resilience to ocean acidification and global warming through pH up-regulation. Nat Clim Chang 2(8):623–627

McKinney D (2009) A survey of the scleractinian corals at Mermaid, Scott, and Seringapatam Reefs, Western Australia. Rec West Aust Mus Suppl 77(1):105–143

McMahon A, Santos IR, Cyronak T, Eyre BD (2013) Hysteresis between coral reef calcification and the seawater aragonite saturation state. Geophysical Research Letters 40(17):4675–4679

McMahon A, Santos IR, Schulz KG, Cyronak T, Maher DT (2018) Determining coral reef calcification and primary production using automated alkalinity, pH and pCO_2 measurements at high temporal resolution. Estuar Coast Shelf Sci 209:80–88

Mehrbach C, Culberson C, Hawley J, Pytkowicx R (1973) Measurement of the apparent dissociation constants of carbonic acid in seawater at atmospheric pressure 1. Limnol Oceanogr 18(6):897–907

Moberg F, Folke C (1999) Ecological goods and services of coral reef ecosystems. Ecol Econ 29(2):215–233
Mongin M, Baird M (2014) The interacting effects of photosynthesis, calcification and water circulation on carbon chemistry variability on a coral reef flat: a modelling study. Ecol Model 284:19–34
Morse JW, Mackenzie FT (1990) Geochemistry of sedimentary carbonates. Elsevier
Orr JC, Fabry VJ, Aumont O, Bopp L, Doney SC, Feely RA, Gnanadesikan A, Gruber N, Ishida A, Joos F (2005) Anthropogenic ocean acidification over the twenty-first century and its impact on calcifying organisms. Nature 437(7059):681–686
Page HN, Andersson AJ, Jokiel PL, Ku'ulei SR, Lebrato M, Yeakel K, Davidson C, D'Angelo S, Bahr KD (2016) Differential modification of seawater carbonate chemistry by major coral reef benthic communities. Coral Reefs 35(4):1311–1325
Page HN, Courtney TA, Collins A, De Carlo EH, Andersson AJ (2017) Net community metabolism and seawater carbonate chemistry scale non-intuitively with coral cover. Front Mar Sci 4:161
Page HN, Courtney TA, De Carlo EH, Howins NM, Koester I, Andersson AJ (2019) Spatiotemporal variability in seawater carbon chemistry for a coral reef flat in Kāne ʻohe Bay, Hawai ʻi. Limnol Oceanogr 64(3):913–934
Palumbi SR, Barshis DJ, Traylor-Knowles N, Bay RA (2014) Mechanisms of reef coral resistance to future climate change. Science 344(6186):895–898
Pandolfi JM, Jackson JB, Baron N, Bradbury RH, Guzman HM, Hughes TP, Kappel C, Micheli F, Ogden JC, Possingham HP (2005) Are US coral reefs on the slippery slope to slime? Am Assoc Adv Sci 307:1725–1726
Phinn SR, Roelfsema CM, Mumby PJ (2012) Multi-scale, object-based image analysis for mapping geomorphic and ecological zones on coral reefs. Int J Remote Sens 33(12):3768–3797
Rees M, Colquhoun J, Smith L, Heyward A (2003) Coral Communities at Ashmore Reef, Cartier Reef and Mermaid Reef, Northwestern Australia
Rogers CS (1990) Responses of coral reefs and reef organisms to sedimentation. Mar Ecol Progr Ser Oldendorf 62(1):185–202
Safaie A, Silbiger NJ, McClanahan TR, Pawlak G, Barshis DJ, Hench JL, Rogers JS, Williams GJ, Davis KA (2018) High frequency temperature variability reduces the risk of coral bleaching. Nat Commun 9(1):1–2
Santos IR, Glud RN, Maher D, Erler D, Eyre BD (2011) Diel coral reef acidification driven by porewater advection in permeable carbonate sands, Heron Island, Great Barrier Reef. Geophys Res Lett 38(3)
Shamberger K, Feely R, Sabine C, Atkinson M, DeCarlo E, Mackenzie F, Drupp P, Butterfield D (2011) Calcification and organic production on a Hawaiian coral reef. Mar Chem 127(1–4):64–75
Shamberger KE, Lentz SJ, Cohen AL (2018) Low and variable ecosystem calcification in a coral reef lagoon under natural acidification. Limnol Oceanogr 63(2):714–730
Shaw EC, McNeil BI, Tilbrook B (2012) Impacts of ocean acidification in naturally variable coral reef flat ecosystems. J Geophys Res Oceans 117(C3)
Smith S, Key G (1975) Carbon dioxide and metabolism in marine environments 1. Limnol Oceanogr 20(3):493–495
Smith S (1978) Calcification and organic carbon metabolism as indicated by carbon dioxide. Coral Reefs Res Methods, pp 469–484
Steven ADL, Pantus F, Brooks D, Trott L (1998) Longterm chlorophyll monitoring in the Great Barrier Reef Lagoon. Status Rep 1:1993–1995 (Great Barrier Reef Marine Park Authority: Townsville)
Stoltenberg L, Schulz KG, Cyronak T, Eyre BD (2020) Seasonal variability of calcium carbonate precipitation and dissolution in shallow coral reef sediments. Limnol Oceanogr 65(4):876–891
Stoltenberg L, Schulz KG, Lantz CA, Cyronak T, Eyre BD (2021) Late afternoon seasonal transition to dissolution in a coral reef: an early warning of a net dissolving ecosystem? Geophys Res Lett 48:e2020GL090811
Sutton AJ, Sabine CL, Maenner-Jones S, Lawrence-Slavas N, Meinig C, Feely R, Mathis J, Musielewicz S, Bott R, McLain P (2014) A high-frequency atmospheric and seawater pCO_2 data set from 14 open-ocean sites using a moored autonomous system. Earth Syst Sci Data 6(2):353–366
Suzuki A, Kawahata H (2003) Carbon budget of coral reef systems: an overview of observations in fringing reefs, barrier reefs and atolls in the Indo-Pacific regions. Tellus B Chem Phys Meteorol 55(2):428–444
Takahashi T, Sutherland SC, Wanninkhof R, Sweeney C, Feely RA, Chipman DW, Hales B, Friederich G, Chavez F, Sabine C (2009) Climatological mean and decadal change in surface ocean pCO_2, and net sea–air CO_2 flux over the global oceans. Deep Sea Res Part II 56(8–10):554–577
Takeshita Y, Cyronak T, Martz TR, Kindeberg T, Andersson AJ (2018) Coral reef carbonate chemistry variability at different functional scales. Front Mar Sci 5:175

Tilbrook B, van Ooijen E, Neill C, Sutton AJ, Sabine CL, Musielewicz S (2012) High-resolution ocean and atmosphere pCO_2 time-series measurements from moorings Heron_Island_152E_23S, Kangaroo_Island_136E_36S and Maria_Island_148E_43S in the Coral Sea, Great Australian Bight and Tasman Sea from 2009-10-09 to 2017-09-04 (NCEI Accession 0100062). Version 3.3. National Oceanographic Data Center, NOAA. Dataset. https://doi.org/10.3334/CDIAC/OTG.TSM_HERON_152E_23S [04/10/2020]

Uppstrom L (1974) The boron/chlorinity ratio of deep-sea water from the Pacific Ocean. Deep Sea Res 21:161–162

Van Heuven S, Pierrot D, Rae J, Lewis E, Wallace D (2011) MATLAB program developed for CO_2 system calculations. ORNL/CDIAC-105b Carbon Dioxide Information Analysis Center, Oak Ridge National Laboratory, US Department of Energy, Oak Ridge, Tennessee 530

Van Hooidonk R, Maynard J, Planes S (2013) Temporary refugia for coral reefs in a warming world. Nat Clim Chang 3(5):508–511

Venti A, Andersson A, Langdon C (2014) Multiple driving factors explain spatial and temporal variability in coral calcification rates on the Bermuda platform. Coral Reefs 33(4):979–997

Walter LM, Morse JW (1985) The dissolution kinetics of shallow marine carbonates in seawater: a laboratory study. Geochim Cosmochim Acta 49(7):1503–1513

Watanabe A, Kayanne H, Hata H, Kudo S, Nozaki K, Kato K, Negishi A, Ikeda Y, Yamano H (2006) Analysis of the seawater CO_2 system in the barrier reef-lagoon system of Palau using total alkalinity-dissolved inorganic carbon diagrams. Limnol Oceanogr 51(4):1614–1628

Wisshak M, Schönberg CH, Form A, Freiwald A (2012) Ocean acidification accelerates reef bioerosion. PLoS ONE 7(9):e45124

Yeakel KL, Andersson AJ, Bates NR, Noyes TJ, Collins A, Garley R (2015) Shifts in coral reef biogeochemistry and resulting acidification linked to offshore productivity. Proc Natl Acad Sci 112(47):14512–14517

Zhang Z, Falter J, Lowe R, Ivey G, McCulloch M (2013) Atmospheric forcing intensifies the effects of regional ocean warming on reef-scale temperature anomalies during a coral bleaching event. J Geophys Res Oceans 118(9):4600–4616

Authors and Affiliations

Samuel A. H. Kekuewa[1] · Travis A. Courtney[1,2] · Tyler Cyronak[3] · Theodor Kindeberg[4] · Bradley D. Eyre[5] · Laura Stoltenberg[5] · Andreas J. Andersson[1]

1 Scripps Institution of Oceanography, University of California San Diego, La Jolla, CA, USA

2 Department of Marine Sciences, University of Puerto Rico Mayagüez, Mayagüez, Puerto Rico

3 Department of Marine and Environmental Sciences, Halmos College of Natural Sciences and Oceanography, Nova Southeastern University, Dania Beach, FL, USA

4 Department of Biology, Lund University, Sölvegatan 37, 223 62 Lund, Sweden

5 Centre for Coastal Biogeochemistry, Faculty of Science and Engineering, Southern Cross University, Lismore, NSW, Australia

Chapter 2, in full, is a reprint of the material as it appears in Kekuewa SAH, Courtney TA, Cyronak T, Kindeberg T, Eyre BD, Stoltenberg L, Andersson AJ. Temporal and Spatial Variabilities of Chemical and Physical Parameters on the Heron Island Coral Reef Platform. *Aquatic Geochemistry* 2021. The dissertation author was the primary investigator and author of this paper.

Chapter 3: Multi-scale coral reef seawater carbonate chemistry variability at Dongsha and Taiping Islands in the South China Sea

Kekuewa SAH, Pezner AK, Courtney TA, Wei Y, Soong K, Rintoul MS, Andersson AJ

Abstract

Coral reefs are composed of various benthic habitats that drive seawater CO_2 chemistry variability on different spatial and temporal scales. Understanding the present-day seawater CO_2 chemistry variability across both habitat-specific and reef-wide scales will allow us to more accurately predict the effects of future environmental change on coral reefs. Here, we utilize autonomous sensors deployed in patch reefs, seagrass beds, and a semi-enclosed lagoon, as well as discrete seawater samples collected across multiple spatial scales ranging from habitat-specific (semi-enclosed lagoon, patch reefs and seagrass; 0.02-0.72 km^2) to reef-wide scales (Dongsha Atoll; 250 km^2) in the South China Sea. Our results illustrate that the daily variability in temperature, pH and oxygen gradually decrease from the lagoon to the seagrass and patch reef environments. The patch reefs of Dongsha experienced similar average aragonite saturation states (Ω_{Ar}) to the entire reef, whereas the seagrass dominated habitats experienced higher average Ω_{Ar} conditions. Based on our observations and the historical increase of 1.15 μmol kg^{-1} $year^{-1}$ in dissolved inorganic carbon near the Ryukyu Islands, we projected future ocean acidification conditions at Dongsha Atoll. By 2050, 52% of our observations for the patch reefs and 89% of our observations for the reef-wide scale will experience $\Omega_{Ar} < 2.92$, the threshold for when coral reef sediments transition from net precipitation to net dissolution. In comparison, only 31% of the observations for the seagrass habitats and 10% of the observations for the semi-enclosed lagoon had a $\Omega_{Ar} < 2.92$ albeit with lower nighttime Ω_{Ar} compared to the patch reefs. These results

demonstrate the need for habitat-specific and spatial scale assessments in projecting ocean acidification impacts on coral reefs.

Introduction

Coral reefs are currently under threat due to global environmental change arising from human industrial and land-use activities causing ocean warming, acidification, and deoxygenation (Hoegh-Guldberg et al., 2007; Doney et al., 2012). This threat is grounded in an increased frequency and severity of coral reef mass bleaching events in response to elevated sea surface temperature (SST) (Hughes et al., 2017), decreased community scale calcification rates due to depressed seawater pH and aragonite saturation state (Ω_{Ar}) (e.g., Silverman et al., 2009; Albright et al., 2018), and increased occurrences of hypoxic events leading to mass mortality of reef organisms (Altieri et al., 2017; Kealoha et al., 2020). However, the effects of warming, acidification, and deoxygenation on global coral reefs will not be uniform and may vary greatly depending on their oceanographic and geographic setting (Guest et al., 2018), as well as local parameters such as community composition, reef metabolism, geomorphology, seawater residence time and hydrodynamics (Marshall et al., 2000; Manzello et al., 2012; Page et al., 2018; Cyronak et al., 2020). As a result, different habitats within coral reefs (e.g., fore reef, back reef, patch reef, lagoon, seagrass, etc.) may have different susceptibilities to short- and long-term environmental change. To understand how future warming, acidification, and deoxygenation may impact coral reef ecosystems, we first need to understand the present-day variability of sea surface temperature (SST), pH, Ω_{Ar}, and dissolved oxygen across different habitats and multiple spatial scales (100s m^2 to 100 km^2) that collectively encompass coral reefs.

It has been well established that seawater chemical conditions in coral reef habitats are often different than open ocean conditions due to the influence of net reef metabolism, which encompasses net community organic carbon production (NCP) and net community calcification (NCC) (e.g., Gattuso et al., 1996; Suzuki and Kawahata, 2003; Watanabe et al., 2006; Andersson

et al., 2014). NCP refers to the net sum of primary production minus total respiration while NCC refers to net sum of calcification minus calcium carbonate ($CaCO_3$) dissolution (Smith and Key, 1975). Positive NCP (i.e., net production or autotrophy) decreases dissolved inorganic carbon (DIC) with little to no change in total alkalinity (TA) and results in an increase in pH and dissolved oxygen (DO). Positive NCC (i.e., net calcification) decreases TA and DIC in a 2:1 ratio and results in a decrease in pH with no influence on DO (Smith and Kinsey, 1978; Aktinson and Smith, 1983). Negative NCP (i.e., net respiration or heterotrophy) and NCC (net dissolution) have the opposite effects on these parameters. Hence, by measuring anomalies in total alkalinity (TA) and dissolved inorganic carbon (DIC) across different habitats relative to offshore conditions, it is possible to assess whether reef habitats are net calcifying or net dissolving, and whether they are net autotrophic or heterotrophic (Suzuki and Kawahata, 2003; Cyronak et al., 2018). Furthermore, the relative influence of NCC and NCP on seawater carbon chemistry can be quantified by assessing their ratio or the slope of TA and DIC changes (Gattuso et al., 1996; Suzuki and Kawahata, 2003; Cyronak et al., 2018).

Natural variations in net reef metabolism drive diel and seasonal changes in seawater chemistry (e.g, pH and DO) on coral reefs that far exceeds the projected changes resulting from climate change in the open ocean by the year 2100 (Hofmann et al., 2011; Shaw et al., 2012; Guadayol et al., 2014; Pezner et al., 2023). However, the extent of modification of seawater chemistry by net reef metabolism is controlled by several properties such as the community composition, light intensity, flow rates, nutrient availability, and carbonate chemistry (Langdon and Atkinson, 2005; Page et al., 2016; Courtney et al., 2018), which vary over multiple spatial and temporal scales. The influence of these properties is further modified by additional factors such as seawater residence time, flow trajectory, and depth (Falter et al., 2013; Koweek et al., 2015; Cyronak et al 2018). For

example, increased residence time and shallower depths allow for greater modification of seawater chemistry (Falter et al., 2013; Zhang et al., 2013) due to longer contact time between the benthos and the seawater, and potentially greater biomass to water volume ratio (Falter et al., 2013; Lowe and Falter, 2015; Page et al., 2019).

To date, most studies focused on seawater biogeochemical variability on coral reefs have been conducted across relatively small spatial scales (Santos et al., 2011; Chou et al., 2018) or targeting specific habitats (e.g., fore reef, patch reef, reef flat, seagrass bed) (Albright et al., 2015; DeCarlo et al., 2017; Chou et al., 2020). This may result in a limited perspective of coral reef seawater biogeochemical variability at the reef scale, which is affected by the cumulative influence of multiple habitats. For example, the highest integrated NCC rate on a coral reef was observed on the eastern reef flat of Dongsha atoll (De Carlo et al., 2017). In contrast, net carbonate dissolution (i.e., negative NCC) has been observed in a seagrass meadow at the same atoll (Chou et al., 2018, 2021), but it is unknown how these extremes contribute to the reef scale biogeochemistry of Dongsha. Thus, it is of interest to understand the biogeochemical footprint and connectivity between different habitats to better understand the relative contribution to the reef scale biogeochemistry. Likewise, seagrass habitats have been hypothesized as a refugia from ocean acidification and hypoxia due to high rates of primary production that increases seawater pH and DO (Manzello et al., 2012; Wallace et al., 2021). However, to understand the magnitude and scale of this buffering, seawater chemistry needs to be characterized both within seagrass habitats and in the adjacent habitats that could be affected (Cyronak et al., 2018; Kapsenberg and Cyronak, 2019). To better understand how anthropogenic change will affect coral reef ecosystems and their habitats, and for developing predictive capacity, it is necessary to understand the biogeochemical

variability within and across multiple spatial and temporal scales to (Andersson et al., 2015; Edmunds et al., 2016).

In this study, we investigated the spatial and diel variability of seawater biogeochemical parameters from 0.02 km^2 to 250 km^2 within and between unique reef habitats (i.e., inner-lagoon, seagrass beds, patch reefs, coral cay) at the Dongsha Atoll and Taiping Island in the South China Sea. The study aimed to address four core questions: (1) What is the range of variability in seawater pH and DO across the Dongsha Atoll and the Taiping Island reef system? (2) How do pH and DO vary within and between different habitats and scales? (3) How do reef chemistry deviate from open ocean conditions and what is the relative influence of NCP and NCC in controlling the chemical variability between habitats? (4) Which habitats are potentially more or less susceptible to ocean acidification and deoxygenation, i.e., what habitats alleviate and/or exacerbate ocean acidification and deoxygenation conditions? Due to ongoing climate change, we hypothesize that Dongsha and Taiping coral reef habitats in general will experience seawater chemistry conditions (pH and DO) that are detrimental to their local fauna and reef accretion during the 21st century. However, we also hypothesize that local seagrass beds may act as a refugia that can buffer local calcifiers from projected acidification and deoxygenation. By analyzing how chemical conditions change across different habitats and spatial scales, this study is a starting point for assessing how individual reef habitats contribute to the reef and atoll scale variability.

Methods

Site Description

Dongsha Atoll Dongsha Atoll, also known as Pratas Atoll, (20.8° N, 116.7° E) is located in the northern South China Sea ~430 km southwest of Kaohsiung, Taiwan. Dongsha is a circular

atoll 28 km in diameter with an area of ~600 km^2 surrounded by a fringing reef which varies from 1-3 km in width along the northern, southern, and eastern sides of the atoll (Dai et al., 2004) (Fig 1). The central lagoon of Dongsha Atoll has an average depth range of 10-15 m with a maximum depth of 23.7 m (Dai, Qin and Zheng, 2013). The lagoon contains thousands of scattered patch reefs of varying size. Dongsha Island is located in the western portion of the atoll and is surrounded by ~11.85 km^2 of seagrass beds. It is bounded by two deeper channels (~5 m) to the north and south of the island that connect the lagoon with the adjacent open ocean (Reid et al., 2020). The island contains a semi-enclosed lagoon (0.64 km^2) with a single inlet located on the western side of the island (Huang et al., 2015). This lagoon is mainly composed of seagrass beds. Dongsha Atoll experiences a wet, warm monsoon season from May to October and a dry, cool season from November to April (Wong et al., 2007).

Taiping Taiping Island (10.377° N, 114.366° E) is the largest island of the Spratly Islands in the southern South China Sea located ~1200 km south of Dongsha (Duan et al., 2016). Taiping Island encompasses an area of 0.57 km^2 surrounded by shallow seagrass beds, a ~50 m wide reef flat (1-4 m), and a steep fore reef that drops off to over 50 m depth (Dai and Fan, 1996). There are few to no corals below the 18 m depth contour. Additionally, 4 km eastward of Taiping Island there is a coral cay (1.12 km^2) covered by seagrass, hard coral, and coral rubble. Both Taiping Island and adjacent reef flat have no barrier reef and are thus fully exposed to oceanic seawater.

Spatial Surveys

Multiple spatial surveys ranging from habitat specific (e.g., patch reef, seagrass; 0.02-0.72 km^2) to the reef scale (i.e., Dongsha Atoll; 250 km^2) were conducted across both Dongsha Atoll and Taiping using small boat, jet ski, or kayak (Table 1). Seawater samples for the reef-wide spatial

scale were collected in a 5L Niskin bottle and transferred to 250 mL Corning Pyrex glass bottles. Samples were immediately poisoned with 100 µL saturated solution of mercuric chloride ($HgCl_2$) to prevent biological modification (Dickson et al., 2007). Due to practical constraints, seawater samples for seagrass, inner-lagoon, and patch reef surveys were collected directly into 250 mL Corning Pyrex glass bottles. Bottles were rinsed three times and then carefully submerged below the surface making sure to not trap air bubbles. Samples collected from kayak for the inner-lagoon and patch reef surveys were immediately poisoned on the kayak whereas samples collected from jet ski for the seagrass survey were transferred to a shore-based team that conducted this task. In parallel with seawater collection, seawater temperature (SST), salinity, and dissolved oxygen (DO), were measured using a handheld multi-parameter instrument (i.e., YSI Pro 2030 m Xylem (±0.3 °C, ±0.1, ±2%), Sontek Castaway (±0.1 °C, ±0.1, no DO), or YSI Professional Plus (±0.2 °C, ±0.1, no DO; Table 1). Detailed descriptions of habitats and sampling scheme for each, unique spatial survey is provided in Table 1.

Autonomous Instruments

Autonomous instruments were deployed in five diverse benthic habitats across Dongsha Atoll and two habitats in Taiping in order to capture high-resolution temporal variability of biogeochemical parameters. The instruments consisted of two Ocean Seven 316 Plus CTD (IDRONAUT S.r.l, Italy) (seawater temperature ±0.003 °C, conductivity ±0.003 mS cm^{-1}, pH_{NBS} ±0.01, dissolved oxygen ±0.01 ppm); one Seafet sensor measuring seawater pH_T via a Durafet pH sensor (±0.02); two Sea-Bird Electronics 16plus V2 Sea CAT (temperature ±0.005 °C, conductivity ±0.0005 S m^{-1}, one sensors was equipped with Aandera Oxygen Sensor 3835 (<12.5 µM)); one Precision Measurement Engineering miniDOT (PME miniDOT®) (DO ± 0.3 mg L^{-1},

temperature ± 0.1 °C); one SeapHOx sensor (temperature ± 0.002 ºC, salinity ± 0.0002, pressure ± 0.1% PSIG, pH_T ± 0.015, DO ± 5%) (Martz et al., 2010).

Prior to deployment all DO sensors were either calibrated to 100% water-saturated air or by the manufacturer. The IDRONAUT pH-sensitive glass electrode was calibrated to multiple standard pH_{NBS} buffers and converted to pH_T via a one-point offset with an in-situ seawater sample collected at the beginning of the deployment. Additionally, both the SeapHOx and Seafet Durafet pH sensors were calibrated against discrete seawater samples collected at the beginning of the deployment following standard procedure (Bresnahan et al., 2014) and compared to additional validation samples collected during the deployment. The accuracy of the SeapHOx and Seafet pH sensors were calculated to be ±0.015 and ±0.02, respectively. The instruments used in Dongsha were initially deployed in proximity to one another in order to cross-calibrate. For all deployments, instruments were secured to nearby reef substrate or cinder blocks. The deployment scheme for all autonomous instruments is detailed in Table 2.

Sample Analysis

Seawater samples collected from Dongsha and Taiping were transported to and analyzed at the Scripps Coastal and Open Ocean Biogeochemistry Lab in La Jolla, CA, USA. Seawater samples were analyzed for both dissolved inorganic carbon (DIC) and total alkalinity (TA). DIC was analyzed via an automated infrared inorganic carbon analyzer (AIRICA, *Marianda*) with a LI-COR 7000. TA was measured via potentiometric, open-cell acid titrations (0.1 N HCl) with a system developed by the Dickon Lab at Scripps Institution of Oceanography (SIO) (Dickson et al. 2007). Accuracy and precision of the instruments were validated against CRMs provided by the Dickson Lab and secondary standards prepared in lab for both DIC and TA (mean offset±1SD; DIC=0.32±1.65 µmol kg^{-1}, n=39; TA=-0.12±2.28 µmol kg^{-1}, n=26). For both DIC and TA, CRMs

were analyzed at the beginning and end of each day and analyzed every 5th sample for DIC and every 10th sample for TA. Seawater samples collected from Dongsha were analyzed in the Scooby Lab in November 2018, 4 months after collection whereas samples collected from Taiping were analyzed in June 2021, 26 months after collection.

Seawater samples from the Dongsha inner lagoon surveys were transported to the Chou lab at the National Taiwan Ocean University and analyzed for DIC and TA via the non-dispersive infrared method on a DIC analyzer (AS-C3, *Apollo SciTech*) and Gran titration on an automatic TA titrator (AS-ALK2, *Apollo SciTech*). Both measurements had accuracies and precisions of ~0.2%. The MATLAB program CO2SYS (v. 1.1) was used to calculate the complete dissolved inorganic carbon chemistry parameters with SST, salinity, TA, and DIC as inputs (Van Heuven et al., 2011) for all seawater samples. Dissociation constants from Mehrbach et al. (1973) refit by Dickson and Millero (1987) were used for all carbonate chemistry calculations.

Future projections

Based on the spatial discrete observations of SST, DIC and DO for each habitat, we calculated future projections in SST, pH, DO, and Ω_{Ar} for the years 2050 and 2100. Region-specific seawater temperature projections from the Coupled Model Intercomparison Project 6 Shared Socio-economic Pathways 8.5 (CMIP6 SSP-8.5) were utilized to calculate the change in SST by 2050 and 2100. The projected temperature increase was added to our observed SST. To project future ocean acidification, we used the historical increase in salinity normalized DIC of 1.15 μmol kg^{-1} year^{-1} observed near the Ryukyu Islands (Kosugi et al., 2023) to calculate future DIC assuming a linear increase. Combined with our SST projection and assuming no secular changes in TA, this allowed us to calculate future pH and Ω_{Ar}. Deoxygenation and future DO conditions for each habitat were calculated based on the site-specific SST projection's influence

on oxygen solubility and biological oxygen demand according to methods in Pezner et al. (2023). For each projection, the percentages of SST observations exceeding 32 °C (a common coral bleaching threshold; Shoepf et al., 2015) were calculated. Similarly, the percentages of observations of pH less than 7.7 (a hypothesized threshold for net reef accretion; Fabricius et al., 2011), Ω_{Ar} less than 2.92 (thresholds for reef sediment net dissolution (Eyre et al., 2018) and less than 1 (thermodynamic threshold for aragonite dissolution) were also calculated. Lastly, the percentages of DO less than 153, 92, and 61 μmol kg^{-1}, representing weak, moderate, and severe hypoxia (Pezner et al., 2023), were calculated for the present, 2050, and 2100.

Results

Diel habitat variability

Data collected via autonomous sensors demonstrated large diurnal variability and extrema in SST, pH, and DO across all benthic habitats and stations (Fig 2, Table 3). For all Dongsha stations, minimum SST was observed in the morning at 07:05±1:12 (mean±1std) while the maximum SST was observed in the late afternoon 17:19±1:07 (Fig 2A; Table 4). Mean SST and diel variability was highest across the inner-lagoon sites (ILI and IL) followed by the seagrass site (SG) and the coral reef sites (CPR, EPR). The mean SST of the inner-lagoon sites ranged from 31.4±0.4 °C (ILI) to 32.8±0.5 °C (IL) with a mean daily variability that ranged from 5.3±1.2 °C to 5.6±0.8 °C (Fig 2A, B; Table 3). The seagrass site experienced a mean SST of 30.7±0.3 °C with a mean daily variability ranging from 2.3±0.2 °C (Fig 2A, B; Table 3). The coral reef habitats experienced mean SST ranging from 29.8±0.1 °C (EPR) to 30.0±0.3 °C (CPR) with mean daily variability ranging from 0.7±0.1 °C (CPR) to 0.8±0.2 °C (EPR) (Fig 2A, B; Table 3).

For Taiping habitats, minimum SST was observed at 06:25±0:53 (mean±1std) while maximum was observed at 14:23±1:04 with mean daily SST values of 28.3±0.1 °C (TPSG) and 28.9±0.1 °C (TPR) and mean daily variability ranging from 1.2±0.0 °C (TPR) to 3.5±0.7 °C (TPSG).

Across all sites, pH and DO were positively correlated with mostly strong correlation coefficients (R^2 >0.65) except at the IL where R^2 =0.18 (Fig S1). The time of daily minimums and maximums for pH and DO values varied between Dongsha habitats. Daily minimum pH and DO first occur at ILI, then CPR, SG, EPR, and lastly IL (Table 5). In comparison, daily maximum pH and DO first occurred at CPR, then EPR, SG, ILI, and lastly IL (Table 5). However, on average for ILI, SG, CPR, and EPR daily minimums of pH and DO were observed at 05:17±0:48 and 05:04±0:51, respectively, while the maximums were observed at 15:01±1:25 and 14:45±1:13, respectively (Fig 2C, E; Table 5). The IL experienced minimum daily pH and DO values at 09:15±0:44 and 07:30±1:12, and maximum values at 18:38±1:44 and 18:08±1:26, respectively (Fig 2C, E; Table 5).

In terms of pH, the inner-lagoon and seagrass sites ((ILI, IL, and SG) qualitatively exhibited higher mean pH conditions (8.03±0.26 (ILI) to 8.60±0.10 (IL)) compared to the coral reef habitats (7.79±0.09 (CPR) to 7.87±0.05 (EPR)) (Fig 2C, D; Table 3). The inner-lagoon and seagrass sites also experienced higher diel pH variability that ranged from 0.41±0.12 (IL) to 0.91±0.09 (ILI) compared to the coral reef sites that ranged from 0.19±0.06 (EPR) to 0.29±0.16 (CPR) (Fig 2C, D; Table 3). Across all Dongsha sites, the lowest pH (7.41) was observed at the ILI while the highest pH (8.89) was observed at the IL (Table 3). In terms of DO, the highest mean DO conditions were observed at the IL site with a value of 150±38 μmol kg^{-1} while the lowest mean DO conditions were observed at the SG and ILI sites which ranged from 115±56 μmol kg^{-1}

(SG) to 124±102 μmol kg^{-1} (ILI) (Fig 2E, F). In comparison, the coral reef sites of CPR and EPR experienced mean DO conditions of 133±29 μmol kg^{-1} and 136±38 μmol kg^{-1}, respectively, intermediate of the other sites (Fig 2E, F; Table 3). Furthermore, the inner-lagoon and seagrass sites experienced higher diel DO variability compared to the coral reef sites with mean diel ranges as low as 142±20 μmol kg^{-1} (IL) and as high as 269±6 μmol kg^{-1} (ILI) (Fig 2E, F; Table 3). In comparison, the coral reef sites on average experienced smaller mean diel ranges that ranged from 100±60 μmol kg^{-1} (CPR) up to 121±45 μmol kg^{-1} (EPR) (Table 3). Across all Dongsha sites, the minimum DO concentration of 0 μmol kg^{-1} was observed at the ILI while the maximum DO concentration of 281 μmol kg^{-1} was observed at the CPR, a coral reef site.

In comparison to the Dongsha habitats, Taiping habitats experienced minimum pH and DO values at 05:23±1:12 and 04:15±0:30, and maximum values at 13:03±0:44 and 12:30±0:22 (Fig 2C, E; Table 5). For these habitats, mean daily pH varied from 7.88±0.02 (TPSG) to 7.93±0.07 (TPR) with mean daily variability ranging from 0.24±0.08 (TPR) to 0.55±0.01 (TPSG) (Fig 2C, D; Table 3). Daily mean DO varied from 155±34 μmol kg^{-1} (TPR) to 160±66 μmol kg^{-1} (TPSG) with mean daily variability ranging from 111±34 μmol kg^{-1} (TPSG) to 123±17 μmol kg^{-1} (TPR) (Fig 2E, F; Table 3).

Spatial habitat variability

The means and ranges of spatial variability of SST, pH, DO, and Ω_{Ar} differed across habitats, spatial scales, and timing of the survey (i.e., early morning, afternoon, late-afternoon). Because of the different duration of surveys and the influence of the timing, here, we mainly focus on the observed variability in each habitat.

In general, the largest spatial variability was observed for the habitats directly associated with the island of Dongsha, i.e., the inner lagoon (0.64 km^2) and the seagrass bed (0.72 km^2). For

individual surveys of these habitats, SST spatial variability ranged from 1.1 to 3.9 °C and 1.0 to 5.0 °C, pH from 0.61 to 1.11 and 0.13 to 0.29 units, DO from 58 to 129 μmol kg^{-1} (DO measurements were not collected in the inner lagoon), and Ω_{Ar} from 5.51 to 9.64 and 0.8 to 3.05 units, respectively (Fig. 3; Table S1). For the inner lagoon, spatial variability was large for all surveys regardless of whether they were conducted in the early morning or mid to late afternoon. In contrast, mid afternoon surveys in the seagrass bed mostly showed reduced variability in pH, DO, and Ω_{Ar} compared to the early morning or late afternoon surveys while SST variability was more variable between surveys. Notably, the inner lagoon experienced the highest SST, pH, and Ω_{Ar} conditions in the late-afternoon with maximum values reaching 35.9 °C, 8.88, and 12.49, respectively (Fig. 3; Table S1). The minimum SST, pH, and Ω_{Ar} conditions were observed in the early morning survey with values as low as 28.3 °C, 7.59, and 1.81, respectively. The observed extremes in the seagrass bed were also notable although not as extreme as for the inner lagoon (28.3-35.5 °C (SST), 7.73-8.49 (pH), 61-393 μmol kg^{-1} (DO), and 2.04-7.88 (Ω_{Ar})) (Fig. 3; Table S1).

The smallest spatial variability was observed for the patch reef habitats, which were also the smallest scale surveys, i.e., Eastern Patch Reef (0.02 km^2) and Central Patch Reef (0.11 km^2). However, only one survey was conducted at each site at 15:00 and 11:00, respectively, with durations < 40 minutes. SST variability was 0.3 °C for both sites, pH variability ranged from 0.08 to 0.11, DO from 25 to 33 μmol kg^{-1}, and Ω_{Ar} from 0.50 to 0.80, respectively.

Although the atoll and reef scale surveys in Dongsha and Taiping stretched from early morning to late afternoon, the observed variability was much reduced compared to the variability observed in the Dongsha inner lagoon and seagrass habitats (Fig. 3; Table S1). Furthermore, the variability around the mean for repeat surveys in the same season was relatively consistent. For

Dongsha atoll taking into account both the current and the Fan et al., (2021) summer surveys (combined n=5), SST observations ranged from 28.1 to 31.2 °C with a mean of 29.9±0.6 °C, pH ranged from 7.77 to 8.08 with a mean of 7.96±0.05, DO ranged from 144 to 245 μmol kg^{-1} with a mean of 192±19 μmol kg^{-1}, and Ω_{Ar} ranged from 2.13 to 3.82 with a mean of 3.11±0.29. Observations from Taiping conducted in March were either within or close to the range of conditions observed on the Dongsha atoll (Fig. 3; Table S1).

Spatial gradients of biogeochemical variability

The observed variability and gradients in pH, Ω_{Ar}, and DO at the study sites were in part influenced by variations in SST and salinity, and in part by biogeochemical and hydrodynamic processes. The main biogeochemical processes (photosynthesis, respiration, calcification, and $CaCO_3$ dissolution) modified pH and Ω_{Ar} through their influence on seawater DIC and TA. The largest spatial gradients for DIC and TA were observed across the semi-enclosed lagoon and seagrass habitats with smaller gradients observed over the patch reefs and the reef-wide surveys for both Dongsha and Taiping (Fig 4; Table S1). DIC and TA were moderately to strongly (R^2 = 0.42 to 0.93) positively correlated in most habitats and scales except for the inner lagoon, some of the seagrass surveys, the Eastern Patch Reef, and the nearshore of Taiping island (Table 5).

At the inner lagoon DIC and TA gradients roughly extended from the inlet to the back of the lagoon, but with several exceptions from this trend. Extreme minimums and maximums of DIC and TA ranged from 1328 to 2504 μmol kg^{-1} and 2157 to 2799 μmol kg^{-1}, respectively (Fig 4; Table S1). In the seagrass habitat, DIC and TA gradients generally followed an inshore-offshore gradient that tracked depth (Fig 4; Table S1). As a result, DIC and TA increased with shoaling depth in the mornings and the opposite during the afternoons. The single surveys at the central

and eastern patch reefs demonstrated a drawdown in DIC and TA from east to west, which tracked the wind direction at the time of the surveys (Fig 4; Table S1).

Across Dongsha atoll, DIC and TA initially decreased from east to west, but then rapidly increased in the western part of the atoll (Fig 4; Table S1). DIC ranged from 1810 to 1937 μmol kg^{-1} and TA ranged from 2074 to 2232 μmol kg^{-1} based on all surveys in 2018 (n=3). Spatial gradients of DIC and TA were near-zero across Taiping but ranged from 1801 to 2034 μmol kg^{-1} and 2157 to 2330 μmol kg^{-1}, respectively, due to one anomalously high DIC and TA station on the eastside of Taiping Island (Fig 4; Table S1).

Biogeochemical modification

Compared to the adjacent open ocean seawater conditions, both repletion and depletion of TA and DIC were observed across the Dongsha and Taiping study sites (Fig 5). On average, observations from the Dongsha habitats were primarily depleted in TA (-dTA) and DIC (-dDIC) relative to the open ocean except for the IL, which was repleted in TA (+dTA) and highly variable in dDIC (Fig 5). We note though that there were only two surveys conducted in the early morning and no surveys conducted at night. For the IL, TA repletion was observed for all surveys (mean dTA = 371±97 μmol kg^{-1}) while DIC repletion was only observed during the early morning survey (mean dDIC = 136±280 μmol kg^{-1}).

The largest mean dTA depletion for any given survey was observed at the central patch reef (-139±15 μmol kg^{-1}; 0.11 km^2), followed by the eastern patch reef (-132±7 μmol kg^{-1}; 0.02 km^2), reef-wide Dongsha surveys (-111±30 μmol kg^{-1}; 250 km^2), and finally the seagrass bed (-89±57 μmol kg^{-1}; 0.72 km^2) (Fig 5; Table 5).The largest mean dDIC depletion for any given survey was observed at the seagrass bed (-330±111 μmol kg^{-1}; 0.72 km^2), followed by the inner-lagoon (-212±231 μmol kg^{-1}; 0.64 km^2), eastern patch reef (-137±16 μmol kg^{-1}; 0.02 km^2), central

patch reef (-89±27 µmol kg^{-1}; 0.11 km^2), and the reef-wide Dongsha surveys (-67±42 µmol kg^{-1}; 250 km^2) (Fig 5; Table 5). Mean positive dDIC was only observed during the early morning survey of the seagrass bed (69±38 µmol kg^{-1}) and inner-lagoon (136±280 µmol kg^{-1}). In Taiping, mean dTA and mean dDIC did not differ from open-ocean conditions (dTA = 1±21 µmol kg^{-1} and dDIC = 1±29 µmol kg^{-1}) although discrete observations revealed distinct anomalies around Taiping Island (Fig 5; Table 5).

Linear regressions (type II) of dTA-dDIC for individual surveys with *p*-values < 0.05 ranged from -0.24 to 1.69 with correlation coefficients (R^2) ranging from 0.29 to 0.93 (Fig 5; Table 5). The larger spatial surveys had the highest slopes (Dongsha atoll 2018: 1.13-1.69; TAO: 1.01-1.51) followed by Taiping Island (0.76), central patch reef (0.48), seagrass bed (0.21-47), and the eastern patch reefs (0.22) (Fig 5; Table 5). dTA-dDIC data from the inner lagoon were mostly not correlated ($R^2 \leq 0.01$) except for one survey that showed a slope of 0.32 with an R^2 of 0.5 and a *p*-value <0.05.

Linear regressions of dDO-$dDIC_{NCP}$ for individual surveys with *p*-values < 0.05 ranged from -1.32 to -0.25 with R^2 ranging from 0.18 to 0.81 (Fig 5; Table 5). The steepest slopes were observed for the larger spatial scale surveys (Dongsha atoll 2018: -0.74 to -1.32; TAO: -0.25 to -1.16) and for the seagrass bed (-0.33 to -1.26) with lesser slopes for the central and eastern patch reefs (-0.55 and -0.35) (Table 5). For the seagrass, it should be noted that the highest slope was associated with the morning survey while the shallower slopes were associated with the afternoon surveys. No oxygen data were collected for the inner lagoon and the Taiping spatial surveys. Property-property plots of dDO and $dDIC_{NCP}$ revealed that the highest pH was associated with the highest dDO and the lowest $dDIC_{NCP}$ (i.e., net production) whereas the lowest pH was associated with the lowest dDO and the highest $dDIC_{NCP}$ (net respiration) (Fig 5).

Future projections

Under the future warming and acidification scenarios explored here, the frequency distributions of SST, pH, Ω_{Ar}, and DO all shifted toward conditions considered more detrimental to coral reef organisms (i.e., higher SST, and lower pH, DO and Ω_{Ar}) (Fig 6).

At present time, SST > 32 °C was only observed in the Dongsha seagrass bed and inner lagoon. For the seagrass, 21% of the observations exceeded this temperature threshold whereas 38% of the observations from the inner lagoon exceeded it (Fig 6A). By 2100 under SSP-5-8.5, 89% of all observations for all habitats were > 32 °C. This included 98% of the observations from the atoll-wide surveys in summer (n=5), 0% for the atoll-wide surveys in winter (n=1), 100% for the inner lagoon, 81% for the seagrass bed, 100% for the patch reefs, and 100% for Taiping surveys (Fig 6A).

The inner lagoon was the only habitat to experience pH < 7.7 (5% of observations) at present time. By the year 2100 following a hypothesized normalized DIC increase of 1.15 μmol $kg^{-1}year^{-1}$ (Kosugi et al., 2023) and projected warming, all habitats except the EPR crossed this threshold for some fraction of the observations (seagrass bed 21%, Dongsha atoll-wide surveys 25%, Dongsha atoll-wide surveys (TAO) 31%, Taiping 4%, inner lagoon 10%, CPR 42%; Fig 6B). Similarly, all habitats except for the EPR experienced $\Omega_{Ar} < 2.92$ for some fraction of observations at present time (Fig 6D). By the end of the century, all habitats except for the seagrass bed (44%), inner lagoon (10%), and EPR (77%) will experience conditions below $\Omega_{Ar} < 2.92$ for 100% of the observations (Fig 6D). Although the seagrass bed and the inner lagoon remained above this threshold for part of the observations, these habitats were predicted to experience the lowest Ω_{Ar} of all the habitats of 1.30 and 1.18, respectively, by the year 2100 (Fig 6D).

At present time, DO < 153 μmol kg^{-1} was observed in the atoll-wide surveys and seagrass bed for 1% and 15% of the observations, respectively (Fig 6C). By the year 2100, this will change to 7% and 21%, respectively (Fig 6C). The seagrass bed was also projected to experience DO < 92 μmol kg^{-1} and < 61 μmol kg^{-1} for 8% and 6% of the observations by 2100, respectively. We note that no DO data was available for the inner lagoon and Taiping.

Discussion

This study utilized both autonomous sensors and discrete seawater samples to characterize the temporal and spatial biogeochemical variability across multiple coral reef habitats and spatial scales across the Dongsha atoll and Taiping Island in the South China Sea. The objective of the measurements was to characterize the current day natural variability in order to set the initial boundaries for assessing future potential changes in seawater chemistry due to ocean warming and acidification. The study also assessed the relative influence of NCP and NCC in controlling the chemical variability between habitats and scales, which may provide clues on what habitats will be more or less susceptible to future ocean acidification and deoxygenation (Kapsenberg and Cyronak, 2019; Wallace et al., 2021). Although the observations were short in duration and not representative of the seasonal range of conditions at the study sites, they reveal important properties and differences between habitats, geomorphological settings, and the scale of observations.

Dongsha and Taiping Biogeochemical Variability

In general, a greater range of seawater pH and DO conditions were observed at the Dongsha atoll compared to Taiping Island and its surrounding habitats (Figure 2 and 4; Table 3, S1). This was mainly due to the semi-enclosed nature, larger size, and greater diversity and complexity of

habitats within the Dongsha atoll compared to the smaller size and non-enclosed nature of the Taiping reef system. The full range of diel pH and DO variability ranged from 7.41-8.89 and 0-281 μmol kg^{-1} in Dongsha, and 7.59-8.14 and 40-306 μmol kg^{-1} in Taiping, respectively. Spatially, pH ranged from 7.59-8.88 in Dongsha and 7.86-8.10 in Taiping.

The Dongsha atoll forms a semi-enclosed system with multiple habitats exposed to a range of residence times, with greater potential for larger modification of DIC and TA the longer a water parcel remains within the atoll due to the cumulative effect of biogeochemical processes that are unbalanced (i.e., NCC and/or NCP $\neq$ 0). The central and eastern regions of the atoll have longer residence time (15-25 days) compared to the western regions near Dongsha Island (<2 days) (Liang et al., 2020; Chen et al., 2023). In addition, the inner lagoon of the Dongsha Island creates a unique habitat with restricted mixing, high biomass to water volume ratio, and thus, an environment conducive to large biogeochemical modifications.

In contrast to Dongsha, Taiping consists of an island and a coral cay with no protective barrier reef. As a result, seawater exchanges rapidly with the surrounding open ocean and the mean seawater pH and DO more closely track open ocean conditions compared to some of the Dongsha habitats. Large diel variability is still detected in Taiping's shallow environments with high biomass to water volume ratio, but because of rapid flushing and short residence times, chemical signatures do not accumulate within this system.

The observed differences between Dongsha and Taiping highlight the uniqueness of these coral reef environments, and the need to understand current day biogeochemical variability for a range of systems in order to develop predictive capacity on the future impacts of environmental change (Disa et al., 2022).

Habitat Specific Biogeochemical Variability

The largest diel and spatial variability as well as the highest mean pH and DO values were observed across the inner lagoon (0.64 km^2) and the seagrass bed (0.72 km^2) proximal to Dongsha Island (Table 3; Table S1). The enhanced variability in these habitats was partly a product of the high density of seagrass (80+%; Huang et al., 2015) combined with the shallow water depth (1-2 m), which allowed for large biogeochemical modification of the overlying seawater due to the high biomass to water volume ratio (Falter et al., 2013; Cyronak et al., 2018). Furthermore, water exchange between the inner lagoon and the surrounding environment was strongly restricted by a narrow inlet roughly 60 m across. Water flow in and out of the lagoon followed the tidal cycle (0.51±0.06 m) with one low tide at 04:00am and one high tide at 09:30am during the study. This further exacerbated the variability in the inner lagoon, but also allowed for biogeochemical signals to accumulate, leading to both mean and extreme pH values (8.38±0.33 and 8.99) well above the pH of other habitats. The elevated pH was likely a result of both aerobic (e.g. metabolic CaCO3 dissolution) and anaerobic processes (e.g., sulfate reduction) producing alkalinity that accumulated within the lagoon due to the restricted mixing (Chou et al., 2018, 2020). The mean TA of the inner lagoon was 2535±167 μmol kg^{-1} (with values as high as 2799 μmol kg^{-1}) compared to the nearby seagrass bed, which had a mean TA of 2188±35 μmol kg^{-1}.

Although both the inner lagoon and the nearby seagrass bed experienced elevated mean pH conditions compared to other habitats, they also experienced the lowest pH conditions, which coincided with hypoxic conditions (DO < 61 μmol kg^{-1}) at night and/or in the early morning. Changes in pH and DO at the seagrass site appeared strongly coupled and correlated (R^2=0.85) while pH and DO were decoupled and only weakly correlated (R^2=0.18) in the inner lagoon. These differences probably arise from the fact that SG is an open, well-flushed habitat where pH and DO variability is most strongly controlled by production and respiration processes. In contrast, the IL

is a semi-enclosed habitat where pH in addition to production and respiration, is strongly influenced by alkalinity generation from $CaCO_3$ dissolution and anerobic processes, which may explain the observed decoupling of pH and DO (Chou et al., 2018, 2020).

In contrast to the IL and the SG, the patch reefs (0.02-0.11 km^2) experienced smaller diel amplitudes in pH and DO and lower mean pH conditions (Fig 2; Table 3, Table S1). The patch reefs were characterized by high abundance of corals, calcifying algae, other calcifiers, and shallow depth (0.5-2 m), but were defined by steep drop offs surrounded by deep lagoonal water (7-15 m). Thus, water transited the patch reefs quickly and was rapidly replenished with lagoonal water dampening local variations in seawater pH and DO.

Previous work across coral reef environments have demonstrated that shallower depths allow for the benthic community to modify the overlying seawater to a greater extent in contrast to deeper depths (Unsworth et al., 2012; Falter et al., 2013; Cyronak et al., 2018; Takeshita et al., 2018; Kekuewa et al., 2021). Therefore, it is likely that the decrease in variability can be attributed to the lower amounts of primary producers and deeper depths around both patch reefs. Slightly larger changes in TA and DIC were observed across CPR compared to EPR, which were attributed to its larger size and longer contact time between the benthos and transiting water.

Biogeochemical Processes across Dongsha and Taiping

The relative effect of NCP and NCC on seawater chemistry across each habitat and spatial scale was assessed based on the repletion (+) and depletion (-) of reef TA, DIC, and DO relative to offshore conditions. Both depletion and repletion of TA, DIC, and DO were observed across each habitat except for the patch reefs that only showed depletion of TA, DIC, and DO. Apart from the inner lagoon surveys, morning seagrass survey, and Taiping survey, every other survey on average demonstrated conditions indicative of net calcification (-dTA) and net organic carbon

production (-dDIC$_{NCP}$), demonstrating that a majority of the Dongsha Atoll and its habitats on average were in a state of net autotrophy and net calcification at the time of observations during the day. The CPR and EPR demonstrated the largest drawdown in TA (Fig 7; Table 5), which could be due to the high NCC rates on the fore reef (De Carlo et al., 2017) or the longer residence times (Liang et al., 2020). These observations match previous work that illustrate, globally coral reefs on average experience net calcification albeit with occasional times of net dissolution (mainly at night) (Fig 7; Cyronak et al., 2018). In particular, our observations indicate that Dongsha Atoll potentially experiences higher rates of net calcification in comparison to other coral reefs (Fig 7). It should be noted that the observed change in seawater carbon chemistry is relative to the offshore seawater biogeochemistry and reflects the accumulation of all biogeochemical modifications that may occur on a reef (Kekuewa et al., 2021, Suzuki and Kawahata, 2003). There is also an important caveat that except for the inner lagoon and seagrass bed habitats, all other spatial surveys lack observations during the early morning and evening, which limits our capacity to assess the full diel signal for each habitat and whether these trends balance out throughout the evening.

In general, the dTA-dDIC slopes were lower across the smaller spatiotemporal surveys, with the seagrass habitat (0.18) and inner lagoon (0.32) having the lowest slopes in comparison to the central patch reef (0.48; Table 5). These results demonstrate that across a smaller spatial and shorter temporal scales, NCP is the primary driver of seawater chemistry variability relative to NCC. The magnitude of variability is controlled by the benthic composition which is further modified by the water depth, residence time, and flow trajectory (Falter et al., 2013; Koweek et al., 2015; Cyronak et al 2018). In contrast the highest dTA-dDIC slopes were observed across the Dongsha atoll-wide surveys during both summer and winter surveys (up to 1.69 and 1.01). The higher slopes in comparison to the smaller habitat surveys is likely a result of the longer duration

of the survey as well as the increased residence time throughout the atoll. Across smaller spatial and time scales, NCP has a more significant effect on the overlying seawater chemistry relative to NCC, however on longer scales NCP is typically balanced (Gattuso et al., 1999; Falter et al., 2013; Andersson et al., 2014; Cyronak et al., 2018; Takeshita et al., 2018). As a result, over prolonged spatial and temporal scales, the impact of NCC on the overlying seawater chemistry becomes more significant compared to NCP (Cyronak et al., 2018). Although these findings demonstrated spatial heterogeneity and complexity of carbon cycling across multiple spatiotemporal scales and habitats throughout Dongsha and Taiping, there is a need to scale these results between smaller functional scales (m^2; e.g. SG or CPR) to larger, system-wide functional scales (km^2; e.g. Dongsha Atoll) (Andersson et al., 2015; Edmunds et al., 2016). This requires additional dedicated spatial surveys to better inform models of the interplay of habitat metabolism and local hydrodynamics to constrain the complexity of coral reef biogeochemical variability and ecosystems connectivity.

Seawater Biogeochemistry under Future Climate Change

As atmospheric CO_2 increases, global ocean SST, and pH, Ω_{Ar}, and DO are expected to increase and decrease, respectively (Kwiakowski et al., 2020). Inevitably, these changes may exceed physiological and functional thresholds, which can impact organism fitness and ecosystem functions (Fabricius et al., 2011; Donner, 2011; Barkley et al., 2017; Eyre et al., 2018; Nelson et al., 2019; Houk et al., 2020). To address this, recent studies have focused on identifying habitats that can alleviate detrimental conditions and/or currently experience highly variable biogeochemical conditions that may provide organismal resistance and resilience against ongoing climate change (Manzello et al., 2012; Tkachenko et al., 2017; Kapsenberg and Cyronak, 2019; Xiao et al., 2021).

In the present study, observations from the different habitats were assessed against proposed thresholds for coral reef net dissolution ($\Omega_{Ar} < 2.92$; Eyre et al., 2018) and accretion (pH < 7.7; Fabricius et al., 2011) as well as hypoxia (DO < 61 μmol kg^{-1}). Discrete seawater samples revealed that almost all habitats across Dongsha and Taiping at some point experienced $\Omega_{Ar} < 2.92$ (thresholds for reef sediment net dissolution (Eyre et al., 2018), with the exception of the EPR, while only the IL experienced pH < 7.7 (a hypothesized threshold for net reef accretion; Fabricius et al., 2011). Only the SG experienced hypoxic conditions (DO < 61 μmol kg^{-1}) (Fig 6). Thus, habitats across Dongsha and Taiping are currently exposed to a combination of acidic and hypoxic conditions, which may be negatively affecting coral reef function.

Notably, the SG and IL experienced the highest average pH and Ω_{Ar} conditions compared to other habitats and spatial scales, which may lead to the interpretation that these habitats may act as OA refugia. However, these habitats also experienced the lowest pH, Ω_{Ar}, and DO conditions with the highest percentage of observations below critical thresholds, which muddles such an interpretation. It is not fully established whether marine organisms will be most sensitive to a decrease in mean pH, Ω_{Ar}, and DO or the increase in magnitude of extremes (Kroeker et al., 2010; Andersson et al., 2014), and how chronic and acute stress events may interact. The magnitude and duration of such events will certainly be important to consider. Regardless, this study shows that the current seagrass habitats already experience potentially detrimental acidic and hypoxic conditions, adding doubts to whether seagrass habitats may act as a refugia for corals under ongoing climate change (Cyronak et al., 2018; Kapsenberg and Cyronak, 2019).

Previous studies have demonstrated that the tolerance, acclimatization, and adaptation potential of coral reef organisms are not fully understood in context to the current day spatiotemporal biogeochemical variability (Anthony et al., 2008; Barkley et al., 2017; Comeau et

al., 2018; Albright et al., 2018; Langdon et al., 2018). For example, marine organisms that experience large diel variability may be better adapted to ongoing climate change and thus more resilient, or potentially they are near their absolute threshold and thus more vulnerable to climate change (Kroeker et al., 2020). Increased coral reef laboratory studies that utilize relevant, *in situ* field observations will be extremely important in assessing organism-specific sensitivity and tolerance levels to future conditions and to better assess which habitats may serve as a refugia.

Based on current emission scenarios, our projections reveal that by the year 2100 all habitats will experience detrimental pH and Ω_{Ar} conditions. However, the inner lagoon, northern shore seagrass bed, and eastern patch reef were projected to experience pH < 7.7 and Ω_{Ar} < 2.92 conditions for a lower percentage of observations compared to the other habitats, suggesting that they may act as an OA refugia (Fig 6). This matches our general understanding of reduced exposure to harmful conditions due elevated pH driven by enhanced NCP in the inner lagoon and seagrass habitats (Manzello et al., 2012; Chou et al., 2018; Chou et al., 2020). These results reveal 10%, 44%, and 77% of the observations in the IL, SG, and EPR by 2100 will be Ω_{Ar} < 2.92 in comparison to 100% of observation from every other habitat. Importantly we observed that there was no change in Ω_{Ar} < 2.92 exposure from current day to the year 2100 in the IL and only a 5% increase in exposure to pH < 7.7. This is likely due to the high TA in the inner lagoon, which buffers the system to future OA conditions, but it also affected by the high SST which would lead to a decrease in pH and increase in Ω_{Ar}.

In comparison to the IL and SG habitats the EPR does not have as high a percentage of seagrass and instead is primarily composed of corals (Tkachenko et al., 2017). Nevertheless, the EPR may still act as an OA refugia due to the external influence of internal waves. The Dongsha Atoll fore reef and reef flat have been observed to be a terminus point for internal waves, which

brings cold, nutrient rich seawater to the local coral community (Davis et al., 2020; Reid et al., 2019). This allochtonous source of nutrition could potentially provide resistance against OA (Towle et al., 2015) and even stimulate high rates of calcification (Yeakel et al., 2015). Previous studies on the Dongsha reef flat documented large diurnal signals with elevated daytime pH and Ω_{Ar} values of 8.5 and 5.5, respectively, which indicate high rates of primary production that also coincided with an estimated NCC rate of 390±90 mmol $CaCO_3$ m^{-2} d^{-1} (De Carlo et al., 2017).

Our DO projections based on discrete seawater suggests that by the year 2100 only the SG habitat will experience hypoxia thresholds ranging from mild to severe (i.e., 153 to < 61 µmol kg^{-1}; Pezner et al., 2023). It is important to note that the discrete seawater samples did not account fully capture the diel minimum at a time point where we would expect to see peak respiration (e.g., prior to sunrise), which was observed via autonomous sensors deployed in the inner lagoon and seagrass habitats (Fig 2). Previous work projects that hypoxic events are likely to also increase in duration, frequency, and intensity under future climate change conditions (Pezner et al., 2023).

Comprehensively, this study captures the natural, current day biogeochemical variability of two coral reef systems in the South China Sea and demonstrates elevated pH and Ω_{Ar} conditions across the seagrass, inner lagoon, and eastern patch reef habitats of Dongsha atoll. However, we note that due to the short duration of the study our observations are limited to the summertime and only the seagrass bed had early morning DO measurements, which limits our capacity to assess whether these projections for each habitat is maintained seasonally and on a diel cycle. Based on our current understanding of seasonal coral reef biogeochemistry variability, we would assume to observe an increase in pH and DO during the wintertime due lower temperatures and decreased respiration and calcification rates (Muehllehner et al., 2016; Ganguly et al., 2017). Increased spatiotemporal observations like this study will enable us to better understand the interplay of

biogeochemical variability, community metabolism, and local hydrodynamics allowing for better constrained models (Cyronak et al., 2018; Kekuewa et al., 2021; Disa et al., 2022).

Table 3.1. Description of habitats and sampling scheme for each spatial survey

Station	Surface area	Survey dates (and time)	Samples per survey	Description of benthic habitat
Dongsha Atoll	**250 km^2**	June 29 (09:04-15:03), July 2 (09:22-16:30), and July 6 (09:32-16:32), 2018	24	Circular atoll 28 km in diameter surrounded by a fringing reef which varies from 1-3 km in width with a central lagoon which has an average depth range of 10-15 m and contains many scattered patch reefs of varying size
Donsha Island Inner Lagoon	**0.64 km^2**	June 27 (10:00-11:26 & 15:30-17:02) and June 30 (06:18-07:20 & 12:30-13:37), 2018	10	A semi-enclosed lagoon with a surface area of 0.64 km^2 and a mean seagrass coverage of 85% with an inlet located on the western side of the lagoon that provides the only source of seawater exchange
Dongsha Island North Shore Seagrass	**0.72 km^2**	June 26 (15:13-16:21), June 27 (11:04-11:56), and June 30 (06:34-07:15 & 12:43-13:27), 2018	12	The survey covered a surface area of ~0.7 km^2 however the entire seagrass meadows extended up to 1 km offshore with a depth range of 0.1-3 m, covering ~1.85 km^2 with scattered coral colonies and 81% mean seagrass cover
Central Patch Reef	**0.11 km^2**	July 8 (11:07-11:43), 2018	12	Located near the center of the atoll lagoon the CPR has an area of ~0.1 km^2 with a depth range of 0.5-1.5 m and was predominately covered by hard coral (60+%) and surrounded by deeper (~8 m) sand flats
Eastern Patch Reef	**0.02 km^2**	July 8 (14:32-15:10), 2018	13	Located 1.5 km from the reef flat on the eastern side of the lagoon the EPR has an area of ~0.02 km^2 with a depth range of 0.5-1 m and was predominately covered by hard coral and surrounded by sand flats (~5 m)
Taiping (all)	**20 km^2**	March 30 (08:31-16:20), 2019	50	Taiping Island is an oceanic reef and the largest island of the Spratly Islands in the southern South China Sea located ~1200 km south of Dongsha
Taiping Island	**1.5 km^2**	March 30 (13:39-14:20), 2019	13	Part of the Spratly islands, Taiping Island is surrounded by shallow seagrass beds that transition into a reef flat (1–4 m in depth) extending ~50 m offshore followed by a steep drop off
Banthan	**1.1 km^2**	March 30 (08:31- 11:00), 2019	21	Located ~4 km east of Taiping Island, Banthan is a coral with a surface area of 1.12 km^2 and is covered by an assemblage of seagrass, hard coral, and coral rubble

Table 3.2. Autonomous sensor deployment locations, dates, instruments, parameters, and benthic habitats

Station	Duration date	Longitude (° N)	Latitude (° E)	Instruments	Parameters measured	Description of benthic habitat
North Shore Seagrass	July 1 – July 8, 2018	20.7074	116.7214	IDRONAUT	T, S, DO, pH (every 15 min)	Seagrass bed at 0.9 m
Inner Lagoon Inlet	June 26 – July 1, 2018	20.7056	116.7117	Seafet Seabird w/ O_2	T, S, pH (every 10 min) T, S, DO (every 10 min)	Seagrass bed at 1.8 m
Inner Lagoon	June 26 – July 1, 2018	20.7016	116.7237	IDRONAUT	T, S, DO, pH (every 15 min)	Seagrass bed at 0.7 m
Central Patch Reef	July 1 – July 8, 2018	20.7059	116.8081	IDRONAUT Seabird	T, S, DO, pH (every 15 min) T, S (every 10 min)	Mixed coral at 2 m
Eastern Patch Reef	July 1 – July 8, 2018	20.7021	116.8896	Seafet Seabird w/ O_2	T, S, pH (every 10 min) T, S, DO (every 10 min)	Mixed coral at 2 m
Taiping Seagrass	March 29 – March 31, 2019	10.3765	114.3700	Seafet MiniDOT	T, S, pH (every 10 min) T, DO (every 10 min)	Seagrass bed at 1 m
Taiping Reef	March 29 – March 31, 2019	10.3756	114.3704	SeapHOx	T, S, P, DO, pH (every 10 min)	Mixed coral at 2.5 m

Table 3.3. Average diel mean (± SD), diel range (± SD), and minimum – maximum seawater pH_T, DO, and temperature from autonomous instrument data across all stations

Site	Habitat	pH_T			DO (µmol kg^{-1})			Temperature (°C)		
		Mean	Range	Min-Max	Mean	Range	Min-Max	Mean	Range	Min-Max
CPR	Coral	7.79±0.09	0.29±0.16	7.61-8.06	133±29	100±60	70-281	30.0±0.3	0.7±0.1	29.3-31.0
EPR	Coral	7.87±0.05	0.19±0.06	7.74-8.03	136±38	121±45	64-267	29.8±0.1	0.8±0.2	29.3-30.6
SG	Seagrass	8.04±0.16	0.53±0.02	7.67-8.36	115±56	187±14	16-217	30.7±0.3	2.3±0.2	29.1-32.1
ILI	Seagrass Lagoon	8.03±0.26	0.91±0.09	7.41-8.54	124±102	269±6	0-273	31.0±0.4	5.6±0.8	27.8-34.9
IL	Seagrass Lagoon	8.60±0.10	0.41±0.12	8.31-8.89	150±38	142±20	46-250	32.8±0.5	5.3±1.2	29.8-36.6
TPSG	Seagrass	7.88±0.02	0.55±0.01	7.59-8.14	160±66	111±34	40-306	28.3±0.1	3.5±0.7	26.6-30.6
TPR	Coral	7.93±0.07	0.24±0.08	7.73-8.02	155±34	123±17	87-222	28.9±0.1	1.2±0.0	28.3-29.6

Table 3.4. Average time of observed daily minimum (± SD) and maximum (± SD) of seawater pH_T, DO, and temperature from autonomous instrument data across all stations

Site	Habitat	pH_T		DO (μmol kg^{-1})		Temperature (°C)	
		Time of Daily Min	Time of Daily Max	Time of Daily Min	Time of Daily Max	Time of Daily Min	Time of Daily Max
CPR	**Coral**	05:08±1:18	13:48±0:35	04:53±1:08	13:40±0:53	06:12±0:38	17:25±1:51
EPR	**Coral**	05:35±0:33	14:22±0:10	05:40±0:27	14:13±1:01	07:47±0:48	17:52±1:06
SG	**Seagrass**	05:25±0:31	15:18±0:58	05:15±0:33	15:25±0:45	07:35±0:59	17:54±0:58
ILI	**Seagrass Lagoon**	04:53±0:29	17:25±0:24	04:10±0:24	16:10±0:08	05:32±0:51	16:53±0:17
IL	**Seagrass Lagoon**	09:15±0:44	18:38±1:44	07:30±1:12	18:08±1:26	08:03±0:23	16:23±0:15
TPSG	**Seagrass**	05:40±0:00	13:30±0:14	04:00±0:00	12:25±0:07	06:55±0:50	14:15±0:36
TPR	**Coral**	5:05±2:00	12:35±0:50	04:30±0:42	12:35±0:35	05:55±0:50	12:30±0:14

Table 3.5. Slope, R^2, and associated *p*-value of dTA-dDIC and dDO-$dDIC_{NCP}$ as well as mean dDIC, dTA, and dDO for all individual spatial surveys.

Site	Area	dTA-dDIC slope (R^2)	*p*-value	dDO-dNCP slope (R^2)	*p*-value	Mean dDIC	Mean dTA	Mean dDO
Atoll mean	**250 km²**	**1.27 (0.82)**	**<0.001**	**-1.00 (0.24)**	**<0.001**	-63±37	-100±46	-1±19
Atoll June 29	-	**1.13 (0.88)**	**<0.001**	**-0.88 (0.35)**	**0.001**	-67±42	-96±47	5±20
Atoll July 2	-	**1.27 (0.93)**	**<0.001**	-0.74 (0.04)	0.295	-57±44	-93±56	-1±18
Atoll July 6	-	**1.69 (0.48)**	**<0.001**	**-1.32 (0.38)**	**<0.001**	-65±21	-111±30	-6±18
IL mean	**0.64 km²**	0.14 (0.01)	0.558	-	-	-45±251	335±181	-
IL June 27 1000	-	7.93 (0.01)	0.765	-	-	-41±156	356±235	-
IL June 27 1600	-	**0.32 (0.50)**	**0.034**	-	-	-212±231	371±97	-
IL June 30 0630	-	-0.03 (0.00)	0.948	-	-	136±280	355±189	-
IL June 30 1300	-	0.13 (0.01)	0.830	-	-	-82±223	247±165	-
Seagrass mean	**0.72 km²**	**0.18 (0.45)**	**<0.001**	**-0.52 (0.89)**	**<0.001**	-94±162	-47±43	30±79
Seagrass June 26 1530	-	0.21 (0.10)	0.329	**-0.34 (0.65)**	**0.001**	-330±111	-89±57	135±42
Seagrass June 27 1130	-	**0.47 (0.88)**	**<0.001**	**-0.33 (0.37)**	**0.035**	-87±160	-42±54	30±44
Seagrass June 30 0700	-	0.24 (0.05)	0.478	**-1.26 (0.68)**	**0.001**	69±38	-25±25	-50±73
Seagrass June 30 1300	-	0.31 (0.30)	0.066	**-0.59 (0.76)**	**<0.001**	-57±58	-43±17	20±46
CPR July 8 1100	**0.11 km²**	**0.48 (0.65)**	**0.002**	**-0.55 (0.81)**	**<0.001**	-89±27	-139±15	-4±12
EPR July 8 1500	**0.02 km²**	0.22 (0.21)	0.116	**-0.35 (0.40)**	**0.021**	-137±16	-132±7	12±7
Taiping mean	**20 km²**	**0.64 (0.56)**	**<0.001**	-	-	1±29	1±21	-
Banthan	**1.1 km²**	**-0.24 (0.29)**	**0.010**	-	-	7±18	0±7	-
Taiping Is.	**1.5 km²**	**0.76 (0.86)**	**<0.001**	-	-	-8±54	3±42	-
TAO Atoll mean	**250 km²**	**1.61 (0.42)**	**<0.001**	**-0.37 (0.40)**	**<0.001**	-31±33	-71±45	2±13
TAO Atoll Aug 2015	-	**1.51 (0.72)**	**<0.001**	**-0.25 (0.18)**	**0.042**	-34±30	-79±42	-1±8
TAO Atoll Aug 2016	-	**1.15 (0.45)**	**<0.001**	**-0.30 (0.57)**	**<0.001**	-30±45	-94±50	-3±13
TAO Atoll Nov 2016	-	**1.01 (0.65)**	**<0.001**	**-1.16 (0.19)**	**0.035**	-29±20	-40±20	9±14

Note. No dissolved oxygen data was collected for Taiping and Dongsha inner lagoon so there is no associated dDO-$dDIC_{NCP}$ comparison. Bold values are significant at $p < 0.05$.

Table S3.1. Mean (± SD), minimum, and maximum values of physical and biogeochemical seawater properties from discrete seawater samples for the mean and each individual spatial survey

Site	Area	TA (µmol kg^{-1})	DIC (µmol kg^{-1})	DO (µmol kg^{-1})	pH_T	Ω_{Ar}	pCO_2 (µatm)	Temp (°C)
Atoll mean	**250 km^2**	2132±38 (2074-2232)	1859±30 (1810-1937)	195±19 (144-245)	7.96±0.04 (7.89-8.04)	3.15±0.21 (2.74-3.64)	463±41 (378-557)	29.9±0.7 (28.1-31.2)
Atoll June 29	-	2137±43 (2074-2227)	1857±40 (1810-1937)	201±20 (144-245)	7.98±0.03 (7.90-8.03)	3.22±0.17 (2.78-3.61)	445±34 (400-554)	29.8±0.8 (28.1-30.9)
Atoll July 2	-	2133±39 (2080-2230)	1860±28 (1819-1937)	195±18 (171-239)	7.97±0.03 (7.92-8.04)	3.15±0.18 (2.84-3.64)	457±31 (388-515)	29.7±0.6 (28.3-30.8)
Atoll July 6	-	2125±30 (2091-2232)	1860±19 (1825-1919)	190±18 (165-242)	7.95±0.04 (7.89-8.04)	3.06±0.23 (2.74-3.59)	485±45 (378-557)	30.1±0.5 (28.8-31.2)
IL mean	**0.64 km^2**	2535±167 (2157-2799)	1863±253 (1328-2504)	-	8.38±0.33 (7.59-8.88)	7.87±3.14 (1.81-12.49)	255±333 (23-1536)	31.7±1.8 (28.3-35.9)
IL June 27 1000	-	2531±197 (2224-2690)	1850±159 (1622-2105)	-	8.41±0.26 (8.05-8.77)	7.99±2.90 (3.99-11.64)	176±122 (41-379)	31.5±0.3 (31.1-32.2)
IL June 27 1600	-	2259±95 (2403-2631)	1684±231 (1328-2051)	-	8.60±0.19 (8.27-8.88)	10.16±1.65 (6.98-12.49)	86±63 (23-229)	34.2±1.0 (32.8-35.9)
IL June 30 0630	-	2577±188 (2237-2799)	2055±278 (1624-2504)	-	8.18±0.43 (7.59-8.70)	6.22±3.71 (1.81-11.45)	525±557 (57-1536)	29.7±1.0 (28.3-31.2)
IL June 30 1300	-	2475±171 (2157-2651)	1844±171 (1501-2201)	-	8.35±0.28 (8.01-8.81)	7.32±2.91 (3.41-11.82)	216±146 (32-436)	32.0±1.1 (29.9-33.8)
Seagrass mean	**0.72 km^2**	2188±35 (2107-2263)	1832±157 (1397-2056)	225±79 (61-393)	8.07±0.18 (7.73-8.49)	4.06±1.42 (2.04-7.88)	391±195 (80-890)	30.4±1.8 (28.3-35.5)
Seagrass June 26 1530	-	2146±37 (2107-2233)	1601±102 (1397-1739)	330±42 (263-393)	8.32±0.11 (8.20-8.49)	6.07±1.14 (4.83-7.88)	162±55 (80-234)	32.9±1.6 (30.5-35.5)
Seagrass June 27 1130	-	2189±7 (2178-2197)	1865±32 (1836-1933)	214±20 (187-245)	8.05±0.05 (7.95-8.09)	3.72±0.38 (2.94-4.11)	378±59 (334-507)	29.7±0.8 (28.7-31.0)
Seagrass June 30 0700	-	2217±24 (2168-2263)	1999±37 (1952-2056)	130±45 (61-190)	7.86±0.08 (7.73-7.97)	2.62±0.39 (2.04-3.15)	653±145 (480-890)	28.6±0.4 (28.3-29.6)
Seagrass June 30 1300	-	2199±17 (2161-2223)	1863±35 (1819-1904)	227±20 (199-260)	8.05±0.05 (7.99-8.12)	3.85±0.31 (3.52-4.32)	372±50 (299-437)	30.3±0.3 (29.8-30.8)
CPR July 8 1100	**0.11 km^2**	2087±13 (2066-2108)	1827±25 (1796-1864)	192±12 (175-208)	7.94±0.03 (7.89-8.00)	3.01±0.17 (2.65-3.35)	487±44 (412-558)	30.7±0.1 (30.5-30.8)

Table S3.1. Mean (± SD), minimum, and maximum values of physical and biogeochemical seawater properties from discrete seawater samples for the mean and each individual spatial survey. (Continued)

EPR July 8 1500	**0.02 km²**	2113±6 (2099-2121)	1796±15 (1774-1827)	208±7 (199-224)	8.02±0.02 (7.98-8.06)	3.61±0.15 (3.35-3.85)	385±26 (345-439)	31.2±0.1 (31.1-31.4)
Taiping mean	**20 km²**	2210±20 (2157-2330)	1914±28 (1801-2034)	-	8.00±0.03 (7.86-8.10)	3.43±0.20 (2.56-4.04)	430±42 (318-637)	29.2±0.7 (28.0-31.9)
Banthan	**1.1 km²**	2209±6 (2195-2221)	1919±17 (1905-1982)	-	8.00±0.04 (7.86-8.03)	3.36±0.23 (2.56-3.56)	434±50 (397-633)	28.7±0.1 (28.5-28.9)
Taiping Is.	**1.5 km²**	2212±43 (2157-2330)	1906±56 (1801-2034)	-	8.01±0.04 (7.95-8.10)	3.55±0.23 (3.33-4.04)	421±5- (318-520)	29.9±1.1 (28.8-31.9)
TAO Atoll mean	**250 km²**	2156±46 (2075-2238)	1883±35 (1796-1985)	189±17 (152-236)	7.97±0.07 (7.77-8.08)	3.15±0.36 (2.13-3.82)	463±90 (348-765)	29.0±1.3 (26.9-31.2)
TAO Atoll Aug 2015	-	2151±42 (2084-2238)	1868±30 (1796-1916)	201±8 (184-226)	7.98±0.04 (7.93-8.05)	3.28±0.26 (2.93-3.82)	450±43 (368-514)	30.2±0.6 (28.5-31.2)
TAO Atoll Aug 2016	-	2128±50 (2075-2220)	1887±45 (1816-1985)	173±13 (152-195)	7.91±0.07 (7.77-8.02)	2.83±0.41 (2.13-3.60)	545±104 (414-765)	29.7±0.4 (29.0-30.3)
TAO Atoll Nov 2016	-	2188±20 (2153-2238)	1895±20 (1866-1953)	193±14 (166-236)	8.03±0.02 (7.99-8.08)	3.33±0.13 (3.08-3.64)	396±23 (348-445)	27.3±0.3 (26.9-27.8)

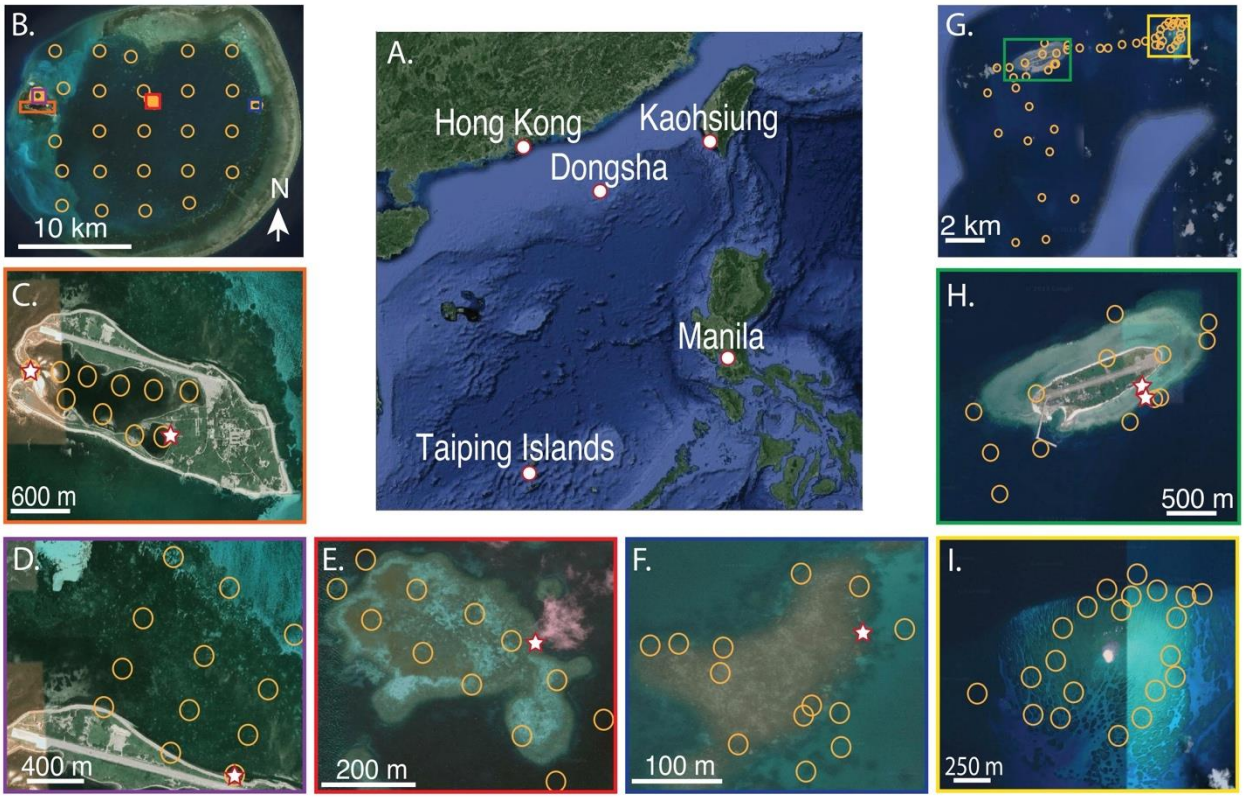

Figure 3.1. (**A**) Map and satellite image (Google Earth) of the South China Sea showing locations of survey locations and major cities in white dots. Spatial surveys are shown for (**B**) Dongsha Atoll, (**C**) Dongsha Inner Lagoon, (**D**) Dongsha Seagrass, (**E**) Central Patch Reef, (**F**) Eastern Patch Reef, (**G**) Taiping, (**H**) Taiping Island, and (**I**) Banthan including location of discrete seawater sampling (orange open circles) and autonomous sensor deployments sites (white stars).

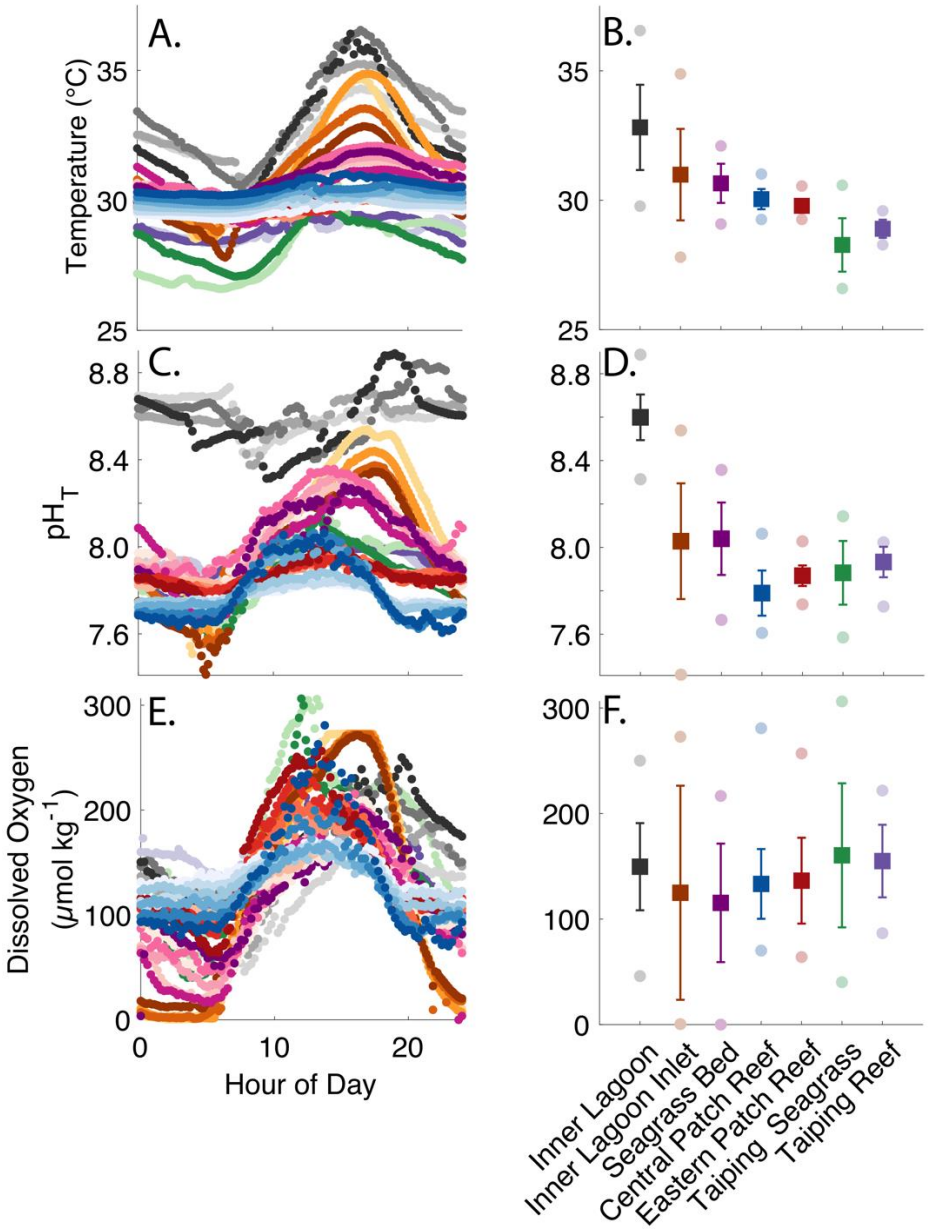

Figure 3.2. Daily climatology and mean conditions of seawater temperature (**A, B**), pH (**C, D**), and dissolved oxygen (**E, F**). Climatology plots (**A, C, E**) are colored from lighter to darker colors, where the lightest color denotes the first day and the darkest color denotes the last day for each specific site. Error plots for each site (**B, D, F**) show mean (± SD), minimum, and maximum.

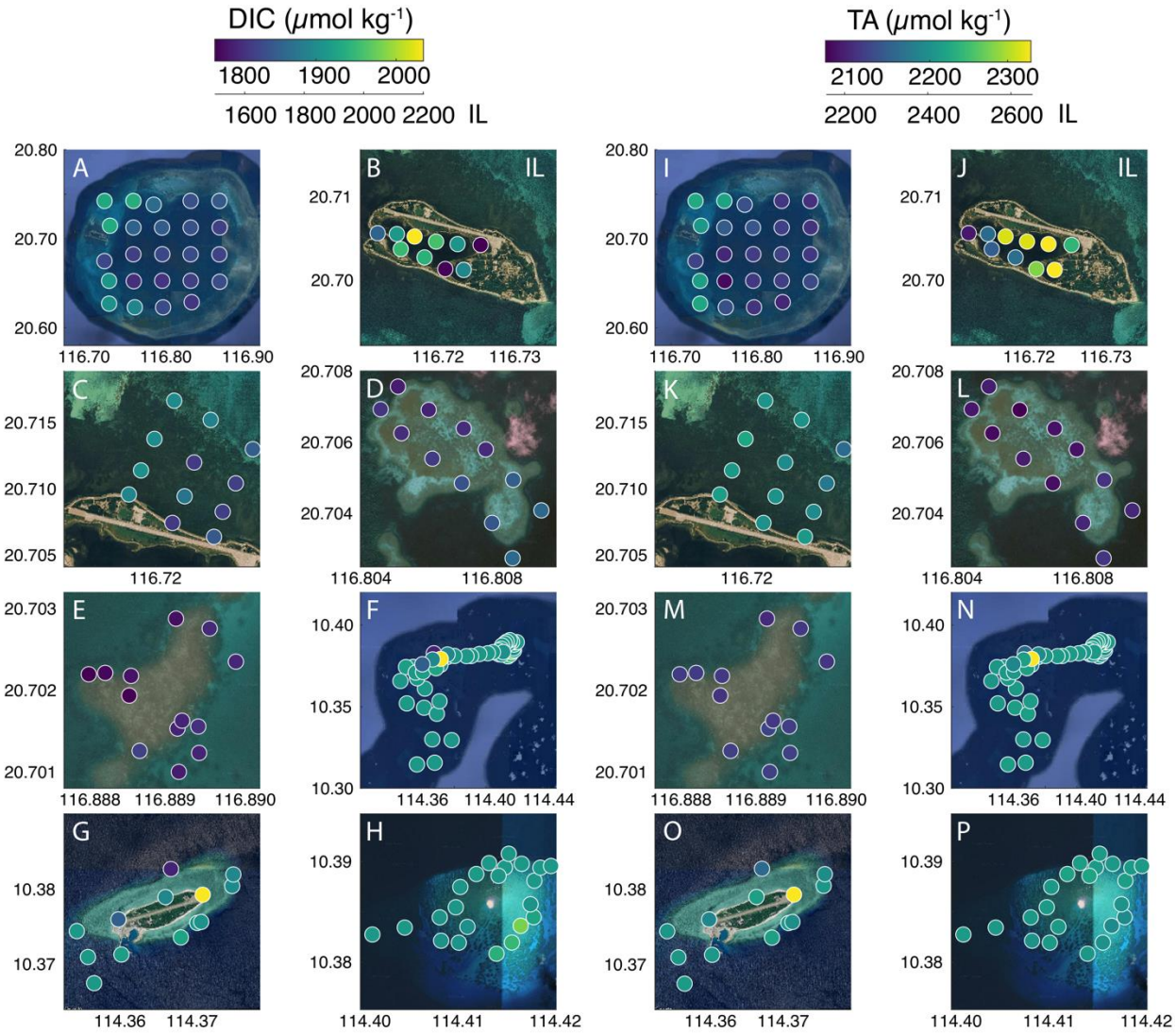

Figure 3.3. Colored scatters dots showing spatial distribution of DIC (**A-H**) on Dongsha Atoll (**A**), Dongsha Inner Lagoon (**B**), Dongsha Seagrass (**C**), Central Patch Reef (**D**), Eastern Patch Reef (**E**), Taiping (**F**) Taiping Island (**G**), and Banthan (**H**) as well as spatial distribution of TA (**I-P**) on Dongsha Atoll (**I**), Dongsha Inner Lagoon (**J**), Dongsha Seagrass (**K**), Central Patch Reef (**L**), Eastern Patch Reef (**M**), Taiping (**N**) Taiping Island (**O**), and Banthan (**P**) for a single afternoon survey. All spatial surveys, besides the IL, share the same colorbar axis (upper) for both DIC and TA. The IL has its' own colorbar axis (lower).

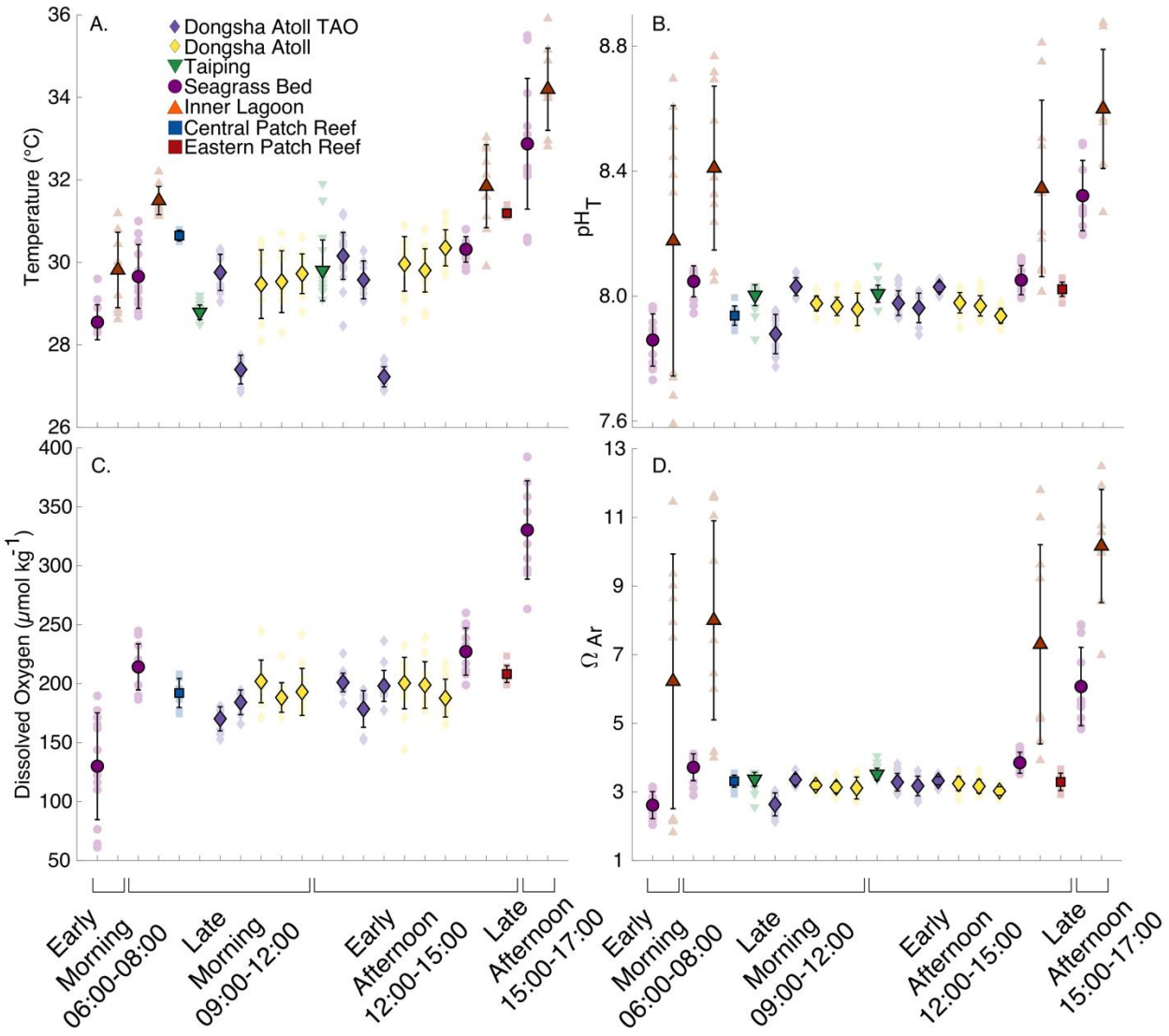

Figure 3.4. Mean (± SD) of seawater temperature (**A**), pH (**B**), DO (**C**), and Ω_{Ar} (**D**) variability for each individual spatial survey organized by the average time of the survey and grouped into early morning (06:00-08:00), late morning (09:00-12:00), early afternoon (12:00-15:00), and late afternoon (15:00-17:00). Shapes denote the type of habitat/spatial survey conducted while the background marks denote the discrete observed values. Large surveys across Dongsha Atoll (yellow and purple diamonds) and Taiping (green triangles) were split into late morning and early afternoon surveys to compare observed differences from time of day.

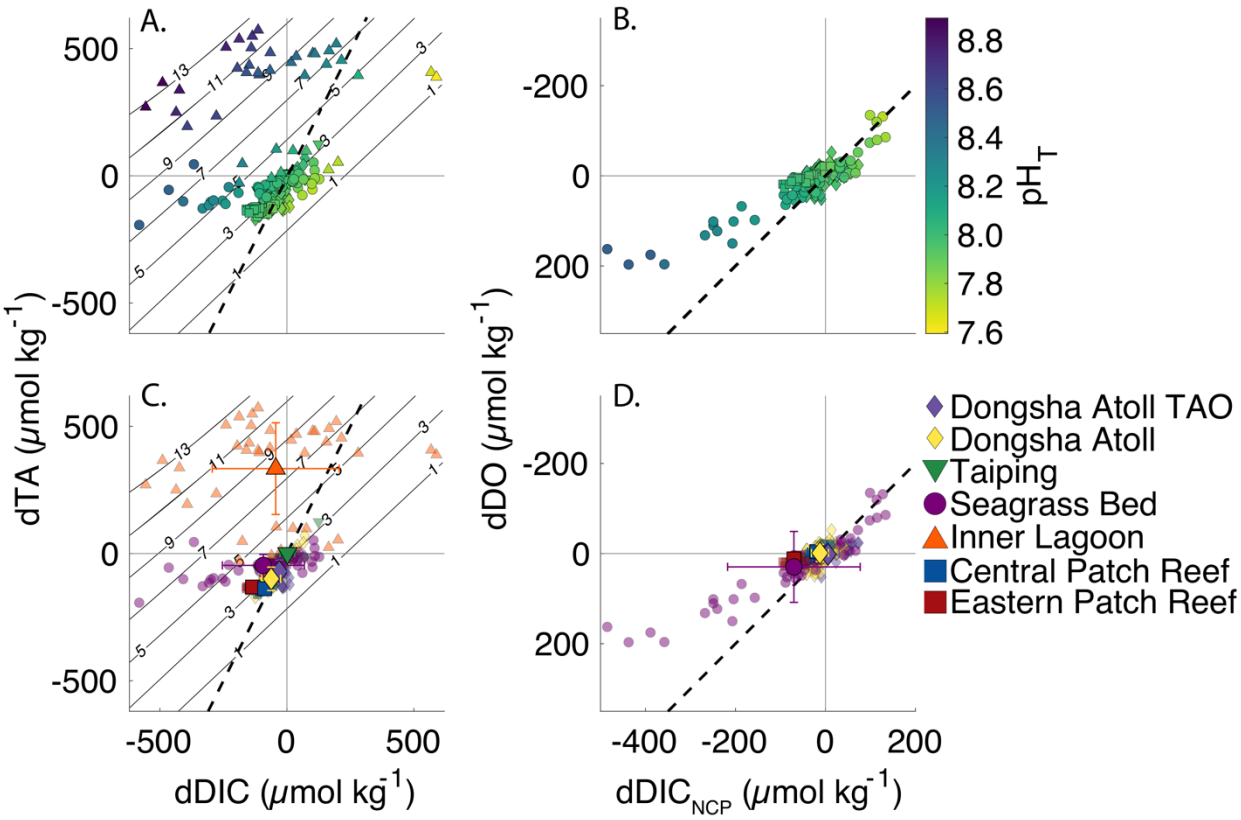

Figure 3.5. Property-property plots of the difference between reef and offshore salinity normalized properties; (**A**, **C**) dTA vs. dDIC and (**B**, **D**) dDO vs. $dDIC_{NCP}$ with colors in (**A**, **B**) indicating pH and in (**C**, **D**) showing the values as well as average for each type of spatial survey. Black contour lines in (**A, C**) show aragonite saturation. Type II linear regressions of dTA vs. dDIC and for dDO vs. $dDIC_{NCP}$ are available in Table 5. Black-dashed line in (**A, C**) demonstrates the TA/DIC 2:1 stoichiometric ratio while in (**B, D**) demonstrates the idealized DO/DIC quotient in coral reefs of -1:1. However it should be noted that for (**B, D**) the y-axis is reversed.

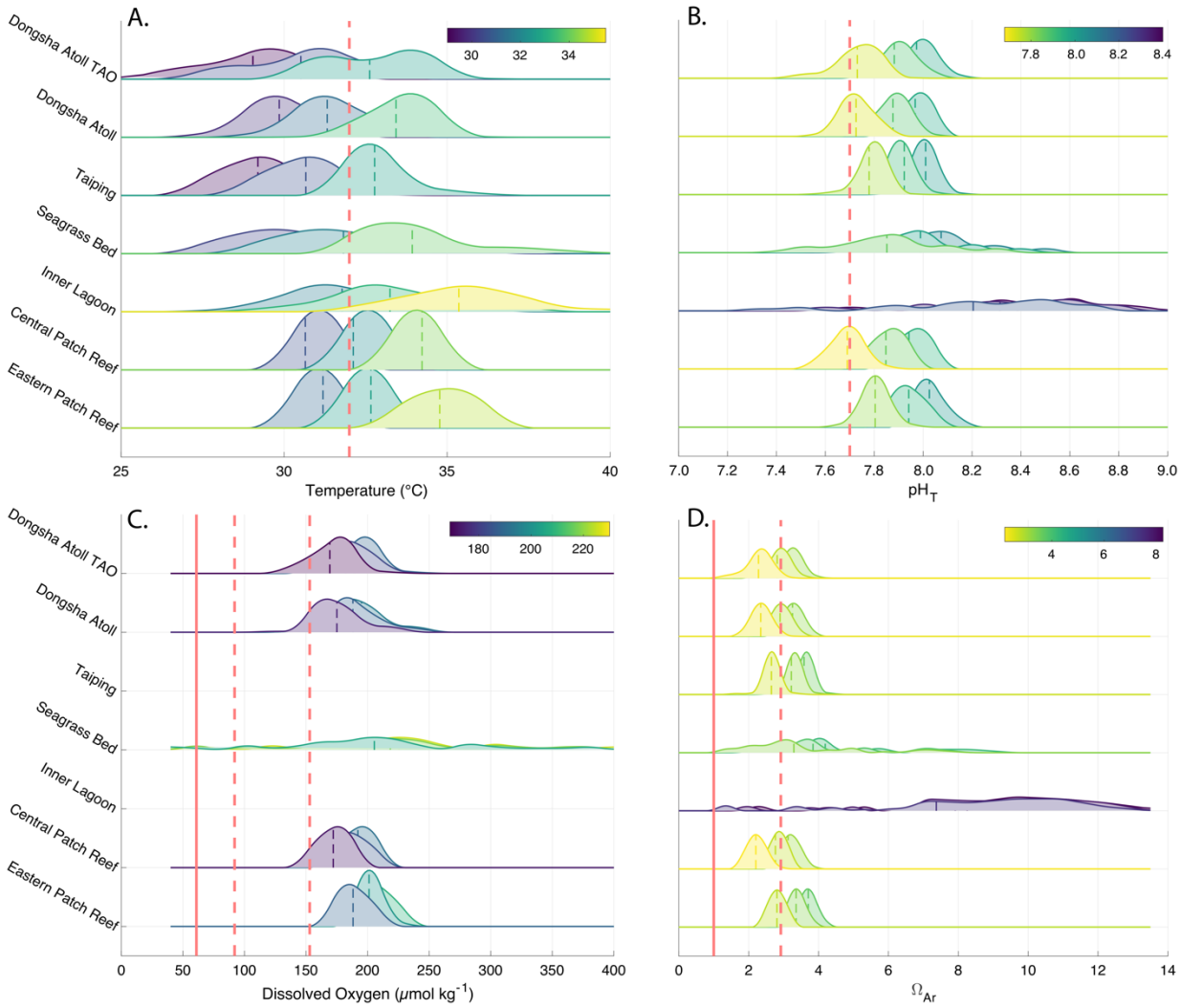

Figure 3.6. Density plots showing frequency distribution of observations of seawater temperature (**A**), pH (**B**), DO (**C**), and Ω_{Ar} (**D**) for all seawater samples across each habitat. Additional peaks show predicted values following CMIP6 RCP 8.5 temperature increases (**A**), an annual 1.15 umol kg^{-1} increase in nDIC following Kosugi et al., 2023 (**B, D**), and predicted decrease in DO following Pezner et al., 2023 (**C**) by the years 2050 and 2100. Red lines for temperature = 32 °C depicts bleaching threshold (Shoepf et al., 2015), pH = 7.7 depicts loss of coral (Fabricius et al., 2011), DO = 153, 92, 61 µmol kg^{-1} depicts weak, moderate, and severe hypoxia (Pezner et al., 2023), and Ω_{Ar} = 2.92 (Bates et al., 2014) is the threshold wherein reef sediments have been observed to shift from net precipitation to net dissolution and Ω_{Ar} = 1 where calcium carbonate is thermodynamically induced to dissolve.

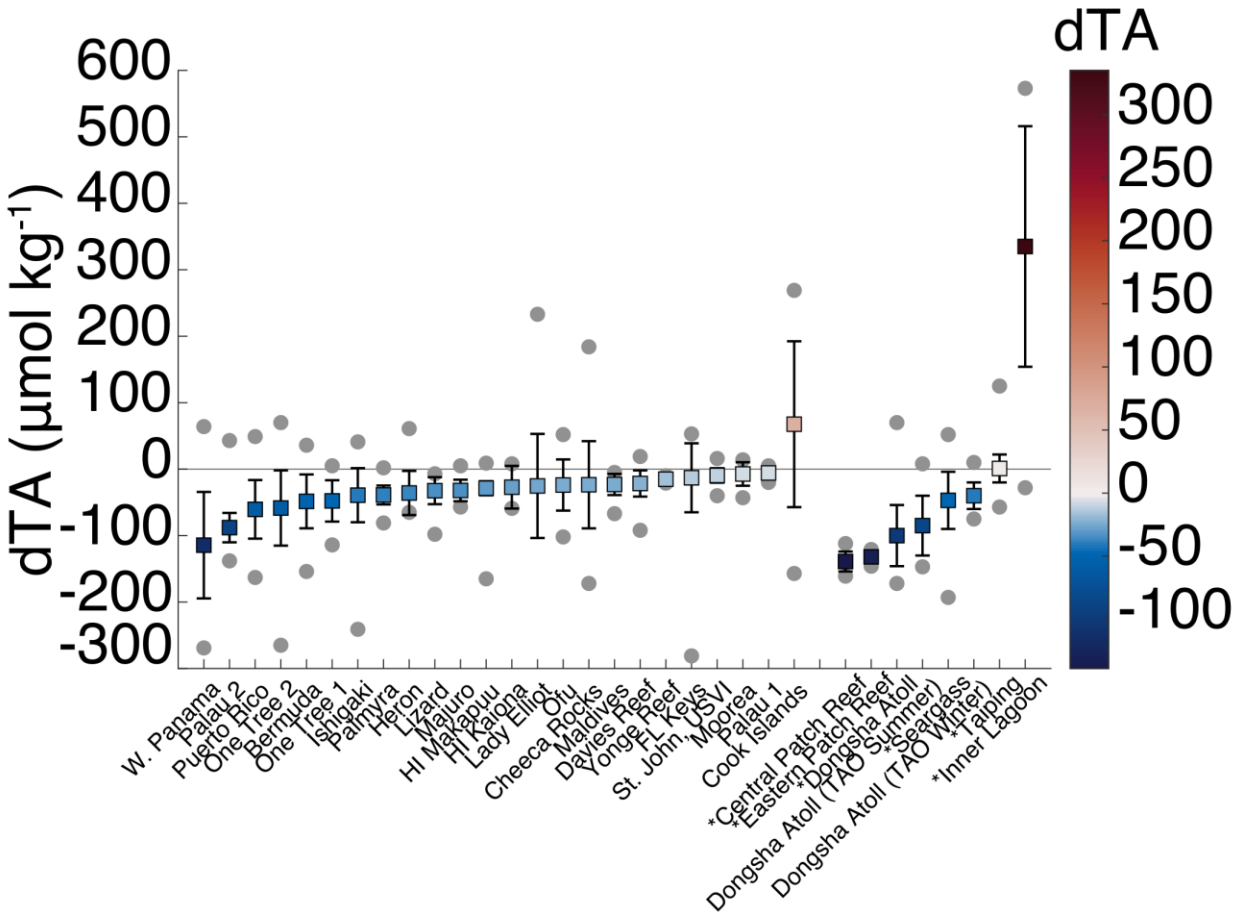

Figure 3.7. Scatter plot of total alkalinity anomalies (dTA) between the open ocean and coral reef concentrations from global coral reef locations (Cyronak et al., 2018) and this study. Negative values indicate enhanced TA drawdown within the reef and represent net calcification (+NCC; blue colors), while positive values indicate an increase in TA and represent net dissolution (-NCC; red colors). Colored squares represent the mean anomaly for each location, while the errorbars represent one standard deviation. Grey circles are the observed maximum and minimum TA anomalies for each location.

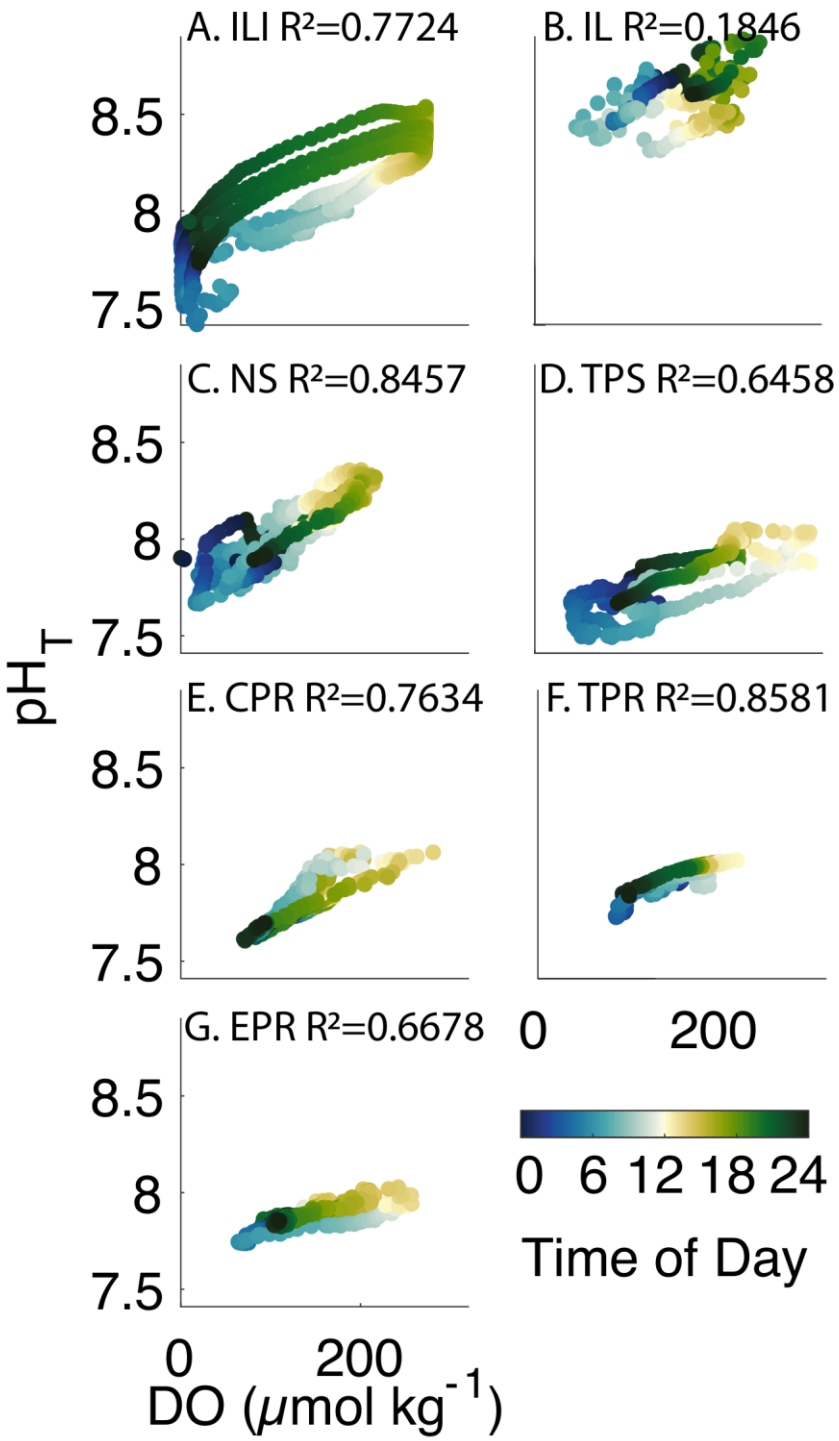

Supplement Figure 3.1. Scatter plots show pH – dissolved oxygen correlation plots for each autonomous sensor site. Points are colored by time of day with correlations (R^2) listed on the top of each subplot.

References

Albright, R., Benthuysen, J., Cantin, N., Caldeira, K. and Anthony, K. (2015) Coral reef metabolism and carbon chemistry dynamics of a coral reef flat, *Geophysical Research Letters,* 42(10), 3980-3988.

Albright, R., Takeshita, Y., Koweek, D. A., Ninokawa, A., Wolfe, K., Rivlin, T., Nebuchina, Y., Young, J. and Caldeira, K. (2018) Carbon dioxide addition to coral reef waters suppresses net community calcification, *Nature*, 555(7697), 516-519.

Altieri, A. H., Harrison, S. B., Seemann, J., Collin, R., Diaz, R. J. and Knowlton, N. (2017) Tropical dead zones and mass mortalities on coral reefs, *Proceedings of the National Academy of Sciences*, 114(14), 3660-3665.

Andersson, A. J., Kline, D. I., Edmunds, P. J., Archer, S. D., Bednaršek, N., Carpenter, R. C., Chadsey, M., Goldstein, P., Grottoli, A. G. and Hurst, T. P. (2015) Understanding ocean acidification impacts on organismal to ecological scales, *Oceanography,* 28(2), 16-27.

Andersson, A. J., Yeakel, K. L., Bates, N. R. and De Putron, S. J. (2014) Partial offsets in ocean acidification from changing coral reef biogeochemistry, *Nature Climate Change,* 4(1), 56-61.

Anthony, K. R., Kline, D. I., Diaz-Pulido, G., Dove, S. and Hoegh-Guldberg, O. (2008) Ocean acidification causes bleaching and productivity loss in coral reef builders, *Proceedings of the National Academy of Sciences,* 105(45), 17442-17446.

Atkinson, M. and Smith, S. (1983) C: N: P ratios of benthic marine plants 1, *Limnology and Oceanography,* 28(3), 568-574.

Barkley, H. C., Cohen, A. L., McCorkle, D. C. and Golbuu, Y. (2017) Mechanisms and thresholds for pH tolerance in Palau corals, *Journal of Experimental Marine Biology and Ecology,* 489, 7-14.

Bresnahan Jr, P. J., Martz, T. R., Takeshita, Y., Johnson, K. S. and LaShomb, M. (2014) Best practices for autonomous measurement of seawater pH with the Honeywell Durafet, *Methods in Oceanography,* 9, 44-60.

Chen, S.-M. (2023) Water Exchange due to wind and waves in a Monsoon Prevailing Tropical Atoll, *Journal of Marine Science and Engineering*, 11(1), 109.

Chou, W.-C., Chu, H.-C., Chen, Y.-H., Syu, R.-W., Hung, C.-C. and Soong, K. (2018) Short-term variability of carbon chemistry in two contrasting seagrass meadows at Dongsha Island: implications for pH buffering and CO_2 sequestration, *Estuarine, Coastal and Shelf Science,* 210, 36-44.

Chou, W.-C., Fan, L.-F., Yang, C.-C., Chen, Y.-H., Hung, C.-C., Huang, W.-J., Shih, Y.-Y., Soong, K., Tseng, H.-C. and Gong, G.-C. (2021) A unique diel pattern in carbonate chemistry in the seagrass meadows of Dongsha Island: The enhancement of metabolic carbonate dissolution in a semienclosed lagoon, *Frontiers in Marine Science*, 8, 717685.

Comeau, S., Cornwall, C. E., DeCarlo, T. M., Krieger, E. and McCulloch, M. T. (2018) Similar controls on calcification under ocean acidification across unrelated coral reef taxa, *Global Change Biology*, 24(10), 4857-4868.

Courtney, T., De Carlo, E., Page, H., Bahr, K., Barro, A., Howins, N., Tabata, R., Terlouw, G., Rodgers, K. and Andersson, A. (2018) Recovery of reef-scale calcification following a bleaching event in Kāneohe Bay, Hawai'i, *Limnology and Oceanography Letters,* 3(1), 1-9.

Cyronak, T., Andersson, A. J., Langdon, C., Albright, R., Bates, N. R., Caldeira, K., Carlton, R., Corredor, J. E., Dunbar, R. B. and Enochs, I. (2018) Taking the metabolic pulse of the world's coral reefs, *PloS one,* 13(1), e0190872.

Cyronak, T., Takeshita, Y., Courtney, T. A., DeCarlo, E. H., Eyre, B. D., Kline, D. I., Martz, T., Page, H., Price, N. N. and Smith, J. (2020) Diel temperature and pH variability scale with depth across diverse coral reef habitats, *Limnology and Oceanography Letters,* 5(2), 193-203.

Dai, C. (2004) Dong-sha Atoll in the South China Sea: Past, present and future. *Islands of the world VIII international conference, Kinmen Island, Taiwan*.

Dai, C., Qin, X. and Zheng, A. (2013) Coral fauna of Dongsha Atoll in the South China Sea, *Marine National Park Headquarters, Construction and Planning Agency, Ministry of the Interior, ROC (In Chinese with English scientific names)*.

Dai, C.-F. and Fan, T.-Y. (1996) Coral fauna of Taiping Island (Itu Aba Island) in the Spratlys of the South China Sea.

Davis, K. A., Arthur, R. S., Reid, E. C., Rogers, J. S., Fringer, O. B., DeCarlo, T. M. and Cohen, A. L. (2020) Fate of internal waves on a shallow shelf, *Journal of Geophysical Research: Oceans*, 125(5), e2019JC015377.

DeCarlo, T. M., Cohen, A. L., Wong, G. T., Shiah, F. K., Lentz, S. J., Davis, K. A., Shamberger, K. E. and Lohmann, P. (2017) Community production modulates coral reef pH and the sensitivity of ecosystem calcification to ocean acidification, *Journal of Geophysical Research: Oceans*, 122(1), 745-761.

Dickson, A. and Millero, F. J. (1987) A comparison of the equilibrium constants for the dissociation of carbonic acid in seawater media, *Deep Sea Research Part A. Oceanographic Research Papers*, 34(10), 1733-1743.

Dickson, A. G., Sabine, C. L. and Christian, J. R. (2007) Guide to best practices for ocean CO_2 measurements.

Dişa, D., Münnich, M., Vogt, M., & Gruber, N. (2022) A space-time mosaic of seawater carbonate chemistry conditions in the north-shore Moorea coral reef system. *Frontiers in Marine Science*, *9*, 1004107.

Doney, S. C., Ruckelshaus, M., Emmett Duffy, J., Barry, J. P., Chan, F., English, C. A., Galindo, H. M., Grebmeier, J. M., Hollowed, A. B. and Knowlton, N. (2012) Climate change impacts on marine ecosystems, *Annual Review of Marine Science*, 4, 11-37.

Donner, S. D. (2011) An evaluation of the effect of recent temperature variability on the prediction of coral bleaching events. *Ecological Applications*, *21*(5), 1718-1730.

Duan, Y., Liu, Y., Li, M., Zhou, M. and Yang, Y. (2016) Survey of reefs based on Landsat 8 operational land imager (OLI) images in the Nansha Islands, South China Sea, *Acta Oceanologica Sinica*, 35, 11-19.

Edmunds, P. J., Comeau, S., Lantz, C., Andersson, A., Briggs, C., Cohen, A., Gattuso, J.-P., Grady, J. M., Gross, K. and Johnson, M. (2016) Integrating the effects of ocean acidification across functional scales on tropical coral reefs, *Bioscience*, 66(5), 350-362.

Eyre, B. D., Cyronak, T., Drupp, P., De Carlo, E. H., Sachs, J. P., and Andersson, A. J. (2018) Coral reefs will transition to net dissolving before end of century. *Science*, *359*(6378), 908-911.

Fabricius, K. E., Langdon, C., Uthicke, S., Humphrey, C., Noonan, S., De'ath, G., Okazaki, R., Muehllehner, N., Glas, M. S. and Lough, J. M. (2011) Losers and winners in coral reefs acclimatized to elevated carbon dioxide concentrations, *Nature Climate Change,* 1(3), 165-169.

Falter, J. L., Lowe, R. J., Zhang, Z. and McCulloch, M. (2013) Physical and biological controls on the carbonate chemistry of coral reef waters: effects of metabolism, wave forcing, sea level, and geomorphology, *PloS one,* 8(1), e53303.

Fan, L.-F., Qiu, S.-Q. and Chou, W.-C. (2021) Carbonate chemistry of the Dongsha Atoll Lagoon in the northern South China Sea, *Terrestrial, Atmospheric & Oceanic Sciences,* 32(3).

Ganguly, D., Singh, G., Ramachandran, P., Selvam, A. P., Banerjee, K., & Ramachandran, R. (2017) Seagrass metabolism and carbon dynamics in a tropical coastal embayment. *Ambio*, *46*, 667-679.

Gattuso, J.-P., Allemand, D. and Frankignoulle, M. (1999) Photosynthesis and calcification at cellular, organismal and community levels in coral reefs: a review on interactions and control by carbonate chemistry, *American Zoologist,* 39(1), 160-183.

Gattuso, J.-P., Pichon, M., Delesalle, B., Canon, C. and Frankignoulle, M. (1996) Carbon fluxes in coral reefs. I. Lagrangian measurement of community metabolism and resulting air-sea CO_2 disequilibrium, *Marine Ecology Progress Series,* 145, 109-121.

Gobler, C. J. and Baumann, H. (2016) Hypoxia and acidification in ocean ecosystems: coupled dynamics and effects on marine life, *Biology Letters,* 12(5), 20150976.

Guadayol, O., Silbiger, N. J., Donahue, M. J. and Thomas, F. I. (2014) Patterns in temporal variability of temperature, oxygen and pH along an environmental gradient in a coral reef, *PloS one,* 9(1), e85213.

Guest, J. R., Edmunds, P. J., Gates, R. D., Kuffner, I. B., Andersson, A. J., Barnes, B. B., Chollett, I., Courtney, T. A., Elahi, R. and Gross, K. (2018) A framework for identifying and characterising coral reef "oases" against a backdrop of degradation, *Journal of Applied Ecology,* 55(6), 2865-2875.

Hoegh-Guldberg, O., Mumby, P. J., Hooten, A. J., Steneck, R. S., Greenfield, P., Gomez, E., Harvell, C. D., Sale, P. F., Edwards, A. J. and Caldeira, K. (2007) Coral reefs under rapid climate change and ocean acidification, *Science*, 318(5857), 1737-1742.

Hofmann, G. E., Smith, J. E., Johnson, K. S., Send, U., Levin, L. A., Micheli, F., Paytan, A., Price, N. N., Peterson, B. and Takeshita, Y. (2011) High-frequency dynamics of ocean pH: a multi-ecosystem comparison, *PloS one*, 6(12), e28983.

Houk, P., Comeros-Raynal, M., Lawrence, A., Sudek, M., Vaeoso, M., McGuire, K., & Regis, J. (2020) Nutrient thresholds to protect water quality and coral reefs. *Marine Pollution Bulletin*, *159*, 111451.

Huang, Y.-H., Lee, C.-L., Chung, C.-Y., Hsiao, S.-C. and Lin, H.-J. (2015) Carbon budgets of multispecies seagrass beds at Dongsha Island in the South China Sea, *Marine Environmental Research*, 106, 92-102.

Hughes, T. P., Kerry, J. T., Álvarez-Noriega, M., Álvarez-Romero, J. G., Anderson, K. D., Baird, A. H., Babcock, R. C., Beger, M., Bellwood, D. R. and Berkelmans, R. (2017) Global warming and recurrent mass bleaching of corals, *Nature*, 543(7645), 373-377.

Kapsenberg, L. and Cyronak, T. (2019) Ocean acidification refugia in variable environments, *Global Change Biology*, 25(10), 3201-3214.

Kealoha, A. K., Doyle, S. M., Shamberger, K. E., Sylvan, J. B., Hetland, R. D. and DiMarco, S. F. (2020) Localized hypoxia may have caused coral reef mortality at the Flower Garden Banks, *Coral Reefs*, 39, 119-132.

Kekuewa, S. A., Courtney, T. A., Cyronak, T., Kindeberg, T., Eyre, B. D., Stoltenberg, L. and Andersson, A. J. (2021) Temporal and spatial variabilities of chemical and physical parameters on the Heron Island coral reef platform, *Aquatic Geochemistry*, 27, 241-268.

Kosugi, N., Ono, H., Toyama, K., Tsujino, H. and Ishii, M. (2023) An empirical projection of ocean acidification in southwestern Japan over the 21st century, *Marine Chemistry*, 255, 104290.

Koweek, D., Dunbar, R. B., Rogers, J. S., Williams, G. J., Price, N., Mucciarone, D. and Teneva, L. (2015) Environmental and ecological controls of coral community metabolism on Palmyra Atoll, *Coral Reefs*, 34, 339-351.

Kroeker, K. J., Kordas, R. L., Crim, R. N. and Singh, G. G. (2010) Meta-analysis reveals negative yet variable effects of ocean acidification on marine organisms, *Ecology Letters*, 13(11), 1419-1434.

Kwiatkowski, L., Torres, O., Bopp, L., Aumont, O., Chamberlain, M., Christian, J. R., Dunne, J. P., Gehlen, M., Ilyina, T. and John, J. G. (2020) Twenty-first century ocean warming, acidification, deoxygenation, and upper-ocean nutrient and primary production decline from CMIP6 model projections, *Biogeosciences*, 17(13), 3439-3470.

Langdon, C., Albright, R., Baker, A. C. and Jones, P. (2018) Two threatened Caribbean coral species have contrasting responses to combined temperature and acidification stress, *Limnology and Oceanography*, 63(6), 2450-2464.

Langdon, C. and Atkinson, M. (2005) Effect of elevated pCO_2 on photosynthesis and calcification of corals and interactions with seasonal change in temperature/irradiance and nutrient enrichment, *Journal of Geophysical Research: Oceans*, 110(C9).

Liang, S.-J., Young, C.-C., Dai, C., Wu, N.-J. and Hsu, T.-W. (2020) Simulation of ocean circulation of Dongsha water using non-hydrostatic shallow-water model, *Water*, 12(10), 2832.

Lowe, R. J. and Falter, J. L. (2015) Oceanic forcing of coral reefs, *Annual Review of Marine Science*, 7, 43-66.

Manzello, D. P., Enochs, I. C., Melo, N., Gledhill, D. K. and Johns, E. M. (2012) Ocean acidification refugia of the Florida Reef Tract.

Marshall, P. and Baird, A. (2000) Bleaching of corals on the Great Barrier Reef: differential susceptibilities among taxa, *Coral reefs*, 19, 155-163.

Martz, T. R., Connery, J. G. and Johnson, K. S. (2010) Testing the Honeywell Durafet® for seawater pH applications, *Limnology and Oceanography: Methods*, 8(5), 172-184.

Mehrbach, C., Culberson, C., Hawley, J. and Pytkowicx, R. (1973) Measurement of the apparent dissociation constants of carbonic acid in seawater at atmospheric pressure 1, *Limnology and Oceanography*, 18(6), 897-907.

Muehllehner, N., Langdon, C., Venti, A., & Kadko, D. (2016) Dynamics of carbonate chemistry, production, and calcification of the Florida Reef Tract (2009–2010): Evidence for seasonal dissolution. *Global Biogeochemical Cycles, 30*(5), 661-688.

Nelson, H. R. and Altieri, A. H. (2019) Oxygen: the universal currency on coral reefs, *Coral Reefs*, 38(2), 177-198.

Page, H. N., Andersson, A. J., Jokiel, P. L., Rodgers, K. u. S., Lebrato, M., Yeakel, K., Davidson, C., D'Angelo, S. and Bahr, K. D. (2016) Differential modification of seawater carbonate chemistry by major coral reef benthic communities, *Coral Reefs*, 35, 1311-1325.

Page, H. N., Courtney, T. A., De Carlo, E. H., Howins, N. M., Koester, I. and Andersson, A. J. (2019) Spatiotemporal variability in seawater carbon chemistry for a coral reef flat in Kāne ʻohe Bay, Hawai ʻi, *Limnology and Oceanography*, 64(3), 913-934.

Pezner, A. K., Courtney, T. A., Barkley, H. C., Chou, W.-C., Chu, H.-C., Clements, S. M., Cyronak, T., DeGrandpre, M. D., Kekuewa, S. A. and Kline, D. I. (2023) Increasing hypoxia on global coral reefs under ocean warming, *Nature Climate Change*, 13(4), 403-409.

Reid, E., Lentz, S., DeCarlo, T., Cohen, A. and Davis, K. (2020) Physical processes determine spatial structure in water temperature and residence time on a wide reef flat, *Journal of Geophysical Research: Oceans*, 125(12), e2020JC016543.

Reid, E. C., DeCarlo, T. M., Cohen, A. L., Wong, G. T., Lentz, S. J., Safaie, A., Hall, A. and Davis, K. A. (2019) Internal waves influence the thermal and nutrient environment on a shallow coral reef, *Limnology and Oceanography*, 64(5), 1949-1965.

Santos, I. R., Glud, R. N., Maher, D., Erler, D. and Eyre, B. D. (2011) Diel coral reef acidification driven by porewater advection in permeable carbonate sands, Heron Island, Great Barrier Reef, *Geophysical Research Letters*, 38(3).

Schoepf, V., Stat, M., Falter, J. L. and McCulloch, M. T. (2015) Limits to the thermal tolerance of corals adapted to a highly fluctuating, naturally extreme temperature environment, *Scientific Reports*, 5(1), 17639.

Shaw, E. C., McNeil, B. I. and Tilbrook, B. (2012) Impacts of ocean acidification in naturally variable coral reef flat ecosystems, *Journal of Geophysical Research: Oceans*, 117(C3).

Silverman, J., Lazar, B., Cao, L., Caldeira, K. and Erez, J. (2009) Coral reefs may start dissolving when atmospheric CO_2 doubles, *Geophysical Research Letters,* 36(5).

Smith, S. and Key, G. (1975) Carbon dioxide and metabolism in marine environments 1, *Limnology and Oceanography,* 20(3), 493-495.

Smith, S. and Kinsey, D. (1978) Calcification and organic carbon metabolism as indicated by carbon dioxide.

Suzuki, A. and Kawahata, H. (2003) Carbon budget of coral reef systems: an overview of observations in fringing reefs, barrier reefs and atolls in the Indo-Pacific regions, *Tellus B: Chemical and Physical Meteorology,* 55(2), 428-444.

Tkachenko, K. S. and Soong, K. (2017) Dongsha Atoll: A potential thermal refuge for reef-building corals in the South China Sea, *Marine Environmental Research,* 127, 112-125.

Towle, E. K., Enochs, I. C., and Langdon, C. (2015) Threatened Caribbean coral is able to mitigate the adverse effects of ocean acidification on calcification by increasing feeding rate. *PloS one*, *10*(4), e0123394.

Van Heuven, S., Pierrot, D., Rae, J., Lewis, E. and Wallace, D. (2011) MATLAB program developed for CO_2 system calculations, *ORNL/CDIAC-105b,* 530.

Wallace, R. B., Peterson, B. J., and Gobler, C. J. (2021) Ecosystem metabolism modulates the dynamics of hypoxia and acidification across temperate coastal habitat types. *Frontiers in Marine Science*, *8*, 611781.

Watanabe, A., Kayanne, H., Hata, H., Kudo, S., Nozaki, K., Kato, K., Negishi, A., Ikeda, Y. and Yamano, H. (2006) Analysis of the seawater CO_2 system in the barrier reef-lagoon system of Palau using total alkalinity-dissolved inorganic carbon diagrams, *Limnology and Oceanography,* 51(4), 1614-1628.

Wong, G. T., Ku, T.-L., Mulholland, M., Tseng, C.-M. and Wang, D.-P. (2007) The SouthEast Asian time-series study (SEATS) and the biogeochemistry of the South China Sea—an overview, *Deep Sea Research Part II: Topical Studies in Oceanography,* 54(14-15), 1434-1447.

Xiao, X., Agustí, S., Yu, Y., Huang, Y., Chen, W., Hu, J., Li, C., Li, K., Wei, F. and Lu, Y. (2021) Seaweed farms provide refugia from ocean acidification, *Science of the Total Environment*, 776, 145192.

Yeakel, K. L., Andersson, A. J., Bates, N. R., Noyes, T. J., Collins, A., and Garley, R. (2015) Shifts in coral reef biogeochemistry and resulting acidification linked to offshore productivity. *Proceedings of the National Academy of Sciences*, *112*(47), 14512-14517.

Zhang, Z., Falter, J., Lowe, R., Ivey, G. and McCulloch, M. (2013) Atmospheric forcing intensifies the effects of regional ocean warming on reef-scale temperature anomalies during a coral bleaching event, *Journal of Geophysical Research: Oceans*, 118(9), 4600-4616.

Chapter 3, in full, is currently being prepared for submission for publication of the material. Kekuewa SAH, Pezner AK, Courtney TA, Wei Y, Soong K, Rintoul MS, Andersson AJ. The dissertation author was the primary researcher and author of this material.

Chapter 4: Effect of seaweed cultivation on spatial seawater carbonate chemistry across Onna-son Reef

Kekuewa SAH, Rintoul MS, Courtney TA, Pezner AK, Mitarai S, Andersson AJ

Abstract

Coral reefs are currently under threat due to ongoing climate change stressors, such as global warming, ocean acidification, and deoxygenation. Seaweed cultivation has been hypothesized as a method to elevate seawater pH relative to source conditions and be established as an ocean acidification refugia. To date, most seaweed aquaculture studies have solely relied on autonomous sensors measuring dissolved oxygen and pH to estimate the primary production and pH buffer capacity inside versus outside of seaweed cultivation plots. While these studies provide high temporal resolution, they lack information about the spatial effect of seaweed aquaculture and whether they provide refugia for proximal and downstream coral reef communities. Herein, we investigate the spatiotemporal variability of seawater carbon chemistry parameters during the fall, winter, and spring across Onna-son reef, with the spring surveys overlapping with the maximum extent of seaweed cultivation prior to harvest. We observed that larger drawdowns in seawater carbon chemistry parameters relative to source water and the largest spatial variability for seawater pH (0.14) and aragonite saturation state (Ω_{Ar}) (0.84) occurred during spring compared to winter and fall. These differences were most likely due to a combination of slower currents, smaller significant wave height, and lower mean sea level, conditions favorable for enhanced biogeochemical modification in spring. Additionally, we revealed that pH buffering was observed across 77-100% of fall afternoon observations (up to 0.10) and 75-92% of spring afternoon observations (up to 0.13). Suggesting that seaweed aquaculture may not be more beneficial than natural macroalgal habitats in buffering OA conditions. Future studies aimed at assessing the

spatial impact of seaweed aquaculture needs to account for local hydrodynamics and the role of natural macroalgal habitats, as this will impact the observed variability in both space and time.

Introduction

Increased atmospheric CO_2 due to anthropogenic activities such as fossil fuel combustion, cement production, deforestation and land use changes has resulted in major changes to the world's oceans. Ocean heat content, seawater temperature, and dissolved CO_2 concentrations have increased while dissolved oxygen concentrations have decreased (Kwiatokski et al., 2020). The oceanic uptake of CO_2 has led to a decrease in seawater pH and aragonite saturation state (Ω_{Ar}), a process known as ocean acidification (OA). By the year 2100, open-ocean average surface pH and Ω_{Ar} are projected to decrease by 0.4 and 1.0 units, respectively (Bates et al., 2014; Kwiatokski et al., 2020). However, many coastal ecosystems such as kelp forests, upwelling regions, seagrass beds, and coral reefs already experience diel and seasonal variations that far exceed the projected changes in open ocean pH and Ω_{Ar} by the year 2100 (Hofmann et al., 2011; Hoegh-Guldberg et al., 2017). The large variability is driven by a number of factors including local biological activity and allochthonous inputs from terrestrial and/or oceanic environments, which are amplified by the shallow water depth and further modified by physical drivers such as flow speed and trajectory (Falter et al., 2013; Cyronak et al., 2020; Rintoul et al., 2022). Understanding the natural biogeochemical variability and the underlying drivers over spatial (m to km) and temporal (diel to seasonal) scales is critical for predicting future chemical conditions in coastal habitats (Page et al., 2019; Kekuewa et al., 2021; Dias et al., 2022).

In the context of global environmental change, coral reefs have received substantial attention due to their unprecedented high biodiversity and ecological services (Moberg and Folke et al., 1999; Costanza et al., 2014; Ferrario et al., 2014), and their perceived high sensitivity to ocean warming, deoxygenation, and acidification (Hughes et al., 2017; Altieri et al., 2017; Breitburg et al., 2018; Edmunds et al., 2024). Over the past several decades, coral reefs have

experienced increasingly frequent and severe mass bleaching and mortality events due to ocean warming (Hughes et al., 2018). Ocean warming also leads to deoxygenation due to reduced oxygen solubility and increased biological oxygen demand, which may increase the frequency of hypoxic events detrimental to coral reef health and function (Altieri et al., 2017; Kealoha et al., 2020; Nelson and Altieri, 2019; Pezner et al., 2023). Similarly, coral reef function may be negatively affected by OA as multiple studies have demonstrated reduced calcification (Andersson and Gledhill, 2013; Eyre et al., 2014; Albright et al., 2015; 2018), increased bioerosion, and increased $CaCO_3$ dissolution rates under future pH and Ω_{Ar} conditions (Cyronak et al., 2013; Eyre et al., 2018; Edmunds et al., 2024). Furthermore, ocean warming, deoxygenation, and OA may interact synergistically to negatively affect corals and coral reefs (Anthony et al., 2008; Dove et al., 2013, 2020). To address and prepare for these threats there have been increasing efforts to identify what coral reefs may be more or less at risk from global environmental change (Guest et al., 2018; Darling et al., 2019; Courtney et al., 2022; Elahi et al., 2022), but also efforts investigating active interventions intended to mitigate the effect of these changes (Natl. Acad. Sci. Eng. Med. 2021; Anthony et al., 2016, Mongin et al., 2016, 2021).

To mitigate the effects of OA on coral reefs, recent studies have proposed that macroalgae dominated habitats or cultivation areas co-located with corals or other calcifiers may alleviate the negative effects of OA and potentially act as a marine carbon dioxide removal (mCDR) strategy (Duarte et al., 2017; Cyronak et al., 2018a; Kapsenberg and Cyronak et al., 2019; Natl. Acad. Sci. Eng. Med. 2021). Particularly, seaweed aquaculture has been suggested as an active OA mitigation strategy due to high rates of primary productivity that elevates local pH and Ω_{Ar} conditions for the benefit of marine calcifiers (e.g., mussels, oysters, clams, coral) (Hurd et al., 2015; Duarte et al., 2017; Gattuso et al., 2018). However, in situ measurements testing this hypothesis and assessing

the biogeochemical footprint and influence of seaweed aquaculture on seawater carbonate chemistry through space and time are scarce (Mongin et al., 2016; Alleway et al., 2019; Xiao et al., 2021). Hence, there is a need for spatiotemporal biogeochemistry surveys across multiple reef habitats and scales, including seaweed and coral cultivation areas, to assess the potential for OA mitigation on reefs. Previous studies have mostly focused on local pH changes directly inside and outside of cultivation areas (e.g., Xiao et al., 2017, 2021; Sato et al., 2022), with limited observations of the relative contribution from different biogeochemical processes and their influence on the seawater chemistry of surrounding habitats and reefs. To fully understand the potential role of seaweed cultivation as an OA mitigation tool, it is necessary to understand how it contributes to the local coral reef biogeochemistry.

Coral reef biogeochemistry is largely controlled by the balance of net community production (NCP = primary organic carbon production –total respiration) and net community calcification (NCC = calcification – $CaCO_3$ dissolution) with additional influence from physical processes and properties (Langdon and Atkinson, 2005; Carilli et al., 2009; Kleypas et al., 2011; Falter et al., 2014; Venti et al., 2014; Lowe and Falter, 2015; Page et al., 2016). Positive NCP implies net organic carbon production that consumes dissolved inorganic carbon (DIC) and produces dissolved oxygen (DO), increasing seawater pH and DO. Negative NCP implies net respiration and decreases seawater pH and DO. NCC is the balance of calcification and $CaCO_3$ dissolution. Positive NCC refers to net calcification, which decreases total alkalinity (TA) and DIC in a ratio of 2:1 leading to a decrease in pH while negative NCC refers to net $CaCO_3$ dissolution and has the opposite effect. Collectively, these processes have been referred to as coral reef metabolism (Frankignoulle et al., 1996; Suszuki and Kawahata, 2003; Cyronak et al., 2018b). On diel time scales, biogeochemical variability on a reef is primarily driven by NCP, which results in

elevated pH and DO conditions during the day and decreased values at night due to the diurnal balance of positive and negative NCP. In contrast, over larger temporal and spatial scales, NCP is often close to 0 and the influence of NCC becomes increasingly important (Watanabe et al., 2006; Takeshita et al., 2018). Consequently, observations of seawater carbonate chemistry within and across coral reefs over different time and spatial scales can be used as a tool to gain insights on the biogeochemical function of individual habitats, both natural and cultivated, as well as entire reef systems (Suzuki and Kawahata, 2003; Watanabe et al., 2006; Andersson et al., 2014; Albright et al., 2015; Takeshita et al., 2018; Courtney et al., 2018; Kekuewa et al., 2021).

In this study, we utilized discrete seawater samples of DIC and TA to assess the spatial and temporal biogeochemical variability across a coral reef in Onna-son, Okinawa, Japan, that hosts extensive areas of seaweed and coral cultivation (Higa et al., 2022). Spatial surveys were conducted in the morning and afternoon during the fall, winter, and spring, the latter surveys overlapping with the maximum extent of seaweed cultivation before harvest. Our explicit goals were to assess how seawater carbonate chemistry was modified across the reef under the presence and absence of seaweeds, and how this influenced the net reef metabolism and relative contribution from NCP and NCC. The observations provide real-world insights into the potential of seaweed cultivation to buffer seawater pH and Ω_{Ar} in proximal and downstream coral reef habitats.

Material and methods

Site Description

The Ryukyu Islands are located south of mainland Japan, bordering the east side of the Kuroshio Current, and composed of six island groups (Yaeyama, Miyako, Okinawa, Amami Oshima, Tokara, and Yakutane). Okinawa is the largest island group and also the most populated.

In general, Okinawa experiences large annual fluctuations of surface seawater temperature of ~10 °C with the lowest temperatures observed in January-February and the highest temperatures observed in July-August (Singh et al., 2022). The seasonal temperature trend coincides with strong northeasterly winds in the winter and weak southerly winds in the summer (Singh et al., 2022). Typhoons regularly occur in Okinawa from May to October with the most intense typhoons generally occurring in August and September (Singh et al., 2022).

The present study focused on a reef system in Onna-son, Okinawa, Japan (26.4497° N, 127.7942° E) (Fig. 1). It is characterized by a ~3 km long fringing reef and 150 m wide reef flat with an average depth of 1.3 m. The reef flat consists of sand, rubble, coral, and algae. The lagoon behind the reef flat ranges from 600-1500 m wide and has a depth range of 2-4 m that consists of sand flats, rubble, patch reefs, algae, and both coral and seagrass cultivation areas. The reef system is also connected to the open-ocean via deeper channels located at the southern edge (deep complex system of channels and patch reefs, < 20 m), in the center, and at the northern edge (~100 m wide, 15 m deep channel).

Seaweed and coral cultivation

Importantly, co-located on Onna-son reef is a seaweed cultivation area, which can cover more than 0.30 km^2 during the growing season. The growing season starts in January and typically ends in late May when SST becomes too high. The Onna-son seaweed farms has been shown to yield between 300 to 1000 tons of a brown algae referred to as Mozuku annually (primarily *Cladosiphon okamuranus*; Higa et al., 2022; Omoto et al., 2024). In addition to seaweed aquaculture, the local Fisheries cooperative have outplanted over 100,000 coral transplants from

2011 to 2017 across ~0.03 km^2 of the Onna-son reef to help facilitate reef diversity and to increase the yield of seaweed through elevated nutrient uptake (Higuchi et al., 2014; Omori et al., 2016).

Spatial Surveys

Reef-wide spatial surveys were conducted in the morning and afternoon via boat to collect discrete seawater samples for DIC and TA across the 3 km long fringing reef in October 2019 (n=4), April 2023 (n=4), and January 2024 (n=2). The surveys took on average ~ 2 hours. Seawater was collected using a 5 L Niskin bottle submerged approximately 0.5 m below the surface. Seawater samples for DIC and TA were collected from the Niskin bottle according to standard protocols (Dickson et al., 2007) into 250 mL Corning Pyrex glass bottles and poisoned with 100 mL saturated mercuric chloride ($HgCl_2$) solution to prevent biological modification. Seawater temperature (± 0.2 °C), salinity (±0.1), and dissolved oxygen (±0.2 mg L^{-1}) were measured in parallel with Niskin sampling using a YSI Pro 2030 m or a YSI Professional Plus. For each day of surveys, at least one off-reef seawater sample was collected as an open ocean reference.

Environmental Data

Tide and current data were aggregated for each spatial survey from a Nortek acoustic doppler current profiler (AquaDopp) deployed in the middle in the lagoon for each survey season. In addition, significant wave height was estimated hourly on the fore reef based on pressure measurements from ADCPs and RBR pressure sensors for the 2019 and 2023 surveys. ADCP directional data were corrected for magnetic declination at the time of each deployment.

Sample and Data Analysis

All seawater samples were transported to and analyzed at Scripps Coastal and Open Ocean Biogeochemistry Lab in La Jolla, CA, USA. DIC was analyzed using an automated infrared inorganic carbon analyzer (AIRICA, *Marianda*) while TA was analyzed using an open-cell potentiometric acid titration system (Dickson et al., 2007). Accuracy and precision of the instruments were validated against CRMs provided by the Dickson Lab at SIO as well as in lab prepared secondary standards. The mean DIC and TA offset±1SD from the standards were -0.30±1.74 μmol kg^{-1} (n=90) and 0.37±2.12 μmol kg^{-1} (n=44), respectively.

The complete seawater dissolved inorganic carbon system was calculated from in situ temperature, salinity, pressure, DIC, and TA using CO2sys for MATLAB (Van Heuven et al., 2011) with K_1 and K_2 dissociation constants from Mehrbach et al. (1973) refit by Dickson and Millero (1987), $KHSO_4$ dissociation constants from Dickson, and $[B]_T$ from Uppstrom (1974) and pH defined on the total hydrogen ion scale. DIC and TA from seawater samples were normalized to a mean salinity across all bottle samples of 34.7 g kg^{-1} to facilitate comparison between seasons. In order to ascertain any statistical significant differences of biogeochemical parameters between individual surveys, one-way analysis of variance (*anova1*) tests were conducted (α=0.05) in MATLAB.

To assess the relative influence of biogeochemical processes on the observed chemical gradients across the reef, the difference between reef and offshore conditions were calculated for TA ($dTA=TA_{reef} - TA_{offshore}$), DIC ($dDIC=DIC_{reef} - DIC_{offshore}$) and DO ($dDO=DO_{reef} - DO_{offshore}$) and analyzed using vector analysis (Deffyes 1965; Cyronak et al., 2018b) and type II liner regressions (*lsqfitma.m*). Negative dTA implies TA consumption and positive NCC whereas positive dTA represents TA production and negative NCC. As dDIC reflects the influence of both NCC and NCP, dDIC was corrected for the influence of NCC ($dDIC_{NCP} = dDIC - 0.5TA$) and

evaluated against dDO to assess the trophic status and the ratio of carbon to oxygen consumption/production ratio (Smith and Key, 1975; Smith and Kinsey, 1978; Atkinson and Smith, 1983). Given the short transit time of water across the Onna reef on the order of hours (Rintoul et al., 2022), the influence of gas exchange was not taken into account.

Results

Environmental conditions

Differences in significant wave height (Hs), current velocity, mean sea level (MSL), and seawater temperature were observed across Onna-son Reef during the survey days in the fall of 2019, winter of 2024, and spring of 2023 (Fig 1). The mean Hs ranged from 0.12±0.01 to 0.15±0.02 m (mean ± 1 SD) during the spring surveys in 2023 compared to 0.41±0.03 to 0.65±0.02 m s^{-1} during the fall surveys in 2019 (Fig 1; Table 1). There were no Hs observations for the winter surveys in 2024. Current speeds were highest during fall surveys (0.04±0.02 to 0.18±0.04 m s^{-1}) followed by the winter surveys (0.09±0.02 to 0.13±0.04 m s^{-1}) and the lowest speeds were observed during the spring surveys (0.02±0.01 to 0.06±0.01 m s^{-1}) (Fig 1; Table 1). Flow direction measured in the lagoon was predominantly from northeast to southwest during the fall surveys, east to west during spring surveys, and west-southwest to east-northeast for the winter surveys (Fig 1). The MSL ranged from -0.40±0.06 to 0.54±0.15 m during the fall surveys, 0.32±0.18 to 0.42±0.22 m during the winter surveys, and -0.29±0.20 to 0.26±0.03 m during the spring surveys (Fig 1; Table 1). Lastly, the highest mean seawater temperatures were observed in the fall (26.2±0.1 to 27.0±0.2 °C) followed by the spring (22.8±0.2 to 24.0±0.3 °C) and the winter surveys (21.6±0.7 to 22.4±0.3 °C) (Table 1).

Seasonal and spatial variability

General observations

Seawater samples collected offshore revealed that the TA outside of the reef was relatively consistent throughout the seasons (2273±5 μmol kg^{-1}; n=12) while DIC was more variable (1963±10 μmol kg^{-1}). The lowest offshores DIC values were observed in the fall (1959±5 μmol kg^{-1}; n=9) with qualitatively slightly higher values in the winter (1966 μmol kg^{-1}; n=1) with the highest values observed in the spring (1981±8 μmol kg^{-1}; n=2). Offshore pH and Ω_{Ar} also varied between seasons, ranging from 8.05±0.00 in the fall to 8.07±0.00 in the spring, and 8.10 in the winter.

In general, chemical gradients across the reef extended in an offshore-onshore direction and were more pronounced at times of higher flow speeds (fall of 2019) compared to slower flow speeds when gradients were less clear and spotty (spring of 2023) (Fig 1-4). Distinct differences were apparent between morning and afternoon surveys, with higher mean TA and DIC, and lower pH and Ω_{Ar}, in the mornings and the opposite trends in the afternoons (Fig 2-4).

Fall 2019

For the fall surveys, TA, DIC, pH, and Ω_{Ar} values ranged between 2234-2285 μmol kg^{-1}, 1869-1999 μmol kg^{-1}, 8.00-8.16, and 3.19-4.37, respectively. Chemical gradients were mostly distinct with TA and DIC decreasing, and pH and Ω_{Ar} increasing in the offshore to inshore direction during the afternoon surveys and the opposite during the one morning survey (Fig 2; Table 1; Fig S1).

Winter 2024

For the winter surveys, TA, DIC, pH, and Ω_{Ar} values ranged between 2260-2300 μmol kg^{-1}, 1954-2040 μmol kg^{-1}, 8.06-8.12 and 2.91-3.49, respectively. Similar to the fall survey, the

morning survey in winter revealed a similar trend of higher TA and DIC, and lower pH and Ω_{Ar} values closer to shore compared to offshore and near the reef crest (Fig 2; Table 1; Fig S2). However, the variability was small for all parameters with pH ranging from 8.06 to 8.08. Compared to the fall surveys, the winter afternoon surveys revealed a different trend with TA and DIC, and pH and Ω_{Ar}, decreasing and increasing, respectively, in a direction from the shore towards the reef crest (Fig. 3), but the range of variability was small for all parameters (Table 1; Table S1). Notably, the winter surveys coincided with seawater flow from the west-southwest to east-northeast, which was largely opposite from the flow observed in the fall (Fig. 1).

Spring 2023

For the spring surveys, TA, DIC, pH, and Ω_{Ar} values ranged between 2140-2285 µmol kg^{-1}, 1819-1990 µmol kg^{-1}, 8.00-8.19 and 2.88-4.02, respectively. Both morning and afternoon surveys showed less uniform and more spotty trends compared to fall and winter surveys. TA and DIC trends were sometimes different. For example, in the morning of April 29, TA increased while DIC decreased in an offshore to onshore direction. Some patterns appeared correlated with specific habitats such as in the afternoon on May 3, large TA and DIC depletion were observed in an area on the reef flat with extensive coral cover and shallow depth (Fig 4; Table 1; Fig S4). The spotty trends in chemical parameters coincided with the slowest flow speeds moving from the east to west.

TA and DIC changes relative to offshore

Throughout each season, both repletion and depletion of TA, DIC, and DO were observed across the Onna-son reef in both morning and afternoon surveys relative to offshore surface samples (Fig 5).

During the fall, both morning and afternoon surveys mostly revealed depletion of TA and DIC relative to offshore (Fig 5 and S4; Table S2). In the morning, TA and DIC drawdown was observed for 89% and 67% of the observations, respectively, with dTA ranging from -18 to 2 µmol kg^{-1} and dDIC ranging from -42 to 35 µmol kg^{-1} (Fig 5; Table S2). Differences in pH and Ω_{Ar} ranged from -0.05 to 0.05 and -0.34 to 0.27, respectively, compared to offshore (Table S2). In the afternoon, TA and DIC drawdown was observed for 83-100% and 94-100% of the observations, respectively. dTA and dDIC ranged from -40 to 8 µmol kg^{-1} and -93 to 6 µmol kg^{-1}, respectively (Fig 5; Table S2). The subsequent change in pH and Ω_{Ar} ranged from -0.04 to 0.10 and -0.41 to 0.45, respectively, compared to offshore (Table S2).

During the winter morning survey, TA and DIC repletion were observed for 69% and 100% of the observations, respectively, with dTA ranging from -5 to 30 µmol kg^{-1} and dDIC ranging from 11 to 74 µmol kg^{-1} (Fig 5 and S4; Table S2). Compared to offshore, pH and Ω_{Ar} differences ranged from -0.04 to 0.00 and -0.47 to -0.02, respectively (Table S2). In contrast, TA and DIC were mostly depleted relative to offshore during afternoon surveys (67% and 53% of observations, respectively) with dTA and dDIC ranging from -11 to 10 µmol kg^{-1} and -12 to 12 µmol kg^{-1}, respectively (Fig 5; Table S2). pH and Ω_{Ar} differed by -0.03 to 0.01 and -0.16 to 0.11, respectively, compared to offshore (Table S2).

During spring surveys, TA and DIC were on average depleted for both morning and afternoon surveys (Fig 5 and S4; Table S2). In the morning, TA and DIC drawdown was observed for 95-96% and 82-83% of the observations, respectively, with dTA ranging from -42 to 4 µmol kg^{-1} and dDIC ranging from -44 to 23 µmol kg^{-1} (Fig 5; Table S2). Differences in reef pH and Ω_{Ar} compared to offshore ranged from -0.06 to 0.07 and -0.41 to 0.45, respectively (Table S2). In the afternoon TA and DIC drawdown ranged from 92-100% and 96-100% with dTA ranging from -

126 to 14 µmol kg^{-1} and dDIC ranging from -157 to 1 µmol kg^{-1} (Fig 5; Table S2). Compared to offshore, pH and Ω_{Ar} differed by -0.02 to 0.13 and -0.16 to 0.77, respectively (Table S2). Across all seasons, DO depletion and repletion were inversely correlated to DIC.

The slopes of the TA-DIC regressions were < 1 for all seasons and each individual survey demonstrating that NCP was the primary driver of variability across the reef relative to NCC. TA-DIC slopes were qualitatively different between seasons ranging from 0.17 to 0.38 during Fall, 0.46 to 0.55 during Winter, and 0.39 to 0.82 during Spring surveys (Table S2). Correlation coefficients (R^2) ranged from 0.05 to 0.89 with six out of 10 surveys having R^2 values equal or greater than 0.54. Distinct differences were noted between morning and afternoon surveys during the spring, with morning TA-DIC slopes ranging from 0.39 to 0.46 and afternoon slopes ranging from 0.69 to 0.82 (Fig S4; Table S2). Across all seasons, assessment of oxygen and DIC changes due to NCP revealed DO-DIC_{NCP} slopes ranging from -0.17 to -1.69 with a mean of –0.79±0.64 for morning surveys and -1.01±0.25 for afternoon surveys (Fig S4; Table S2). In general, correlations coefficients were stronger compared to TA-DIC relationships, but no clear trend of the slopes were discerned as a function of season.

Discussion

Seawater Carbonate Chemistry Variability

Here, we assessed seawater carbonate chemistry gradients and variability across the Onna-son reef in fall, winter, and spring, with the spring survey coincident with the maximum extent of seaweed cultivation. In general, the spatial biogeochemical variability across the reef was influenced by the time of day, tidal phase, hydrodynamics, and sample location for any given survey. Gradients in TA, DIC, pH and Ω_{Ar} were observed across all surveys, but in general were more pronounced during afternoon surveys than morning surveys demonstrating the influence of

daytime primary productivity and calcification across the reef (Fig 2-4). Cross reef gradients were also more uniform at times of larger Hs and faster flow speed moving from the northwest to southeast (i.e., fall surveys). When waves break at the reef crest, the resulting wave setup becomes the dominant force of circulation on the reef. At flow speeds exceeding 0.10 m s^{-1}, the flow across the reef and lagoon converges on a remarkable uniform flow direction, which is revealed by striations in the benthos (Rintoul et al., 2022; Rintoul, 2024). Under these conditions, biogeochemical fluxes result in distinct chemical gradients across the reef (Fig 2). In contrast, when the wave setup is small or absent, the circulation on the reef is more strongly influenced by tides and winds, and the flow becomes more variable (Rintoul, 2024), which is also observed in chemical gradients (Fig 4).

Some seasonal differences were observed in TA, DIC, pH, and Ω_{Ar} across the reef, which have been previously reported for other reefs in Okinawa (Kurihara et al., 2019). The seasonal variations in pH, and Ω_{Ar} were influenced by the differential modification of TA and DIC by reef metabolism, but also the thermodynamic effects of temperature (winter: 22.0±0.5 ºC, spring: 23.4±0.3 ºC, fall: 26.7±0.2 ºC) on the solubility of CO_2 and the acid-base equilibrium with dpH/dSST: -0.014 $°C^{-1}$ and $d\Omega_{Ar}$/dSST: +0.020 $°C^{-1}$. Consequently, ranges of seawater pH and Ω_{Ar} overlapped between all seasons (fall: 8.00-8.16 and 3.20-4.36; winter: 8.05-8.12 and 2.90 to 3.49; spring: 8.00-8.19 and 2.89-4.02; Table S1), but with different maximum and minimum values. Notably, at times of high light conditions and warm seawater, primary production is favored and increases pH and $\Omega_{Ar,}$ with the observed changes counteracted and exacerbated, respectively, by warmer temperatures.

The maximum spatial variabilities of TA (130 µmol kg^{-1}), DIC (158 µmol kg^{-1}), pH (0.14), and Ω_{Ar} (0.84) were larger in spring compared to both fall and winter (Fig 2-4; Fig S1-3). These

differences were partly due to smaller Hs that led to slower current speeds and increased residence time (Fig 1; Rintoul et al., 2022), allowing more time for chemical modification by the benthos (Falter et al., 2013). Although we are unable to accurately determine the specific residence times during each survey, small Hs coincident with slow flow speed and extended residence times have been well-documented by multiple current sensors and drifter experiments across the Onna reef (Rintoul et al., 2022).The spring surveys also coincided with shallow MSL conditions (-0.29±0.20 to 0.26±0.03 m), which can further explain the enhanced biogeochemical variability in the shallow regions of the reef flat due to the enhanced biomass to water volume ratio (Fig 1) (e.g., Page et al., 2018; Cyronak et al., 2020). These results highlight the importance of tidal regimes, currents, and flow trajectory in influencing the variability of seawater carbon chemistry in shallow reef environments but makes it challenging to assess whether the presence of seaweed cultivation during the spring surveys had any major influence on the seawater chemistry relative to the background signal.

To date, most seaweed aquaculture studies have relied on autonomous sensors measuring DO and pH to estimate the NCP and pH buffer capacity inside versus outside of seaweed cultivation plots (Xiao et al., 2021; Sato et al., 2022; Chou et al., 2023). While these studies provide high temporal resolution in contrasting habitats (i.e., no seaweed versus seaweed), they lack information about the spatial effect of seaweed aquaculture and whether they provide refugia for proximal calcifying communities. One of the goals of this study was to address this shortcoming, and although the results demonstrated the strongest spatial chemical gradients and variability coincident with the seasonality of seaweed cultivation in Onna, we were unable to assign direct attribution to the seaweeds due to the reasons discussed above (i.e., small Hs, slow flow speeds, shallow MSL). However, the results do not refute the hypothesis that seaweed cultivation may

modulate OA for proximal calcifying communities but highlight the complexities that need to be taken into account in assessing it. An increased number of surveys in each season under different light, tide, and flow conditions could have assisted our analysis, but resource availability is a real constraint in this type of studies.

Regardless of the potential role of seaweed cultivation at this particular site, based on the relatively shallow slopes of dTA-dDIC regressions across all seasons (fall: 0.17-0.38; winter: 0.46-0.55; spring: 0.39 to 0.82), and the strong relationship between dDO and $dDIC_{NCP}$ (Fig. 5; Table S2), it can be concluded that the spatial variability in seawater pH and Ω_{Ar} was primarily driven by NCP relative to NCC. The steeper slopes of dTA-dDIC observed during the spring surveys reveal relatively higher rates of NCC at this time. This could be due to higher rates of organismal calcification, lower rates of carbonate sediment dissolution, or a combination of both. Although this is the hypothesized outcome in an OA mitigation scenario, it cannot be unequivocally determined whether the relative increase in NCC had anything to do with the presence of seaweed or simply a result of higher light or any other factor coincident with the spring surveys.

OA Mitigation

Recent work has projected that coral reefs will respond negatively to OA under future gas emission scenarios (Edmunds et al., 2024). It has been proposed that co-located seaweed aquaculture or macroalgal habitats can buffer coral reefs from future OA conditions. By examining the change in pH from discrete seawater samples off the reef we can ascertain the amount of pH buffering (i.e., higher pH on the reef) as well as the percent of observation per survey, which showed elevated pH (Cyronak et al., 2018b). Off-reef pH was relatively stable throughout the seasons and varied from 8.05-8.07. Our results show that ecosystem-scale pH amelioration was

observed by up to ~0.1 for both the fall and spring surveys. Further, based on the off-reef pH values we observed that pH was elevated on the reef for 11% of the morning and 92% of the afternoon observations in the fall, 0% of the morning and 53% of the afternoon observations in the winter, and 40% of the morning and 83% of the afternoon observations in the spring. If we assess the ranges of individual surveys, pH was elevated from 11-100% during the fall, 0-53% during the winter, and 29-92% during the spring with the lower percentages observed in the morning and higher percentages in the afternoon. This reflects the shift from OA intensification due to nighttime respiration and amelioration due to daytime primary productivity. These observations reveal that there are no radical differences in pH elevation between fall and spring, suggesting that the seaweed farms are not intrinsically better than the natural macroalgal habitats in mitigating OA (Sato et al., 2022).

Lastly, it is important to note that the spatial surveys do not account for diel extremes (e.g., early morning at sunrise and late afternoon following peak light intensity) at time points where we would expect to see peak respiration and dissolution signals, which has been observed via autonomous sensors deployed in seagrass habitats located in coral reefs and spatial surveys (Cyronak et al.,2018a; Chou et al., 2018, 2021; Kekuewa et al., 2021). Under future climate change conditions increased biological oxygen demand, decreased calcification, and increased dissolution rates are projected to occur (Vaquer-Sunyer et al., 2012; Eyre et al., 2014; Edmunds et al., 2024). These projections would result in an increase in reef-wide deleterious seawater chemistry conditions. Further studies that capture both tidal and diel extremes across reef-wide spatial surveys are thus needed to better determine whether reef habitats can act as a refugia to ongoing climate change conditions.

Table 4.1 Summary of measured environmental data (mean ± SD), measured mean seawater temperature, salinity-normalized TA, DIC, and DO (mean ± SD) for each individual survey in the fall, winter, and spring

Date and Time	Mean Sea Level (m)	Current Velocity (m s^{-1})	Hs (m)	Temperature (°C)	TA (µmol kg^{-1})	DIC (µmol kg^{-1})	DO (µmol kg^{-1})
17-Oct-19 08:50-11:25	0.54±0.15	0.18±0.04	-	26.2±0.1	2267±6	1964±17	192±10
17-Oct-19 14:49-16:25	-0.40±0.06	0.11±0.03	0.55±0.05	26.8±0.3	2259±12	1919±26	220±20
21-Oct-19 13:43-15:32	0.25±0.06	0.17±0.03	0.65±0.02	27.0±0.2	2263±8	1926±22	218±21
22-Oct-19 12:52-14:42	0.31±0.05	0.04±0.02	0.41±0.03	26.8±0.2	2255±9	1925±20	206±18
18-Jan-24 09:01-11:45	0.42±0.22	0.13±0.04	-	21.6±0.7	2275±9	1991±17	184±6
18-Jan-24 12:20-15:23	0.52±0.18	0.09±0.02	-	22.4±0.3	2269±6	1967±9	198±10
29-Apr-23 09:05-11:27	0.09±0.02	0.04±0.02	0.13±0.01	23.6±0.3	2257±12	1969±14	198±10
29-Apr-23 13:49-15:36	0.26±0.03	0.04±0.01	0.13±0.01	24.0±0.3	2243±23	1933±27	227±17
3-May-23 09:06-11:45	-0.29±0.20	0.02±0.01	0.12±0.01	22.8±0.2	2256±9	1965±14	205±14
3-May-23 13:15-15:14	-0.21±0.22	0.06±0.01	0.15±0.02	23.1±0.2	2246±27	1932±36	220±20

Table S4.1 Summary of measured environmental data (mean ± SD), calculated mean pCO_2, pH, and aragonite saturation state (mean ± SD) for each individual survey in the fall, winter, and spring

Date and Time	Mean Sea Level (m)	Current Velocity (m s^{-1})	pCO_2 (µatm)	pH	Ω_{Ar}
17-Oct-19 08:50-11:25	0.54±0.15	0.37±0.04	396±25	8.04±0.02	3.44±0.14
17-Oct-19 14:49-16:25	-0.40±0.06	0.35±0.04	338±27	8.10±0.03	3.83±0.21
21-Oct-19 13:43-15:32	0.25±0.06	0.24±0.03	347±25	8.09±0.02	3.81±0.18
22-Oct-19 12:52-14:42	0.31±0.05	0.19±0.03	355±29	8.08±0.03	3.71±0.20
18-Jan-24 09:01-11:45	0.42±0.22	0.13±0.04	363±9	8.08±0.01	3.16±0.09
18-Jan-24 12:20-15:23	0.52±0.18	0.09±0.02	341±13	8.10±0.01	3.35±0.08
29-Apr-23 09:05-11:27	0.09±0.02	0.04±0.02	382±28	8.06±0.03	3.22±0.18
29-Apr-23 13:49-15:36	0.26±0.03	0.04±0.01	344±25	8.09±0.02	3.45±0.18
3-May-23 09:06-11:45	-0.29±0.20	0.02±0.01	363±21	8.07±0.02	3.24±0.12
3-May-23 13:15-15:14	-0.21±0.22	0.06±0.01	328±34	8.11±0.04	3.47±0.21

Table S4.2 Summary of mean and min-max dTA, dDIC, dDO, $dDIC_{NCP}$, ΔpH, and $\Delta\Omega_{Ar}$ drawdowns relative to the offshore end member (mean ± SD), and corresponding dTA:dDIC and dDO:$dDIC_{NCP}$ slopes and R^2 for each individual survey in the fall, winter, and spring

Date and Time	dTA (µmol kg^{-1})	dDIC (µmol kg^{-1})	dTA:dDIC slope (R^2)	$dDIC_{NCP}$ (µmol kg^{-1})	dDO (µmol kg^{-1})	dDO:$dDIC_{NCP}$ slope (R^2)	ΔpH	$\Delta\Omega_{Ar}$
17-Oct-19 08:50-11:25	-10±6 -18 to 2	-1±17 -42 to 35	0.28 (0.54)	4±15 -35 to 34	-1±10 -13 to 30	-0.62 (0.77)	-0.01±0.02 -0.05 to 0.05	-0.10±0.14 -0.34 to 0.27
17-Oct-19 14:49-16:25	-18±12 -40 to 8	-46±26 -93 to -6	0.38 (0.58)	-37±22 -83 to -5	27±20 -1 to 75	-0.90 (0.55)	0.04±0.03 0.00 to 0.10	0.29±0.20 0.01 to 0.82
21-Oct-19 13:43-15:32	-12±8 -30 to -1	-32±22 -88 to 1	0.29 (0.58)	-26±19 -76 to 2	25±21 -4 to 85	-1.10 (0.96)	0.03±0.02 -0.00 to 0.09	0.21±0.18 -0.03 to 0.67
22-Oct-19 12:52-14:42	-13±9 -29 to 6	-29±20 -57 to 6	0.17 (0.09)	-22±19 -51 to 16	21±18 -17 to 44	-0.94 (0.88)	0.02±0.03 -0.04 to 0.06	0.16±0.20 -0.27 to 0.46
18-Jan-24 09:01-11:45	5±9 -5 to 30	25±17 11 to 74	0.55 (0.89)	22±12 11 to 59	1±6 -10 to 9	-0.17 (0.09)	-0.02±0.01 -0.04 to 0.00	-0.20±0.10 -0.47 to -0.02
18-Jan-24 12:20-15:23	-1±6 -11 to 10	1±9 -12 to 12	0.46 (0.24)	1±8 -9 to 13	15±10 -2 to 30	-1.46 (0.51)	-0.00±0.01 -0.03 to 0.02	-0.02±0.08 -0.16 to 0.11
29-Apr-23 09:05-11:27	-24±12 -42 to 4	-17±14 -44 to 4	0.39 (0.05)	-5±14 -41 to 21	-16±10 -38 to 6	-0.68 (0.74)	-0.01±0.03 -0.06 to 0.07	-0.08±0.17 -0.41 to 0.45
29-Apr-23 13:49-15:36	-39±23 -110 to 14	-53±27 -99 to -13	0.82 (0.62)	-34±19 -67 to -2	14±17 -15 to 51	-0.92 (0.86)	0.02±0.02 -0.02 to 0.06	0.15±0.17 -0.16 to 0.43
3-May-23 09:06-11:45	-10±9 -38 to 3	-10±14 -42 to 23	0.46 (0.33)	-5±12 -33 to 21	3±14 -12 to 60	-1.69 (0.06)	-0.00±0.02 -0.04 to 0.05	-0.00±0.12 -0.20 to 0.30
3-May-23 13:15-15:14	-20±27 -126 to 4	-43±36 -157 to 1	0.69 (0.69)	-33±27 -94 to 3	18±20 -5 to 85	-0.73 (0.81)	0.04±0.04 -0.01 to 0.13	0.22±0.21 -0.07 to 0.77

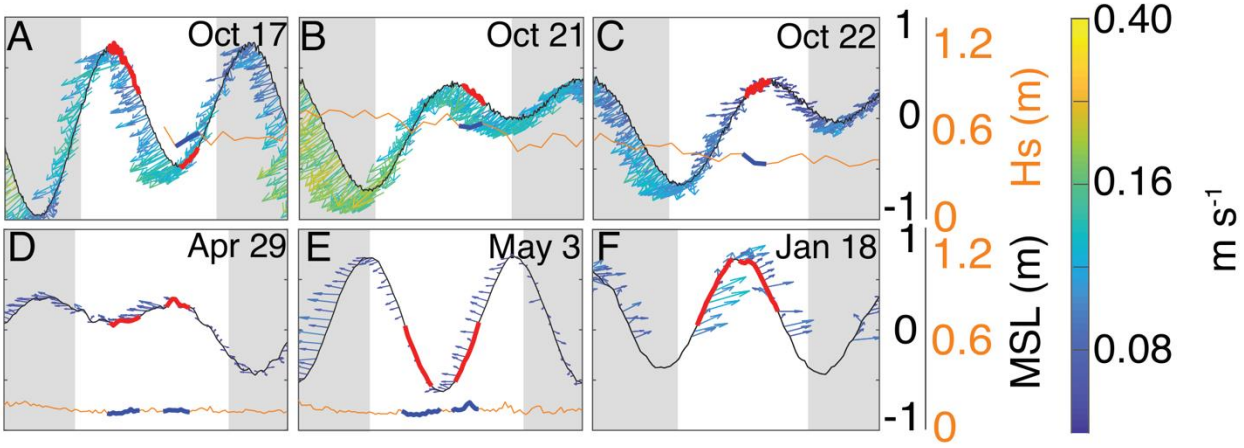

Figure 4.1. Depth integrated current velocity and direction (vectors) in relationship to mean sea level (MSL; black line) for each day of surveys from the middle of the lagoon and corresponding significant wave height (Hs; orange line) (A-F). Thicker red and blue lines depict the time of day when spatial surveys were conducted.

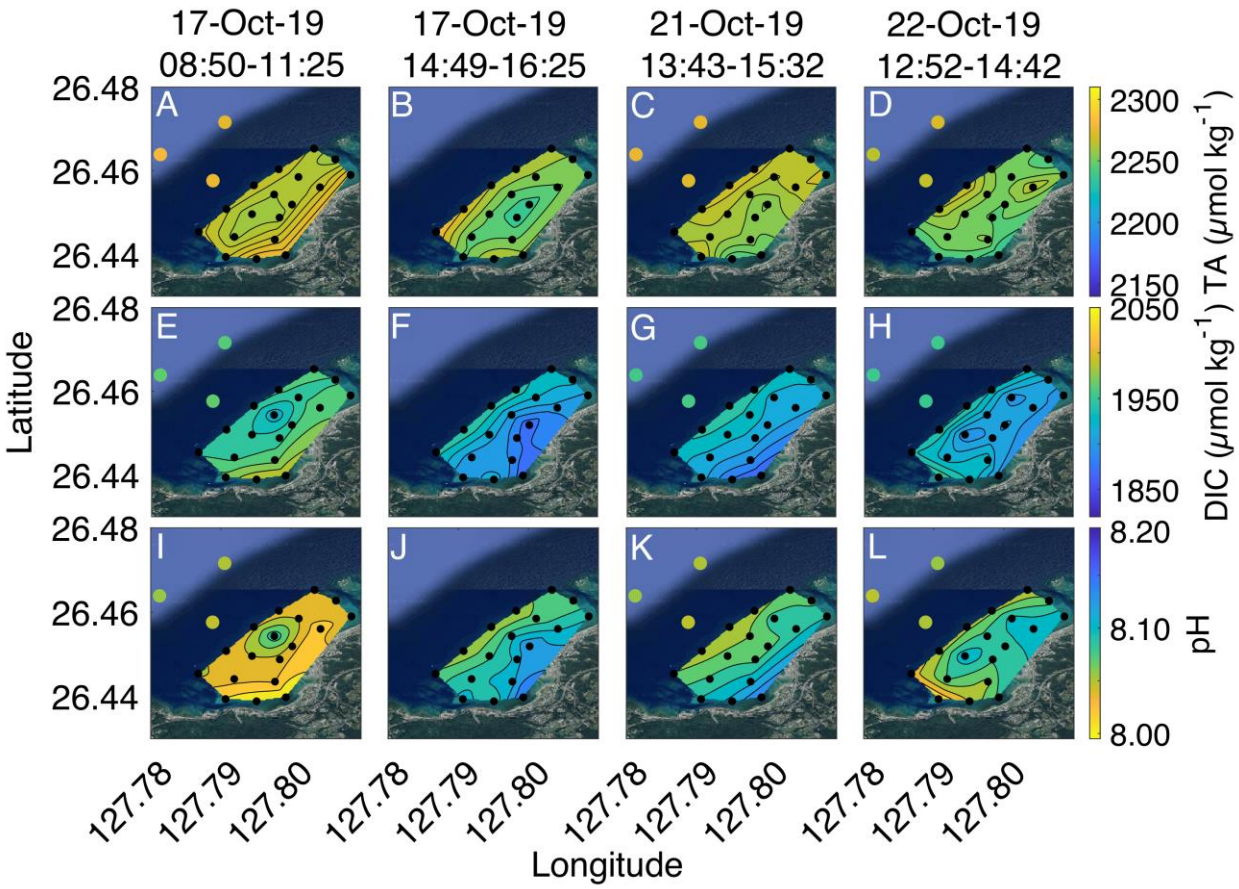

Figure 4.2. Spatial variability of measured TA (A-D), DIC (E-H), and calculated pH (I-L) for Fall, 2019 morning and afternoon surveys with color gradients representing the range of values and black dots representing location of samples.

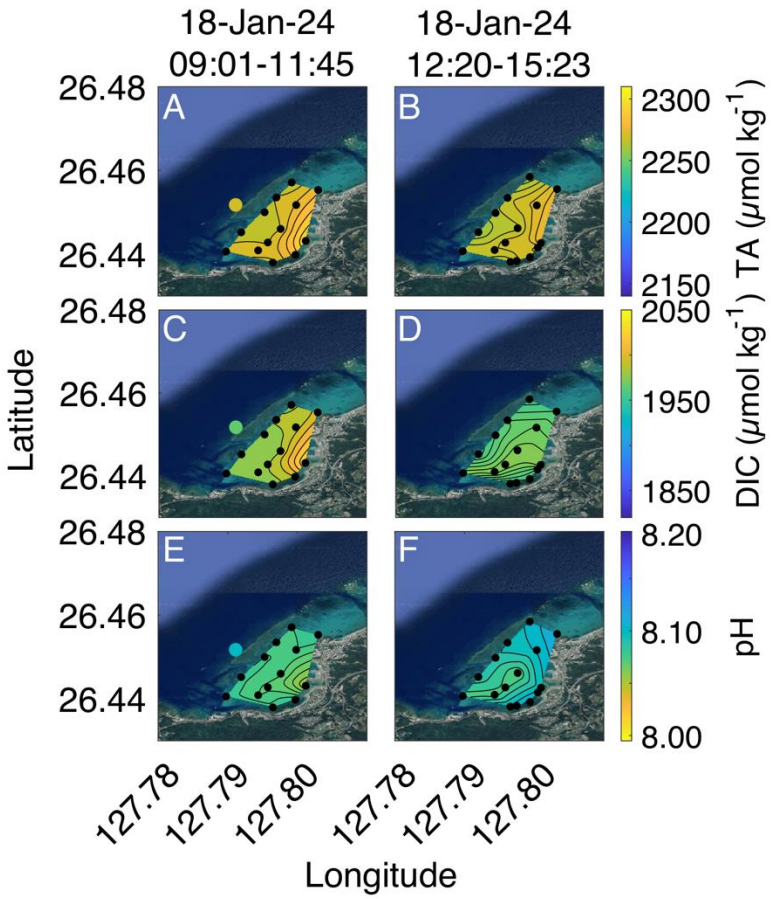

Figure 4.3. Spatial variability of measured TA (A, B), DIC (C, D), and calculated pH (E, F) for Winter, 2024 morning and afternoon surveys with color gradients representing the range of values and black dots representing location of samples.

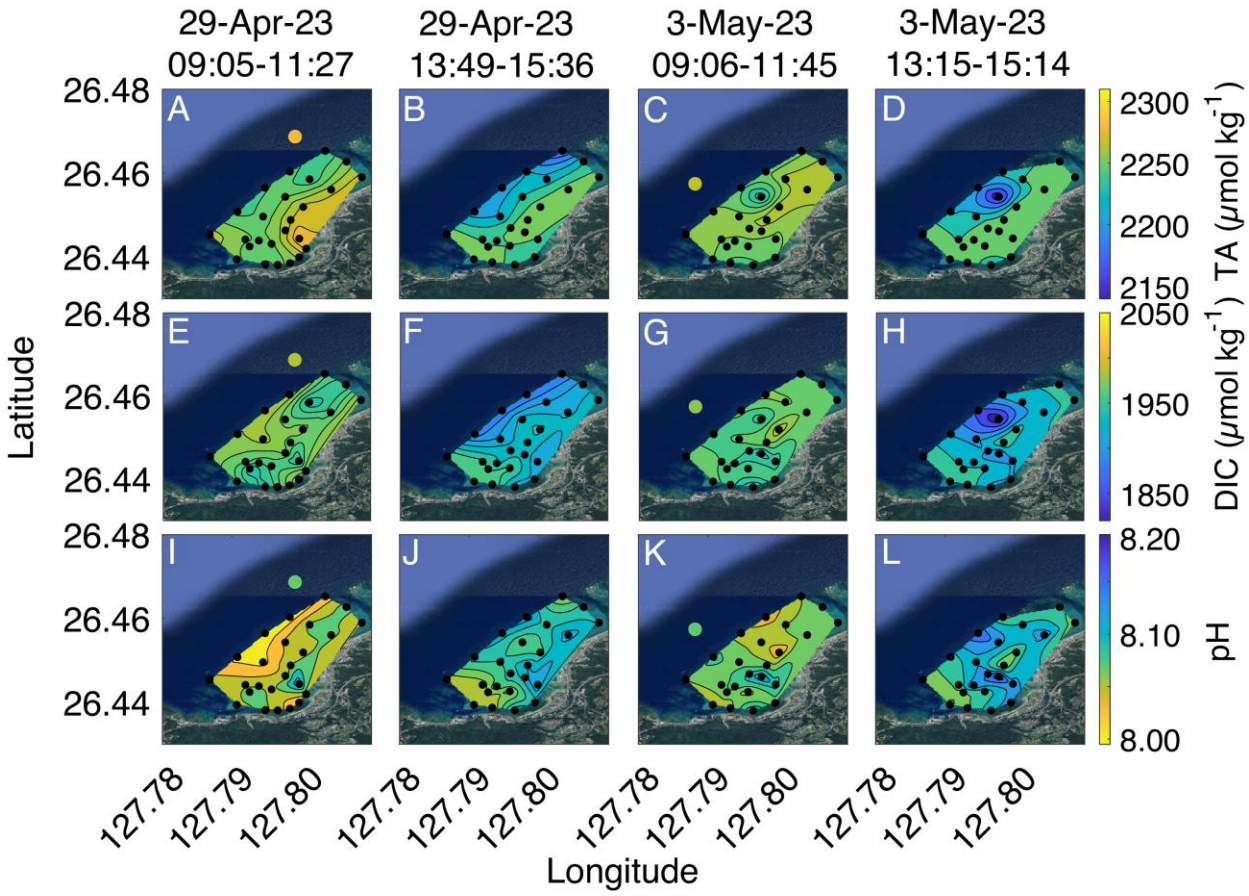

Figure 4.4. Spatial variability of measured TA (A-D), DIC (E-H), and calculated pH (I-L) for Spring, 2023 morning and afternoon surveys with color gradients representing the range of values and black dots representing location of samples.

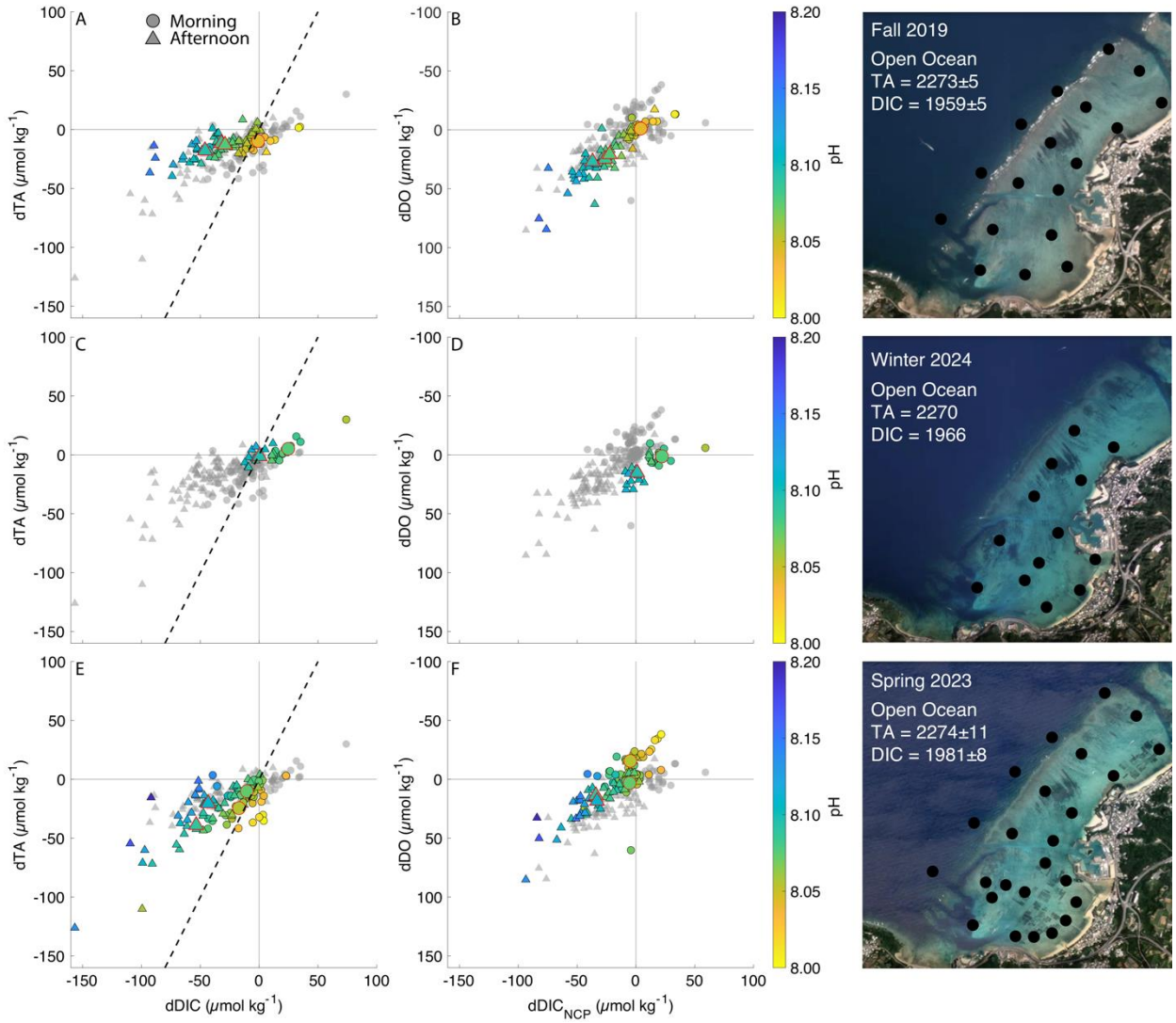

Figure 4.5. Property-property plots of the difference between reef and offshore salinity normalized properties; (A, C, E) dTA vs. dDIC and (B, D, F) dDO vs. $dDIC_{NCP}$ with colors indicating pH, the circles indicating morning surveys, and the triangles indicating afternoon surveys for the Fall (A, B), Winter (C, D), and Spring (E, F) spatial surveys. Larger, red-outlined shapes depict the mean for each individual survey. Black dashed line (A, C, E) demonstrates the TA/DIC 2:1 stoichiometric ratio. Corresponding maps on the right depict the locations for discrete seawater sampling, open-ocean TA and DIC conditions, and demonstrate differences in extent of seaweed farms.

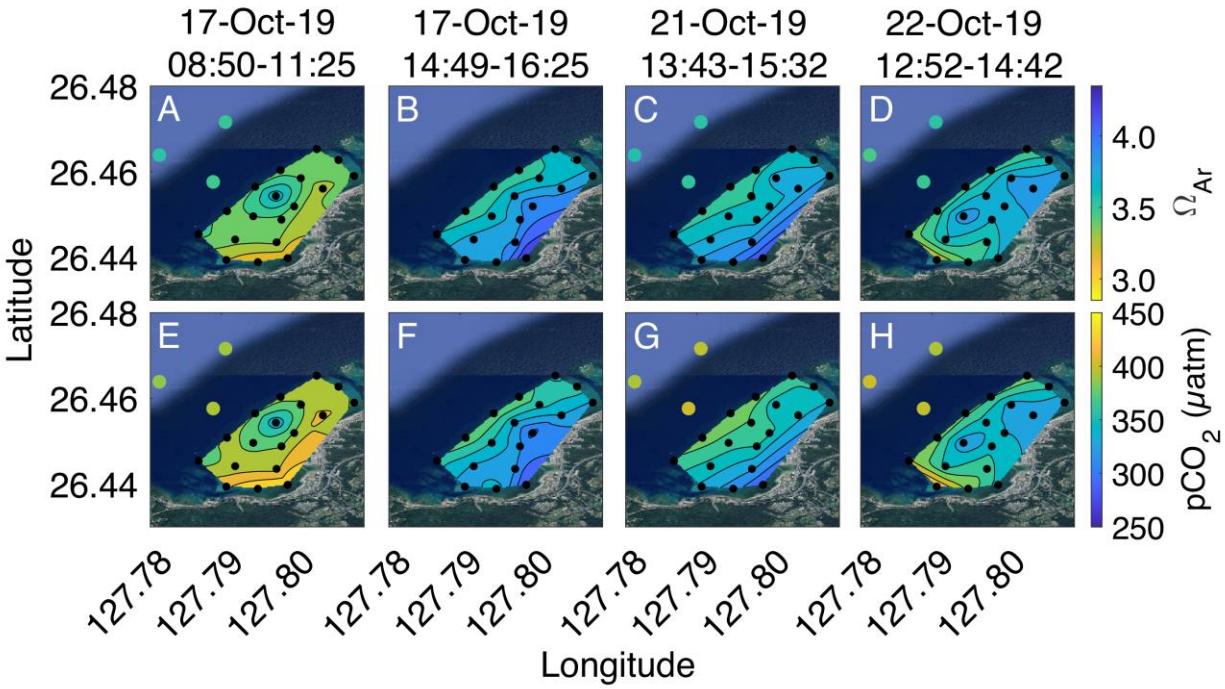

Figure S4.1. Spatial variability of calculated aragonite saturation state (A-D) and pCO_2 (µatm) (E-H) for Fall, 2019 morning and afternoon surveys with color gradients representing the range of values and black dots representing location of samples.

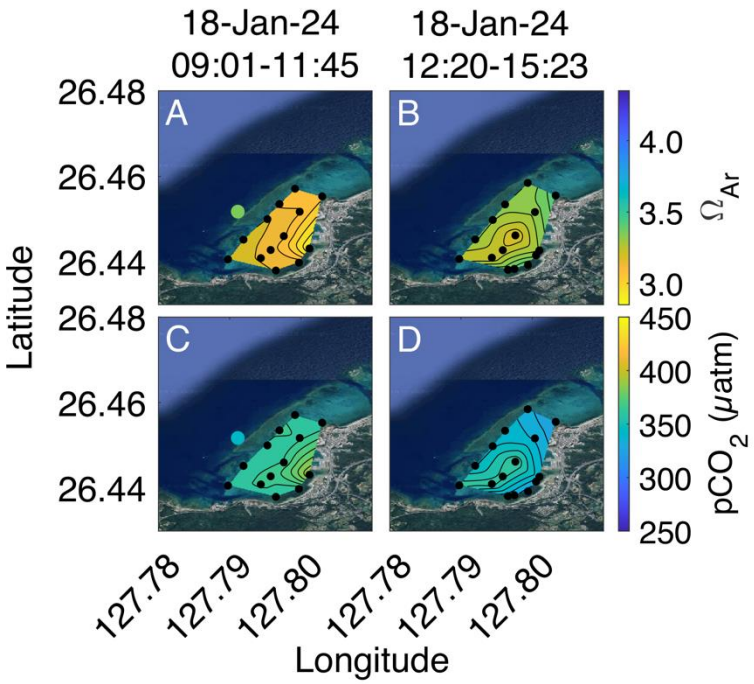

Figure S4.2. Spatial variability of calculated aragonite saturation state (A, B), and pCO_2 (µatm) (C, D) for Winter, 2024 morning and afternoon surveys with color gradients representing the range of values and black dots representing location of samples.

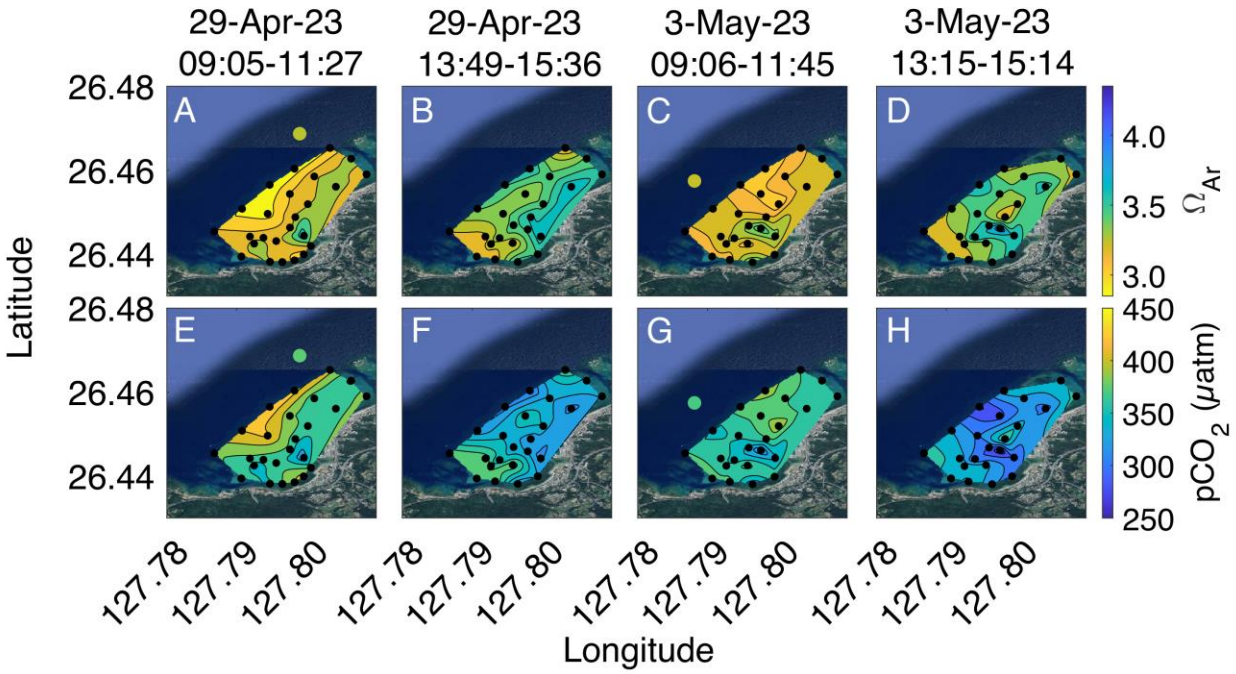

Figure S4.3. Spatial variability of calculated aragonite saturation state (A-D) and pCO_2 (µatm) (E-H) for Spring, 2023 morning and afternoon surveys with color gradients representing the range of values and black dots representing location of samples.

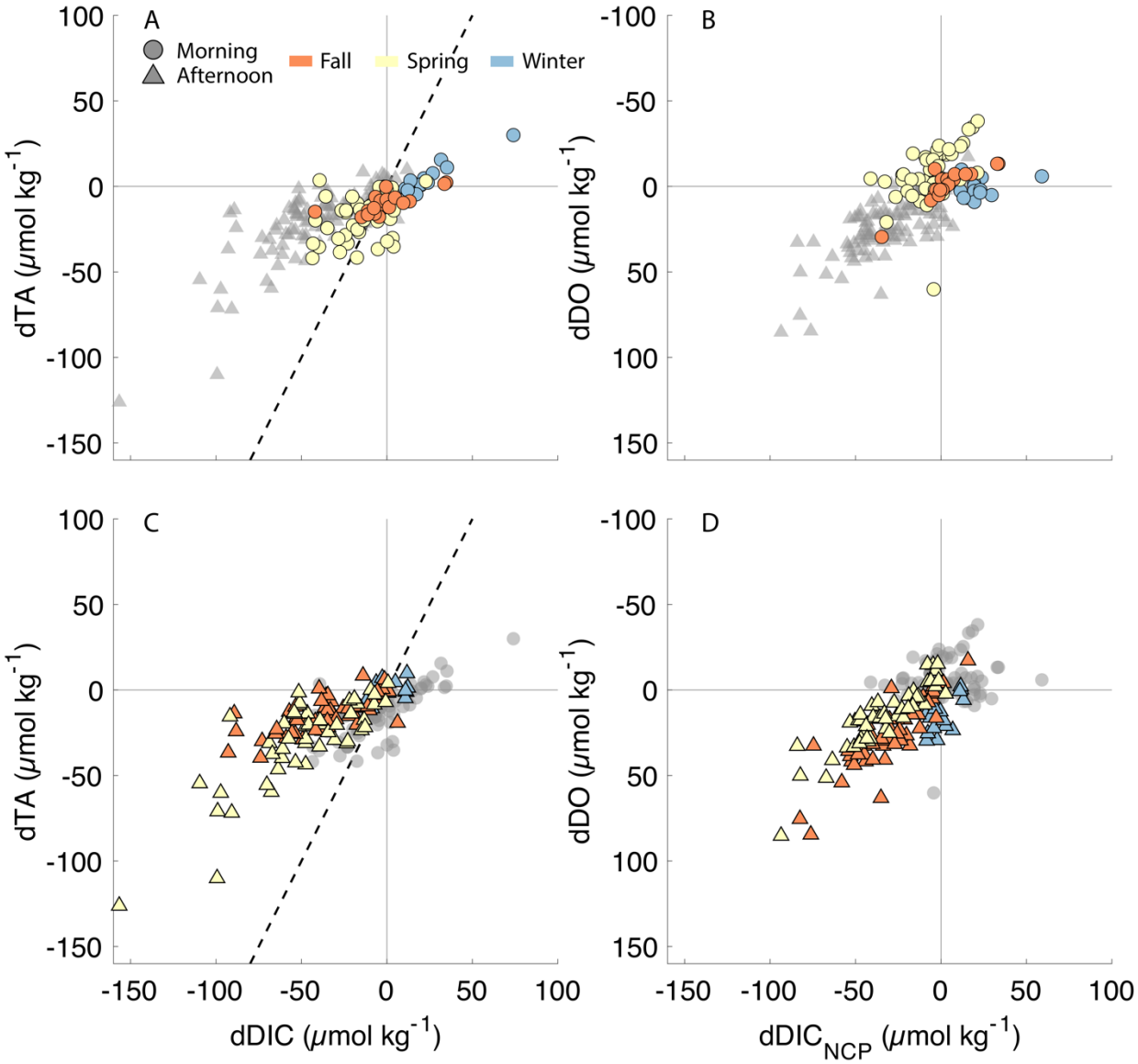

Figure S4.4. Property-property plots of the difference between reef and offshore salinity normalized properties; (A, C) dTA vs. dDIC and (B, D) dDO vs. $dDIC_{NCP}$ with colors Fall, Spring, or Winter surveys and the circles and triangles indicating morning (A, B) and afternoon (C, D) surveys, respectively. Black dashed line (A, C) demonstrates the TA/DIC 2:1 stoichiometric ratio.

References

Albright, R., J. Benthuysen, N. Cantin, K. Caldeira, and K. Anthony (2015), Coral reef metabolism and carbon chemistry dynamics of a coral reef flat, *Geophysical Research Letters*, *42*(10), 3980-3988.

Albright, R., Y. Takeshita, D. A. Koweek, A. Ninokawa, K. Wolfe, T. Rivlin, Y. Nebuchina, J. Young, and K. Caldeira (2018), Carbon dioxide addition to coral reef waters suppresses net community calcification, *Nature*, *555*(7697), 516-519.

Alleway, H. K., C. L. Gillies, M. J. Bishop, R. R. Gentry, S. J. Theuerkauf, and R. Jones (2019), The ecosystem services of marine aquaculture: valuing benefits to people and nature, *BioScience*, *69*(1), 59-68.

Altieri, A. H., S. B. Harrison, J. Seemann, R. Collin, R. J. Diaz, and N. Knowlton (2017), Tropical dead zones and mass mortalities on coral reefs, *Proceedings of the National Academy of Sciences*, *114*(14), 3660-3665.

Andersson, A. J., and D. Gledhill (2013), Ocean acidification and coral reefs: effects on breakdown, dissolution, and net ecosystem calcification, *Annual review of marine science*, *5*(1), 321-348.

Andersson, A. J., K. L. Yeakel, N. R. Bates, and S. J. De Putron (2014), Partial offsets in ocean acidification from changing coral reef biogeochemistry, *Nature Climate Change*, *4*(1), 56-61.

Anthony, K. R. (2016), Coral reefs under climate change and ocean acidification: challenges and opportunities for management and policy, *Annual Review of Environment and Resources*, *41*(1), 59-81.

Anthony, K. R., D. I. Kline, G. Diaz-Pulido, S. Dove, and O. Hoegh-Guldberg (2008), Ocean acidification causes bleaching and productivity loss in coral reef builders, *Proceedings of the National Academy of Sciences*, *105*(45), 17442-17446.

Atkinson, M., and S. Smith (1983), C: N: P ratios of benthic marine plants 1, *Limnology and Oceanography*, *28*(3), 568-574.

Bates, N. R., Y. M. Astor, M. J. Church, K. Currie, J. E. Dore, M. González-Dávila, L. Lorenzoni, F. Muller-Karger, J. Olafsson, and J. M. Santana-Casiano (2014), A time-series view of changing surface ocean chemistry due to ocean uptake of anthropogenic CO_2 and ocean acidification, *Oceanography*, *27*(1), 126-141.

Breitburg, D., L. A. Levin, A. Oschlies, M. Grégoire, F. P. Chavez, D. J. Conley, V. Garçon, D. Gilbert, D. Gutiérrez, and K. Isensee (2018), Declining oxygen in the global ocean and coastal waters, *Science*, *359*(6371), eaam7240.

Carilli, J. E., R. D. Norris, B. A. Black, S. M. Walsh, and M. McField (2009), Local stressors reduce coral resilience to bleaching, *Plos one*, *4*(7), e6324.

Chisholm, J. R., and J. P. Gattuso (1991), Validation of the alkalinity anomaly technique for investigating calcification of photosynthesis in coral reef communities, *Limnology and Oceanography*, *36*(6), 1232-1239.

Chou, W.-C., H.-C. Chu, Y.-H. Chen, R.-W. Syu, C.-C. Hung, and K. Soong (2018), Short-term variability of carbon chemistry in two contrasting seagrass meadows at Dongsha Island: implications for pH buffering and CO_2 sequestration, *Estuarine, Coastal and Shelf Science*, *210*, 36-44.

Chou, W.-C., L.-F. Fan, C.-C. Hung, Y.-Y. Shih, W.-J. Huang, H.-K. Lui, and T.-Y. Chen (2023), Dynamics of O_2 and pCO_2 in a Southeast Asia seagrass meadow: Metabolic rates and carbon sink capacity, *Frontiers in Marine Science*, *10*, 1076991.

Chou, W.-C., L.-F. Fan, C.-C. Yang, Y.-H. Chen, C.-C. Hung, W.-J. Huang, Y.-Y. Shih, K. Soong, H.-C. Tseng, and G.-C. Gong (2021), A unique diel pattern in carbonate chemistry in the seagrass meadows of dongsha island: the enhancement of metabolic carbonate dissolution in a semienclosed lagoon, *Frontiers in Marine Science*, *8*, 717685.

Costanza, R., R. De Groot, P. Sutton, S. Van der Ploeg, S. J. Anderson, I. Kubiszewski, S. Farber, and R. K. Turner (2014), Changes in the global value of ecosystem services, *Global environmental change*, *26*, 152-158.

Courtney, T., E. De Carlo, H. Page, K. Bahr, A. Barro, N. Howins, R. Tabata, G. Terlouw, K. Rodgers, and A. Andersson (2018), Recovery of reef-scale calcification following a bleaching event in Kāne'ohe Bay, Hawai'i, *Limnology and Oceanography Letters*, *3*(1), 1-9.

Courtney, T. A., H. C. Barkley, S. Chan, C. S. Couch, T. L. Kindinger, T. A. Oliver, D. J. Kriegman, and A. J. Andersson (2022), Rapid assessments of Pacific Ocean net coral reef carbonate budgets and net calcification following the 2014–2017 global coral bleaching event, *Limnology and Oceanography*, *67*(8), 1687-1700.

Cyronak, T., I. R. Santos, and B. D. Eyre (2013), Permeable coral reef sediment dissolution driven by elevated pCO_2 and pore water advection, *Geophysical Research Letters*, *40*(18), 4876-4881.

Cyronak, T., A. J. Andersson, S. D'Angelo, P. Bresnahan, C. Davidson, A. Griffin, T. Kindeberg, J. Pennise, Y. Takeshita, and M. White (2018a), Short-term spatial and temporal carbonate chemistry variability in two contrasting seagrass meadows: implications for pH buffering capacities, *Estuaries and Coasts*, *41*, 1282-1296.

Cyronak, T., A. J. Andersson, C. Langdon, R. Albright, N. R. Bates, K. Caldeira, R. Carlton, J. E. Corredor, R. B. Dunbar, and I. Enochs (2018b), Taking the metabolic pulse of the world's coral reefs, *PloS one*, *13*(1), e0190872.

Cyronak, T., Y. Takeshita, T. A. Courtney, E. H. DeCarlo, B. D. Eyre, D. I. Kline, T. Martz, H. Page, N. N. Price, and J. Smith (2020), Diel temperature and pH variability scale with depth across diverse coral reef habitats, *Limnology and Oceanography Letters*, *5*(2), 193-203.

Darling, E. S., T. R. McClanahan, J. Maina, G. G. Gurney, N. A. Graham, F. Januchowski-Hartley, J. E. Cinner, C. Mora, C. C. Hicks, and E. Maire (2019), Social–environmental drivers inform strategic management of coral reefs in the Anthropocene, *Nature ecology & evolution*, *3*(9), 1341-1350.

Deffeyes, K. S. (1965), Carbonate equilibria: A graphic and algebraic approach 1, *Limnology and Oceanography*, *10*(3), 412-426.

Dişa, D., M. Münnich, M. Vogt, and N. Gruber (2022), A space-time mosaic of seawater carbonate chemistry conditions in the north-shore Moorea coral reef system, *Frontiers in Marine Science*, *9*, 1004107.

Dove, S. G., K. T. Brown, A. Van Den Heuvel, A. Chai, and O. Hoegh-Guldberg (2020), Ocean warming and acidification uncouple calcification from calcifier biomass which accelerates coral reef decline, *Communications Earth & Environment*, *1*(1), 55.

Dove, S. G., D. I. Kline, O. Pantos, F. E. Angly, G. W. Tyson, and O. Hoegh-Guldberg (2013), Future reef decalcification under a business-as-usual CO_2 emission scenario, *Proceedings of the National Academy of Sciences*, *110*(38), 15342-15347.

Duarte, C. M., J. Wu, X. Xiao, A. Bruhn, and D. Krause-Jensen (2017), Can seaweed farming play a role in climate change mitigation and adaptation?, *Frontiers in Marine Science*, *4*, 100.

Edmunds, P. J., S. S. Doo, and R. C. Carpenter (2024), Effects of year-long exposure to elevated pCO_2 on the metabolism of back reef and fore reef communities, *Limnology and Oceanography*, *69*(3), 533-547.

Elahi, R., P. J. Edmunds, R. D. Gates, I. B. Kuffner, B. B. Barnes, I. Chollett, T. A. Courtney, J. R. Guest, E. A. Lenz, and L. T. Toth (2022), Scale dependence of coral reef oases and their environmental correlates, *Ecological Applications*, *32*(7), e2651.

Eyre, B. D., A. J. Andersson, and T. Cyronak (2014), Benthic coral reef calcium carbonate dissolution in an acidifying ocean, *Nature climate change*, *4*(11), 969-976.

Eyre, B. D., T. Cyronak, P. Drupp, E. H. De Carlo, J. P. Sachs, and A. J. Andersson (2018), Coral reefs will transition to net dissolving before end of century, *Science*, *359*(6378), 908-911.

Falter, J. L., R. J. Lowe, Z. Zhang, and M. McCulloch (2013), Physical and biological controls on the carbonate chemistry of coral reef waters: effects of metabolism, wave forcing, sea level, and geomorphology, *PloS one*, *8*(1), e53303.

Falter, J. L., Z. Zhang, R. J. Lowe, F. McGregor, J. Keesing, and M. T. McCulloch (2014), Assessing the drivers of spatial variation in thermal forcing across a nearshore reef system and implications for coral bleaching, *Limnology and Oceanography*, *59*(4), 1241-1255.

Ferrario, F., M. W. Beck, C. D. Storlazzi, F. Micheli, C. C. Shepard, and L. Airoldi (2014), The effectiveness of coral reefs for coastal hazard risk reduction and adaptation, *Nature communications*, *5*(1), 1-9.

Frankignoulle, M., J.-P. Gattuso, R. Biondo, I. Bourge, G. Copin-Montégut, and M. Pichon (1996), Carbon fluxes in coral reefs. II. Eulerian study of inorganic carbon dynamics and measurement of air-sea CO_2 exchanges, *Marine Ecology Progress Series*, *145*, 123-132.

Gattuso, J.-P., A. K. Magnan, L. Bopp, W. W. Cheung, C. M. Duarte, J. Hinkel, E. Mcleod, F. Micheli, A. Oschlies, and P. Williamson (2018), Ocean solutions to address climate change and its effects on marine ecosystems, *Frontiers in Marine Science*, *5*, 337.

Guest, J. R., P. J. Edmunds, R. D. Gates, I. B. Kuffner, A. J. Andersson, B. B. Barnes, I. Chollett, T. A. Courtney, R. Elahi, and K. Gross (2018), A framework for identifying and characterising coral reef "oases" against a backdrop of degradation, *Journal of Applied Ecology*, *55*(6), 2865-2875.

Guo, W. (2019), Seawater temperature and buffering capacity modulate coral calcifying pH, *Scientific Reports*, *9*(1), 1189.

Higa, Y., A. Takeuchi, and S. Yanaka (2022), Connecting Local Regions and Cities through Mozuku Seaweed Farming and Coral Reef Restoration: Onna Village, Okinawa, in *Satoumi Science: Co-Creating Social-Ecological Harmony between Human and the Sea*, edited, pp. 193-215, Springer.

Higuchi, T., K. K. Takagi, K. Matoba, S. Kobayashi, R. Tsurumi, S. Arakaki, Y. Nakano, H. Fujimura, T. Oomori, and M. Tsuchiya (2014), The nutrient and carbon dynamics that mutually benefit coral and seagrass in mixed habitats under the influence of groundwater at Bise coral reef, Okinawa, Japan, *International Journal of Marine Science*, *4*.

Hoegh-Guldberg, O., E. S. Poloczanska, W. Skirving, and S. Dove (2017), Coral reef ecosystems under climate change and ocean acidification, *Frontiers in Marine Science*, *4*, 158.

Hofmann, G. E., J. E. Smith, K. S. Johnson, U. Send, L. A. Levin, F. Micheli, A. Paytan, N. N. Price, B. Peterson, and Y. Takeshita (2011), High-frequency dynamics of ocean pH: a multi-ecosystem comparison, *PloS one*, *6*(12), e28983.

Hughes, T. P., J. T. Kerry, M. Álvarez-Noriega, J. G. Álvarez-Romero, K. D. Anderson, A. H. Baird, R. C. Babcock, M. Beger, D. R. Bellwood, and R. Berkelmans (2017), Global warming and recurrent mass bleaching of corals, *Nature*, *543*(7645), 373-377.

Hughes, T. P., K. D. Anderson, S. R. Connolly, S. F. Heron, J. T. Kerry, J. M. Lough, A. H. Baird, J. K. Baum, M. L. Berumen, and T. C. Bridge (2018), Spatial and temporal patterns of mass bleaching of corals in the Anthropocene, *Science*, *359*(6371), 80-83.

Hurd, C. L. (2015), Slow-flow habitats as refugia for coastal calcifiers from ocean acidification, *Journal of phycology*, *51*(4), 599-605.

Kapsenberg, L., and T. Cyronak (2019), Ocean acidification refugia in variable environments, *Global Change Biology*, *25*(10), 3201-3214.

Kealoha, A. K., S. M. Doyle, K. E. Shamberger, J. B. Sylvan, R. D. Hetland, and S. F. DiMarco (2020), Localized hypoxia may have caused coral reef mortality at the Flower Garden Banks, *Coral Reefs*, *39*, 119-132.

Kekuewa, S. A., T. A. Courtney, T. Cyronak, T. Kindeberg, B. D. Eyre, L. Stoltenberg, and A. J. Andersson (2021), Temporal and spatial variabilities of chemical and physical parameters on the Heron Island coral reef platform, *Aquatic Geochemistry*, *27*, 241-268.

Kleypas, J. A., K. R. Anthony, and J. P. Gattuso (2011), Coral reefs modify their seawater carbon chemistry–case study from a barrier reef (Moorea, French Polynesia), *Global change biology*, *17*(12), 3667-3678.

Kurihara, H., J. Wouters, and N. Yasuda (2019), Seasonal calcification of the coral Acropora digitifera from a subtropical marginal Okinawa reef under ocean acidification, *Coral Reefs*, *38*, 443-454.

Kwiatkowski, L., O. Torres, L. Bopp, O. Aumont, M. Chamberlain, J. R. Christian, J. P. Dunne, M. Gehlen, T. Ilyina, and J. G. John (2020), Twenty-first century ocean warming, acidification, deoxygenation, and upper-ocean nutrient and primary production decline from CMIP6 model projections, *Biogeosciences*, *17*(13), 3439-3470.

Langdon, C., and M. Atkinson (2005), Effect of elevated pCO_2 on photosynthesis and calcification of corals and interactions with seasonal change in temperature/irradiance and nutrient enrichment, *Journal of Geophysical Research: Oceans*, *110*(C9).

Lowe, R. J., and J. L. Falter (2015), Oceanic forcing of coral reefs, *Annual review of marine science*, *7*(1), 43-66.

Moberg, F., and C. Folke (1999), Ecological goods and services of coral reef ecosystems, *Ecological economics*, *29*(2), 215-233.

Mongin, M., and M. Baird (2014), The interacting effects of photosynthesis, calcification and water circulation on carbon chemistry variability on a coral reef flat: A modelling study, *Ecological modelling*, *284*, 19-34.

Mongin, M., M. E. Baird, S. Hadley, and A. Lenton (2016), Optimising reef-scale CO_2 removal by seaweed to buffer ocean acidification, *Environmental Research Letters*, *11*(3), 034023.

Mongin, M., M. E. Baird, A. Lenton, C. Neill, and J. Akl (2021), Reversing ocean acidification along the Great Barrier Reef using alkalinity injection, *Environmental Research Letters*, *16*(6), 064068.

National Academies of Sciences, E., and Medicine (2021), *A research strategy for ocean-based carbon dioxide removal and sequestration*.

Nelson, H. R., and A. H. Altieri (2019), Oxygen: the universal currency on coral reefs, *Coral Reefs*, *38*(2), 177-198.

Nishihira, M. (1988), *Field guide to hermatypic corals of Japan*, 東海大学出版会.

Omori, M., Y. Higa, C. Shinzato, Y. Zayasu, T. Nagata, R. Nakamura, A. Yokokura, and S. Janadou (2016), Development of active restoration methodologies for coral reefs using asexual reproduction in Okinawa, Japan, paper presented at Proceedings of the 13th International Coral Reef Symposium.

Page, H. N., T. A. Courtney, E. H. De Carlo, N. M. Howins, I. Koester, and A. J. Andersson (2019), Spatiotemporal variability in seawater carbon chemistry for a coral reef flat in Kāne ʻohe Bay, Hawai ʻi, *Limnology and Oceanography*, *64*(3), 913-934.

Page, H. N., A. J. Andersson, P. L. Jokiel, K. u. S. Rodgers, M. Lebrato, K. Yeakel, C. Davidson, S. D'Angelo, and K. D. Bahr (2016), Differential modification of seawater carbonate chemistry by major coral reef benthic communities, *Coral Reefs*, *35*, 1311-1325.

Pezner, A. K., T. A. Courtney, H. N. Page, S. N. Giddings, C. M. Beatty, M. D. DeGrandpre, and A. J. Andersson (2021), Lateral, vertical, and temporal variability of seawater carbonate chemistry at Hog Reef, Bermuda, *Frontiers in Marine Science*, *8*, 562267.

Rintoul, M., T. Courtney, J. Dohner, S. Giddings, S. Kekuewa, S. Mitarai, S. Monismith, A. Pezner, and A. Andersson (2022), The effects of light intensity and flow speed on biogeochemical variability within a fringing coral reef in Onna-son, Okinawa, Japan, *Journal of Geophysical Research: Oceans*, *127*(12), e2021JC018369.

Rintoul, M (2024) The influence of physical factors on biogeochemical variability on coral reefs. University of California, San Diego.

Sato, Y., G. N. Nishihara, A. Tanaka, D. F. Belleza, A. Kawate, Y. Inoue, K. Hinode, Y. Matsuda, S. Tanimae, and K. Tozaki (2022), Variability in the net ecosystem productivity (NEP) of seaweed farms, *Frontiers in Marine Science*, *9*, 861932.

Singh, T., F. Sinniger, Y. Nakano, S. Nakamura, S. Kadena, M. Jinza, H. Fujimura, and S. Harii (2022), Long-term trends and seasonal variations in environmental conditions in Sesoko Island, Okinawa, Japan, *Galaxea, Journal of Coral Reef Studies*, *24*(1), 121-133.

Smith, S., and G. Key (1975), Carbon dioxide and metabolism in marine environments 1, *Limnology and Oceanography*, *20*(3), 493-495.

Smith, S., and D. Kinsey (1978), Calcification and organic carbon metabolism as indicated by carbon dioxide.

Suzuki, A., and H. Kawahata (2003), Carbon budget of coral reef systems: an overview of observations in fringing reefs, barrier reefs and atolls in the Indo-Pacific regions, *Tellus B: Chemical and Physical Meteorology*, *55*(2), 428-444.

Takeshita, Y., T. Cyronak, T. R. Martz, T. Kindeberg, and A. J. Andersson (2018), Coral reef carbonate chemistry variability at different functional scales, *Frontiers in Marine Science*, *5*, 175.

Van Heuven, S., D. Pierrot, J. Rae, E. Lewis, and D. Wallace (2011), MATLAB program developed for CO_2 system calculations, *ORNL/CDIAC-105b. Carbon Dioxide Information Analysis Center, Oak Ridge National Laboratory, US Department of Energy, Oak Ridge, Tennessee*, *530*.

Vaquer-Sunyer, R., C. M. Duarte, G. Jordà, and S. Ruiz-Halpern (2012), Temperature dependence of oxygen dynamics and community metabolism in a shallow Mediterranean macroalgal meadow (Caulerpa prolifera), *Estuaries and Coasts*, *35*, 1182-1192.

Venti, A., A. Andersson, and C. Langdon (2014), Multiple driving factors explain spatial and temporal variability in coral calcification rates on the Bermuda platform, *Coral Reefs*, *33*, 979-997.

Watanabe, A., H. Kayanne, H. Hata, S. Kudo, K. Nozaki, K. Kato, A. Negishi, Y. Ikeda, and H. Yamano (2006), Analysis of the seawater CO_2 system in the barrier reef-lagoon system of Palau using total alkalinity-dissolved inorganic carbon diagrams, *Limnology and Oceanography*, *51*(4), 1614-1628.

Xiao, X., S. Agusti, F. Lin, K. Li, Y. Pan, Y. Yu, Y. Zheng, J. Wu, and C. M. Duarte (2017), Nutrient removal from Chinese coastal waters by large-scale seaweed aquaculture, *Scientific reports*, *7*(1), 46613.

Xiao, X., S. Agustí, Y. Yu, Y. Huang, W. Chen, J. Hu, C. Li, K. Li, F. Wei, and Y. Lu (2021), Seaweed farms provide refugia from ocean acidification, *Science of the Total Environment*, *776*, 145192.

Chapter 4, in full, is currently being prepared for submission for publication of the material. Kekuewa SAH, Rintoul MS, Courtney TA, Pezner AK, Mitarai S, Andersson AJ. The dissertation author was the primary researcher and author of this material.

CHAPTER 5: Conclusion

By the year 2100, global ocean surface seawater temperatures are projected to increase by 3.5 °C under the RCP 8.5 emission scenario, which will be accompanied by decreases in average surface ocean pH and DO by about 0.40 and 13 μmol kg^{-1}, respectively (Kwiatowski et al., 2020). These major shifts in ocean physicochemical parameters are anticipated to be detrimental to ecosystem function and health in coastal habitats (Hughes et al., 2017; Altieri et al., 2017; Edmunds et al., 2024). For coral reefs, global warming may lead to increased frequency and severity of coral bleaching and mass mortality events (Hughes et al., 2018), ocean acidification has been demonstrated to reduce calcification (Kroeker et al., 2013; Perry et al., 2018; Kornder et al., 2018; Cornwall et al., 2021; Davis et al., 2021) and increase $CaCO_3$ dissolution (Eyre et al., 2018; Edmunds et al., 2024) while hypoxia has been shown to result in mass morality events (Altieri et al., 2017; Kealoha et al., 2019). Nonetheless, our understanding of the current day, natural spatiotemporal variability of seawater carbonate chemistry over coral reefs is limited. Thus, this dissertation leverages autonomous sensors and discrete seawater samples deployed and collected over a range of spatial and temporal scales across coral reef habitats to assess the natural seawater carbonate chemistry across space and time of three unique coral reefs. Together, these observations help elucidate the relative impact of habitat metabolism (e.g., NCP and NCC), benthic composition, and hydrodynamic processes in modifying the observed chemistry variability and provides crucial observations to improve our predictive capacity and modelling efforts on how coral reefs fill fair in the future.

In Chapter 2 of this dissertation, we characterized the physicochemical spatiotemporal variability on Heron Reef Platform in the Great Barrier Reef, Australia. Our results revealed that the local geomorphology resulted in isolation of the platform during low tide and rapid fooding

during rising tides, which led to distinct spatial gradients depending on the timing of high tide. As a result, seawater during low tide was observed in different parts of the reef leading to unexpected seawater CO_2 chemistry trends both temporally and spatially. For example, during the evening high tide survey we observed elevated pH, Ω_{Ar}, and DO and decreased TA and DIC across the shallow, western region of the reef – patterns associated with the low tide, daytime processes (+NPC, +NCC). Further insights were gained when our observations were compared to spatial biogeochemical models from Mongin and Baird, 2014. The model comparison revealed contrasting findings, wherein we observed an increase in Ω_{Ar} and pH in the western region of the reef while Mongin and Baird, 2014 projected a decrease. We hypothesized this to be due to a combination of a mismatch in timing and amplitude between low and high tide, parametrization of NCP and NCC, and the difference in season between the model and our observations. These results demonstrate the need for dedicated spatial surveys to assess spatiotemporal physicochemical variability across a range of tidal and diel cycle extremes to capture the full natural range of variability and better inform biogeochemical models.

In Chapter 3, we assessed the seawater carbonate chemistry variability across multiple spatial scales and habitats in two contrasting coral reef systems, Dongsha Atoll and Taiping, in the South China Sea. Observations from autonomous sensors revealed that the daily variability in temperature, pH and oxygen gradually decrease from the lagoon to the seagrass and patch reef environments. In particular, the tidally isolated inner lagoon site appeared to be influenced by metabolic carbonate dissolution which resulted in elevated TA and thus pH conditions. Discrete seawater samples relative to offshore seawater samples revealed that all habitats across Dongsha, except the inner lagoon, on average experienced net calcification and that on larger spatial scales NCC is the predominant driver of seawater carbonate chemistry variability. Projections of our

observations utilizing a historical increase of 1.15 μmol $kg^{-1}year^{-1}$ in DIC near the Ryukyu Islands and a regional CMIP6 RCP 8.5 warming increase we projected future ocean acidification conditions at Dongsha Atoll. By 2050, 52% of our observations for the patch reefs and 89% of our observations for the reef-wide scale will experience Ω_{Ar}<2.92, the threshold for when coral reef sediments transition from net precipitation to net dissolution. In comparison, only 31% of the observations for the seagrass habitats and 10% of the observations for the semi-enclosed lagoon had a Ω_{Ar}<2.92. These results highlight the capacity for the inner lagoon, seagrass beds, and eastern patch reefs of Dongsha Atoll to act as a refugia to ongoing climate change conditions. Further, these findings demonstrate the necessity for increased monitoring to better understand the complex interplay between hydrodynamics and various reef habitats to better assess the resiliency and adaptability of coral reefs to future climate change conditions. Combined, the first two chapters of this dissertation demonstrate the individuality of coral reefs environments and the importance of system-wide spatiotemporal surveys to evaluate the function of carbon cycling in coral reefs.

Seaweed cultivation and marine macroalgal habitats in general have been hypothesized to play an important role in marine carbon dioxide removal and to buffer calcifying organisms from ocean acidification conditions via photosynthesis driven pH amelioration. In Chapter 4, we conducted reef wide spatial surveys for seawater carbonate chemistry analysis in the fall, winter, and spring, the latter of which coincides with the maximum extent of seaweed cultivation. These observations were used to assess the biogeochemical footprint and impact of a seaweed farm on the downstream Onna-son reef. Spatial seawater carbonate chemistry variability was greatest in spring, followed by fall and then winter. In particular, the largest maximum drawdown in TA and DIC relative to an open-ocean source was observed in the spring during seaweed cultivation, suggesting a potential increase in calcification. However, despite the observed spatial variability,

there was no evidence of significantly elevated pH buffering in spring relative to fall. More research is needed to assess how seaweed cultivation effects the natural spatial variability of seawater carbonate chemistry across coral reefs and whether seaweed farms can act as a spatial refugia to ongoing climate change.

Collectively, this dissertation bridges a critical gap in our knowledge of the extent coral reef communities can modify seawater chemistry. It is evident that some communities have a higher potential to ameliorate the change in pH due to climate change whereas others can potentially exacerbate it. Co-deployed biogeochemical and hydrodynamic sensors in addition to dedicated spatiotemporal surveys are needed to evaluate the role, resilience, adaptability, and function of different coral reef communities in the future.

References

Altieri, A. H., Harrison, S. B., Seemann, J., Collin, R., Diaz, R. J. and Knowlton, N. (2017) Tropical dead zones and mass mortalities on coral reefs, *Proceedings of the National Academy of Sciences*, 114(14), 3660-3665.

Cornwall, C.E., Comeau, S., Kornder, N.A., Perry, C.T., van Hooidonk, R., DeCarlo, T.M., Pratchett, M.S., Anderson, K.D., Browne, N., Carpenter, R. and Diaz-Pulido, G., (2021) Global declines in coral reef calcium carbonate production under ocean acidification and warming. *Proceedings of the National Academy of Sciences*, *118*(21), p.e2015265118.

Davis, K.L., Colefax, A.P., Tucker, J.P., Kelaher, B.P. and Santos, I.R., (2021) Global coral reef ecosystems exhibit declining calcification and increasing primary productivity. *Communications Earth & Environment*, *2*(1), p.105.

Eyre, B. D., Cyronak, T., Drupp, P., De Carlo, E. H., Sachs, J. P., and Andersson, A. J. (2018) Coral reefs will transition to net dissolving before end of century. *Science*, *359*(6378), 908-911.

Hughes, T. P., Kerry, J. T., Álvarez-Noriega, M., Álvarez-Romero, J. G., Anderson, K. D., Baird, A. H., Babcock, R. C., Beger, M., Bellwood, D. R. and Berkelmans, R. (2017) Global warming and recurrent mass bleaching of corals, *Nature*, 543(7645), 373-377.

Hughes, T.P., Kerry, J.T., Baird, A.H., Connolly, S.R., Dietzel, A., Eakin, C.M., Heron, S.F., Hoey, A.S., Hoogenboom, M.O., Liu, G. and McWilliam, M.J., (2018) Global warming transforms coral reef assemblages. *Nature*, *556*(7702), pp.492-496.

Kealoha, A. K., Doyle, S. M., Shamberger, K. E., Sylvan, J. B., Hetland, R. D. and DiMarco, S. F. (2020) Localized hypoxia may have caused coral reef mortality at the Flower Garden Banks, *Coral Reefs*, 39, 119-132.

Kornder, N.A., Riegl, B.M. and Figueiredo, J., (2018) Thresholds and drivers of coral calcification responses to climate change. *Global change biology*, *24*(11), pp.5084-5095.

Kroeker, K.J., Kordas, R.L., Crim, R., Hendriks, I.E., Ramajo, L., Singh, G.S., Duarte, C.M. and Gattuso, J.P., (2013) Impacts of ocean acidification on marine organisms: quantifying sensitivities and interaction with warming. *Global change biology*, *19*(6), pp.1884-1896.

Kwiatkowski, L., Torres, O., Bopp, L., Aumont, O., Chamberlain, M., Christian, J. R., Dunne, J. P., Gehlen, M., Ilyina, T. and John, J. G. (2020) Twenty-first century ocean warming, acidification, deoxygenation, and upper-ocean nutrient and primary production decline from CMIP6 model projections, *Biogeosciences,* 17(13), 3439-3470.

Perry, C.T., Alvarez-Filip, L., Graham, N.A., Mumby, P.J., Wilson, S.K., Kench, P.S., Manzello, D.P., Morgan, K.M., Slangen, A., Thomson, D.P. and Januchowski-Hartley, F., (2018) Loss of coral reef growth capacity to track future increases in sea level. *Nature*, *558*(7710), pp.396-400